Politecnico di Torino

POLITECNICO di TORINO

Tesi di Laurea Magistrale

Effects of selected environmental conditions on the stability of reinforced-soil dams

Corso di Laurea Magistrale in Building Engineering

Supervisors

Prof. Monica Barbero (DISEG)

Dr. Gianmarco Vallero

Candidate

Davood Kalantari

March 2026

Table of Contents

Table of Figures

List of Tables

Introduction

Dams are among the most complex and essential civil-engineering structures, designed to store, regulate, and utilize water resources for multiple purposes such as hydropower generation, irrigation, flood control, and domestic supply. By forming artificial reservoirs, dams allow the regulation of river flows over time, reducing the impacts of seasonal variability and extreme hydrological events while ensuring a more consistent availability of water. Despite their societal benefits, dams remain vulnerable systems in which hydraulic, geotechnical, and environmental processes interact continuously, sometimes in ways that can threaten their long-term safety and performance. An important question, therefore, arises: can the water stored within a reservoir, intended as a resource, also become a potential threat to the structural integrity of the dam itself?

From an engineering perspective, dams are commonly classified according to construction material, geometric configuration, and overall dimensions (such as height and crest length), resulting in categories including concrete gravity dams, arch dams, and earth or rockfill embankment dams. Among these, earth and rockfill embankment dams are predominant because of their cost efficiency, adaptability to various foundations, and the use of local materials. Their stability, however, is highly sensitive to the mechanical and hydraulic behaviour of the compacted soil mass and to the complex interactions between seepage, pore-pressure evolution, and external loading conditions.

In recent years, the role of vegetation in improving soil stability has attracted growing attention within geotechnical and environmental engineering. Vegetation can reinforce surface layers mechanically through root anchorage and tensile resistance, while also influencing hydraulic behaviour via evapotranspiration and suction. Nevertheless, these effects are not always beneficial. Root growth, particularly the uncontrolled proliferation of roots and shrubs, their decay, and water infiltration can alter drainage pathways, create preferential flow paths, and compromise the structural integrity of earth dams. Determining whether vegetation acts as a stabilizing or destabilizing factor thus represents a central question in contemporary dam-safety research.

This thesis investigates the combined mechanical and hydraulic effects of vegetation on reinforced-soil embankment dams. Moreover, the possible influence of reservoir water level and waves travelling on the water surface is also investigated. These waves are related to the impact of landslides within the reservoir basin, which can generate additional hydrodynamic loading on the dam body. As a result, the effect of wave-induced forces acting on the upstream face of the earth dam and their potential influence on the factor of safety is analysed. The study integrates a critical review of existing literature with numerical modelling performed using Slide2, a limit-equilibrium-based slope-stability software developed by Rocscience. Through this tool, multiple scenarios were analysed to quantify the influence of support spacing, permeability, vegetation coverage, and hydrodynamic wave action on the factor of safety and probability of failure.

The thesis is structured in five chapters. **Chapter 1** provides a structured overview of dams, with emphasis on embankment dams, introducing key components and the main hazards and failure mechanisms relevant to dam safety. **Chapter 2** examines the dual role of vegetation in reinforced-soil embankment systems, addressing both stabilizing contributions and potential adverse interactions with drainage and reinforcement elements. **Chapter 3** describes the modelling strategy and numerical methodology adopted in this research, including the reference geometry, material and hydraulic parameters, and the scenario framework implemented in Slide2. **Chapter 4** presents and interprets the numerical results, comparing the stability

response of vegetated and non-vegetated reinforced embankments under different reservoir levels, seepage conditions, and wave loading. **Chapter 5** summarises the main findings, outlines their engineering implications, and discusses limitations and directions for future work.

.

Abstract

This thesis analyses the combined mechanical and hydraulic effects of vegetation on reinforced-soil embankment dams. While vegetation is widely recognized for influencing slope stability through root reinforcement and hydrological processes such as evapotranspiration, its role in reinforced embankment dams particularly under varying reservoir levels, seepage conditions, and wave-induced loading remains insufficiently understood.

The research adopts an integrated approach combining literature review and numerical modelling. Using Slide2, a limit-equilibrium slope-stability software, a series of parametric analyses was conducted to evaluate the factor of safety and probability of failure under varying reinforcement spacing, permeability conditions, vegetation coverage assumptions, and hydrodynamic loading. The results highlight that hydraulic conditions, and especially seepage-related pore-pressure development, strongly control stability sensitivity to reservoir level and wave action. Vegetation may improve near-surface resistance through root-related mechanisms, but unfavourable interactions such as locally reduced reinforcement continuity within the root-affected zone in conservative scenarios can reduce stability margins and increase susceptibility to shallow instability.

The thesis is organised into five chapters: (1) a structured overview of dams with emphasis on embankment components, hazards, and failure mechanisms; (2) an analysis of vegetation effects in reinforced-soil embankment systems; (3) the numerical modelling procedure and scenario development in Slide2; (4) presentation and interpretation of stability results under different hydraulic and loading conditions; and (5) conclusions, engineering implications, and recommendations for future work. Overall, the findings emphasise the importance of coordinating vegetation management with reinforcement layout and seepage control to balance ecological benefits with structural safety in reinforced embankment dams under variable hydraulic conditions.

Chapter 1

Hazards on Dams

1.1 Introduction

Dams are among the most important civil-engineering structures, providing vital services such as hydro-power generation, irrigation, flood regulation, and water supply. Yet, the long-term safety of these structures remains a major engineering challenge because of the complex interactions between hydrological, geotechnical, and structural processes acting within and around the dam body (Masi et al., 2021; Olinic et al., 2024). Dams can be classified according to several criteria, including construction material, geometric configuration, and overall size. Based on construction material, the main categories include concrete dams, embankment dams (earth and rockfill), and mixed-type dams that combine different structural solutions. In terms of dimensions, dams are commonly distinguished as small, medium, or large structures, depending primarily on their height and storage capacity. A concise overview of these classification criteria and indicative ranges is provided in Table below.

Classification criterion	Order	Main classes	Typical height range (H, m)
Construction material	1	Concrete dams	~20–250
	2	Embankment dams (earth fill)	~5–100
	3	Embankment dams (rockfill)	~10–200
	4	Mixed / composite dams	~5–200
Geometric configuration	5	Gravity (concrete)	~20–200
	6	Arch (concrete)	~50–300
	7	Buttress (concrete)	~15–150
	8	Embankment (earth/rockfill)	~5–200
Overall size (by height & capacity)	9	Small	H < 15 (typical engineering usage)
	10	Medium	15 ≤ H ≤ 30 (typical)
	11	Large	H > 30 (typical)

Table 1. Dam classification by construction material, geometric configuration, and size, with indicative height ranges and commonly used size thresholds (ICOLD definition included). (ICOLD, International Commission on Large Dams)

Note: Height ranges are indicative and may vary across national regulations and project contexts; the ICOLD threshold is shown because it is widely used internationally.

Among these categories, embankment dams represent the most widespread type worldwide, owing to their adaptability to different foundation conditions and the possibility of using locally available materials. Figure 1 presents a schematic representation of a typical embankment dam, illustrating its principal components such as the impervious core, upstream and downstream shells, slopes, drainage and filter zones, and the crest, which are used as reference elements throughout this chapter.

In this thesis, the focus is on small earth embankment dams, which are the most relevant typology for the reinforced-soil and vegetation-related analyses developed in the following chapters. Accordingly, this chapter emphasizes dam components, hazards, and failure mechanisms that are directly applicable to embankment structures, while broader dam-safety topics are mentioned only insofar as they support this scope.

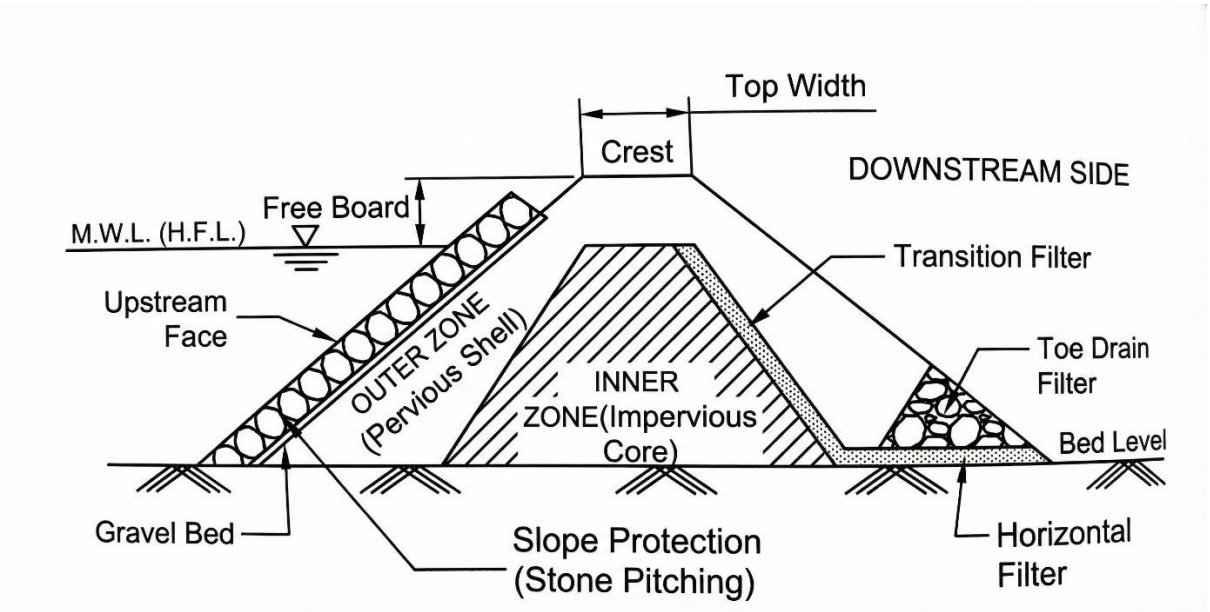

Figure 1. Schematic cross-section of a zoned embankment earth dam showing the main components (impervious core/inner zone, pervious outer shells, transition and horizontal filters, toe drain filter, crest and freeboard, and upstream slope protection). Source: Civil Practical Knowledge (n.d.) Types of dams.

Early field investigations in mountainous and forested terrain showed that slope instability and dam failures often arise from the combined influence of pore-pressure rise, seepage, and mechanical weakening of soils (Bishop & Stevens, 1964; Ziemer, 1981). In both natural slopes and engineered embankments, failure typically develops from local damage to partial failure and/or global collapse (Frydman, 2000).

Recent advances in numerical and experimental modelling have improved the understanding of how hydraulic loading and mechanical response interact. Physically based hydrological, geotechnical models now couple rainfall, infiltration, and internal stress to predict the onset of instability (Arnone et al., 2016; Cislaghi et al., 2017). Experimental erosion studies further clarify how rainfall-driven flow affects the stability of the dam faces and changes in internal water flows (Olinic et al., 2024).

Environmental and climatic variations increasingly influence dam performance. Changes in precipitation intensity, extended droughts, and temperature fluctuations modify pore-pressure regimes and material behaviour (Masi et al., 2021). Such interlinked factors make dam-hazard assessment a multidisciplinary problem that requires both probabilistic and mechanistic approaches.

1.2 Classification of Hazards Affecting Dams

Dam safety is challenged by diverse hazards that can be grouped into structural, hydraulic, geotechnical, seismic, climatic, and anthropogenic categories (Masi et al., 2021; Olinic et al., 2024). Each class contributes differently to overall risk, yet failures frequently occur through their combined action.

1.2.1 Structural hazards

Structural hazards arise from material degradation, construction-related deficiencies, and time-dependent deformations that reduce the integrity of the dam system. In embankment dams, these hazards are commonly associated with non-uniform compaction and differential settlement, which may lead to cracking and local stress concentrations. The progressive ageing or malfunction of internal filters and drains can further aggravate these conditions by promoting uncontrolled seepage concentrations and increasing susceptibility to internal erosion (Frydman, 2000). Field observations in logged terrains in Alaska also indicate that deformation and

weakening of adjacent or supporting slopes can compromise alignment and contribute to gradual deterioration of engineered earth structures (Bishop & Stevens, 1964). For these reasons, appropriate construction quality control and the preservation of drainage efficiency through maintenance are central to limiting progressive degradation in embankment dams (Masi et al., 2021).

1.2.2 Hydraulic hazards

Hydraulic hazards are among the most common causes of dam failure. Flow regimes over a dam crest can change rapidly during floods, as illustrated in Figure 2, which shows the hydraulic transition that occurs during overtopping and how it leads to erosion of the downstream slope. Overtopping, seepage, and internal erosion result from excessive inflow, inadequate spillway capacity, or poor drainage design. Laboratory rainfall-simulation experiments demonstrated that higher flow intensity rapidly accelerates surface erosion and removes protective layers (Olinic et al., 2024). Similarly, field studies showed that uncontrolled seepage generates internal channels and piping that propagate toward the downstream face (Ziemer, 1981). Once continuous flow paths form, the factor of safety decreases abruptly, often leading to breach formation (Bishop & Stevens, 1964).

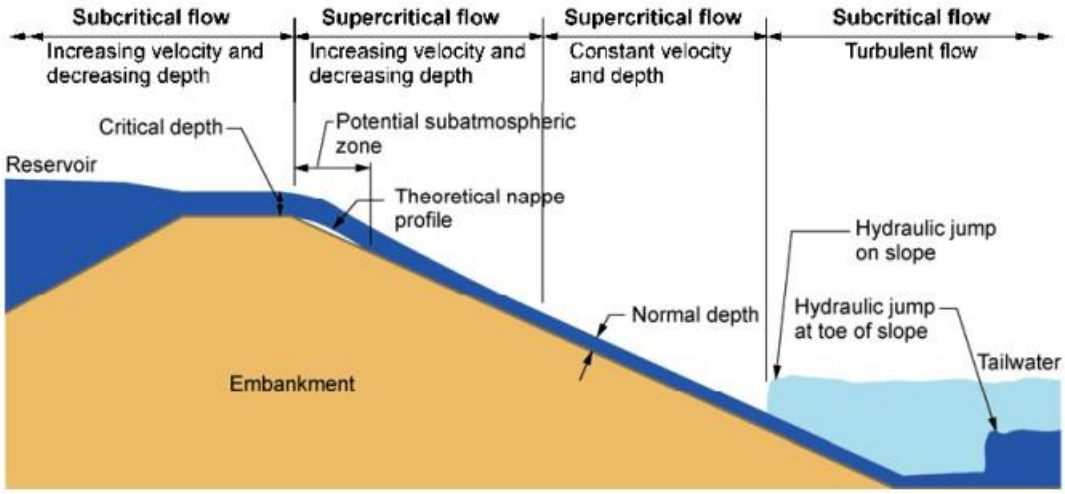

Figure 2. Typical hydraulic regimes during overtopping: transition from subcritical approach to critical depth at the crest and supercritical flow down the downstream slope (after Reclamation, FEMA P-1015, p. 8). Public domain.

1.2.3 Geotechnical hazards

Geotechnical hazards originate from the mechanical response of soils and foundations to stress changes and variations in soil water content. An increase in pore-water pressure associated with higher water content reduces effective stress, thereby decreasing shear strength and potentially leading to shear failure and settlement (Ziemer, 1981; Frydman, 2000). Probabilistic three-dimensional stability analyses have shown that small variations in cohesion or permeability may double the computed failure probability (Cislaghi et al., 2017; Arnone et al., 2016). Inadequate compaction or heterogeneous strata can create weak layers that initiate differential movement and subsequent cracking (Masi et al., 2021).

1.2.4 Seismic hazards

Earthquakes can impose extreme dynamic actions causing stress states that can exceed the design capacity of the dam. Under such conditions, pore pressure rises and shear strength declines, producing settlement or sliding in embankments (Ziemer, 1981; Frydman, 2000). Although direct dam-scale seismic tests are limited, analogous slope studies confirm that cyclic stress leads to loss of stiffness and potential liquefaction in saturated foundations.

1.2.5 Climatic and hydrological hazards

Intense or prolonged rainfall, snowmelt, and drought cycles alter hydraulic regimes and soil properties. Water infiltration resulting from rainfall and/or snow melting events increases pore pressure, while desiccation during drought produces shrinkage cracks that later act as preferential seepage paths (Masi et al., 2021). Historical field data demonstrate strong temporal correlations between rainfall events and slope movements (Bishop & Stevens, 1964).

1.2.6 Anthropogenic hazards

Human activities such as rapid reservoir drawdown, poor maintenance, or excessive loading frequently amplify natural processes. Insufficient monitoring or outdated design criteria can lead to unnoticed degradation (Frydman, 2000; Masi et al., 2021). Logging and land-use changes near dam abutments have also been observed to accelerate erosion and slope instability (Bishop & Stevens, 1964).

1.3 Risk Assessment Framework

Evaluating dam safety requires a comprehensive quantitative risk-assessment framework that links hazard, structural vulnerability, and potential consequences. Conceptually, total risk $\boldsymbol{R}$ can be expressed as:

$$\boldsymbol{R = H \times V \times E \times W}$$

where $\boldsymbol{H}$ represents the hazard, $\boldsymbol{V}$ the vulnerability of the structure, $\boldsymbol{E}$ the exposure of elements at risk and $\boldsymbol{W}$ their worth (UNISDR, 2009).

In this framework, the hazard ($\boldsymbol{H}$) describes the probability and intensity of potentially damaging events. The vulnerability ($\boldsymbol{V}$) represents the probability of the dam to suffer a certain level of damage or failure when subjected to a given hazard, depending on its design, material properties, and structural condition. The exposure ($\boldsymbol{E}$) refers to the probability of presence of elements at risk that may be affected by dam failure, including population, infrastructure, and environmental assets; ($\boldsymbol{W}$) is related to the worth of the elements at risk, usually given with indices or in monetary terms.

Dam-safety evaluation follows three complementary phases: risk assessment, risk management, and risk communication. Each phase builds upon the previous one to transform hazard data into practical management actions.

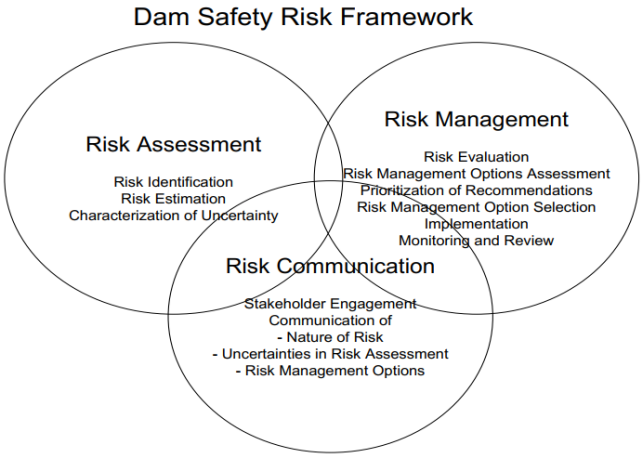

Figure 3. Dam Safety Risk Framework illustrating the interaction between risk assessment, risk management, and risk communication. Source: U.S. Army Corps of Engineers, ER 1110-2-1156, Safety of Dams – Policy and Procedures (Public Domain).

This process provides the foundation for consistent decision-making across all phases of dam operation and maintenance.

1.4 Mechanisms of Dam Failure

Dam failure usually results from a sequence of interacting mechanisms rather than a single event, including seepage and internal erosion, slope instability, overtopping, and progressive degradation of material strength (Masi et al., 2021; Olinic et al., 2024).

1.4.1 Internal erosion and piping

Seepage is the slow movement of water through the pores and voids of soil or rock under a hydraulic gradient, driven by differences in water level between the upstream and downstream sides of a dam. In embankment dams, seepage occurs primarily through the dam body, its foundation, or along interfaces between different materials, and is an inherent hydraulic process that must be controlled through appropriate zoning, filters, and drainage systems.

When seepage is not adequately controlled, the flow of water can detach and transport fine soil particles once hydraulic gradients exceed critical values, leading to internal erosion and the progressive enlargement of flow channels, commonly referred to as piping. This failure mechanism is characteristic of earth and rockfill embankment dams, where soil permeability and particle size distribution govern seepage behaviour. Field observations in Southeast Alaska documented similar piping behaviour following intense rainfall and logging disturbance (Bishop & Stevens, 1964). Laboratory evidence further confirms that increased pore-water pressure reduces effective stress and shear strength, thereby accelerating erosion processes (Frydman, 2000).

1.4.2 Overtopping and surface erosion

When reservoir inflows exceed the discharge capacity of the spillway system, water may flow over the dam crest; this phenomenon is referred to as overtopping. In embankment dams, overtopping is particularly critical because flowing water can rapidly erode downstream slope materials, leading to progressive surface degradation and, in severe cases, breach formation. Controlled rainfall and overtopping experiments have shown that erosion rates increase markedly with increasing flow depth and slope inclination (Olinic et al., 2024). During overtopping events, erosion may be further aggravated when water infiltrates cracks or preferential flow paths in near-surface layers, increasing local pore-water pressures and reducing soil strength. Once protective cover layers are compromised, erosion can accelerate, potentially exposing the impervious core and initiating uncontrolled breach development if no corrective measures are taken.

1.4.3 Slope and foundation instability

Instability of the dam body or its foundation commonly arises from elevated pore-water pressures or rapid drawdown conditions, which reduce effective stress and, consequently, shear resistance within the soil mass (Ziemer, 1981; Frydman, 2000). In embankment dams, these conditions may affect both upstream and downstream slopes as well as foundation materials, depending on drainage efficiency and the history of hydraulic loading. Probabilistic modelling of slope performance has demonstrated that even minor spatial heterogeneities in strength parameters or permeability can significantly influence the computed factor of safety and the associated failure probability (Cislaghi et al., 2017; Arnone et al., 2016). Weak strata, anisotropic layering, or differential settlement within the dam body or foundation frequently act as initiation zones for deep-seated or rotational failure mechanisms (Masi et al., 2021).

1.4.4 Seismic and cyclic loading effects

Although large earthquakes are infrequent, cyclic stress from seismic motion or repeated reservoir fluctuations can degrade soil stiffness and promote crack formation. Studies of cyclic shear behaviour in saturated soils show that transient pore-pressure rise may lead to localized

liquefaction (Ziemer, 1981). Periodic loading from water-level changes has similar cumulative effects, producing settlement and fatigue over long operational periods (Masi et al., 2021).

1.4.5 Progressive deformation and material fatigue

Even in the absence of external shocks, gradual material deterioration reduces stability. Thermal expansion and contraction, chemical reactions, and stress cycling generate micro-cracks and settlement that compromise filter performance (Frydman, 2000; Masi et al., 2021). Without consistent monitoring, these incremental deformations can evolve into large-scale structural problems.

1.5 Conceptual Framework of Dam Hazard Analysis

- ***Interacting processes***

Dams operate as coupled systems in which hydrological forcing, geotechnical response, and structural behaviour are interdependent. Rainfall infiltration alters suction and pore pressure, reducing soil strength and initiating deformation (Ziemer, 1981; Frydman, 2000). Internal strain modifies permeability, further changing the hydraulic regime, a feedback loop that can accelerate instability.

- ***Framework domains***

The dam-hazard system can be represented by three domains:

1) Hydrological: rainfall, reservoir level, and seepage conditions.
2) Geotechnical: material strength, pore pressure, and deformation.
3) Structural: stress distribution and integrity of the dam body and appurtenant works

Interactions among these domains explain why local hydraulic changes can induce mechanical failure, and why deformation affects flow paths (Bishop & Stevens, 1964; Masi et al., 2021).

- ***Modelling and validation***

Physically based models such as those proposed by Arnone et al. (2016) and Cislaghi et al. (2017) couple rainfall infiltration with mechanical response to predict stability evolution. Laboratory tests on rainfall-induced erosion (Olinic et al., 2024) and field observations in logged terrains (Bishop & Stevens, 1964) validate these conceptual linkages. Combining deterministic simulation with stochastic input parameters allows the framework to represent both expected performance and uncertainty, forming a bridge between theory and real monitoring data (Masi et al., 2021).

- ***Framework application***

Applied within risk management, the conceptual model provides a structure for interpreting monitoring results, prioritizing maintenance, and planning emergency measures. It supports continuous, adaptive safety assessment rather than periodic static evaluation (Olinic et al., 2024).

1.6 Research Gaps and Future Challenges

- ***Multi-Hazard integration***

Although numerous studies examine single mechanisms, few address simultaneous hydraulic, geotechnical, and seismic interactions. Developing fully coupled numerical models remains a research priority (Arnone et al., 2016; Cislaghi et al., 2017).

- ***Uncertainty and parameter calibration***

Probabilistic models rely on an accurate statistical representation of input data. Yet field-scale information on permeability, cohesion, and compaction variability is limited, constraining model reliability (Masi et al., 2021; Frydman, 2000).

- ***Climate and aging effects***

Climate change introduces new boundary conditions, more intense rainfall, longer droughts, and wider temperature ranges, that alter design assumptions. Many older dams were built before such extremes were anticipated (Ziemer, 1981; Olinic et al., 2024). Long-term monitoring and adaptive design criteria are needed to address aging materials and changing hydrology.

- ***Data integration and digitalization***

While sensor technology has advanced, integration into predictive models and decision-support systems is uneven. Future work should focus on standardized digital twins and data-fusion platforms linking measurements, models, and management actions (Masi et al., 2021).

- ***Governance and risk communication***

Technical progress must be matched by institutional capacity. Effective dam safety requires transparent communication between engineers, authorities, and communities, ensuring that monitoring results translate into timely preventive action (Olinic et al., 2024).

Chapter 2

Effect of Vegetation on Reinforced Soil Dams

2.1 Introduction

As discussed in Chapter 1, embankment dams constitute one of the most widespread dam typologies worldwide, owing to their adaptability to diverse foundation conditions and the extensive use of compacted soil materials. Within this category, reinforced soil dams represent a specific class of embankment structures in which artificial inclusions such as geosynthetics, geogrids, or other reinforcing elements are incorporated to enhance shear resistance and overall slope stability. Vegetation plays a dual and highly complex role in the stability of reinforced soil dams.

Plant roots can substantially enhance soil mechanical and hydraulic properties, thereby contributing to the long-term integrity of dam slopes. The reinforcing action of roots is primarily achieved through mechanical interlocking and tensile resistance, which increase the apparent cohesion of the soil and may modify its shear strength parameters (Giadrossich et al., 2017; Li et al., 2022). Numerous laboratory and field studies have confirmed that well-developed root systems can improve the shear strength of near-surface soils and delay the onset of shallow slope failures (Leung et al., 2015; Löbmann et al., 2020). At the same time, vegetation exerts significant hydrological influences by regulating infiltration, evapotranspiration, and pore-water pressure distribution within the dam body (Masi et al., 2021; Wang et al., 2023). These combined mechanical and hydraulic effects have led to the increasing adoption of vegetation as a component of modern bioengineering strategies for slope protection and erosion control (Cazzuffi et al., 2014; Olinic et al., 2024).

In the specific case of reinforced soil dams, vegetation interacts not only with the natural soil matrix but also with artificial reinforcing layers. When appropriately designed, the integration of vegetation with reinforcement systems may produce synergistic benefits, combining the adaptability of biological systems with the strength and reliability of engineered materials (Powrie & Smethurst, 2018; Olinic et al., 2024). Vegetation can mitigate surface erosion through canopy interception, while root networks contribute to anchoring shallow soil layers and improving soil-reinforcement interaction. This combined action enhances resistance to rainfall-induced shallow sliding, surface scouring, and hydraulic erosion.

However, the same interaction that promotes stability may also introduce adverse effects if vegetation is not properly selected or controlled. Roots penetrating reinforcement zones or drainage layers can disturb their integrity, create preferential seepage paths, or induce localized stress concentrations. Furthermore, seasonal vegetation cycles involving growth, decay, and desiccation can cause variations in soil suction and moisture conditions, potentially leading to differential settlements or surface fissuring (Deng et al., 2020). These processes can gradually weaken near-surface zones of the dam, highlighting the necessity for integrated ecological-geotechnical design approaches that explicitly consider root-infrastructure interactions.

Recent advances in experimental testing and numerical modelling have enabled a more realistic quantification of these processes. Direct shear, triaxial, and pull-out tests on rooted soils, together with hydro-mechanical modelling of root reinforcement, now provide improved insight into both the stabilizing and potentially detrimental effects of vegetation on reinforced

soil structures (Bordoloi & Ng, 2020; Giadrossich et al., 2017; Olinic et al., 2024). These approaches support the development of reinforced soil dams that effectively exploit the beneficial functions of vegetation while avoiding configurations that may compromise long-term structural safety.

The objective of this chapter is therefore to provide a critical review and analytical synthesis of the mechanisms through which vegetation influences the behaviour of reinforced soil dams. The chapter first examines mechanical reinforcement mechanisms associated with root-soil interaction, followed by the hydrological influence of vegetation on moisture dynamics and pore-water pressure. It then addresses the combined performance of vegetation and geosynthetic systems, outlines experimental and numerical approaches used to assess these interactions, and concludes with a discussion of environmental and climatic factors governing the long-term efficiency of bio-reinforced dam structures.

2.2 Vegetation and Soil-Structure Interaction

The interaction between vegetation and the soil matrix in reinforced embankments or dams is governed by both mechanical and biological processes that evolve over time. Plant roots act as natural reinforcements, transmitting tensile forces to the surrounding soil, bridging potential failure planes, and modifying the stress-strain response of the soil-structure system. This contribution is particularly significant in the upper one to two metres of the dam shell, where root density is typically highest and where hydrological fluctuations are most pronounced (Löbmann et al., 2020; Giadrossich et al., 2017).

In Figure 4, a cross section of how vegetation, reinforcement, and drainage are practically integrated in a earth dam, is reported.

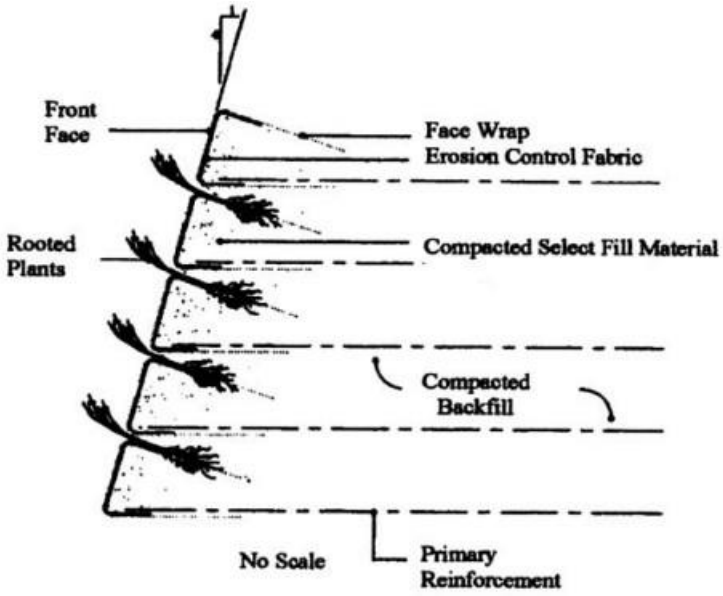

Figure 4. Vegetated reinforced slope (VRSS) showing geosynthetic layers, live cuttings, and drainage. Source: FHWA, NHI-10-025 Vol. II Fig. 8-6, p. 8-17. Public Domain.

2.2.1 Mechanical reinforcement mechanisms

Root systems enhance the mechanical stability of soils primarily by increasing apparent cohesion and, to a lesser degree, by modifying the internal friction angle. When external shear stress is applied, the roots act as fibrous inclusions that resist deformation through tensile strength and anchorage effects. As observed in numerous laboratory tests, such as tensile and shear-box experiments, the peak shear strength of rooted soil can exceed that of bare soil by

20-300 %, depending on the plant species, root diameter, and water content (Giadrossich et al., 2017; Li et al., 2022).

Mechanically, the reinforcement process can be described by an adaptation of the Mohr-Coulomb criterion, in which a root-induced cohesion term (c_a) is added to the classical shear strength equation. This term represents the tensile contribution of roots crossing the failure plane and their interaction with the surrounding soil matrix. Experimental studies have shown that the tensile strength of individual roots may range between 5 and 80 MPa, values comparable to those of mild steel on a per-area basis (Leung et al., 2015). However, the effective reinforcement perceived at the macro-scale depends on root density, spatial orientation, and bonding at the root-soil interface (Bordoloi & Ng, 2020).

2.2.2 Influence of root geometry and distribution

The geometry, orientation, and depth of root systems vary greatly across plant species and significantly influence their stabilising potential. Deep, vertically oriented taproots typically improve basal shear resistance, while lateral and fibrous root systems are more effective in confining surface soils and mitigating shallow slips (Frydman & Olinic, 2000; Löbmann et al., 2020). Quantitative analyses indicate that root density often decreases exponentially with depth, meaning that reinforcement is strongest in the near-surface layers, precisely the zones most exposed to rainfall infiltration and erosion.

Root distribution anisotropy can also influence the shape and size of potential failure zones. When roots are preferentially aligned in the downslope direction, they contribute to tensile restraint; conversely, horizontally oriented networks promote shear transfer along bedding planes. Laboratory direct shear tests by Leung et al. (2015) and Giadrossich et al. (2017) demonstrated that the presence of crossed or mixed-orientation root networks increases overall shear strength more effectively than uniform arrangements.

Species selection, therefore, plays a pivotal role in bio-reinforcement. Gramineae species, with their dense fibrous systems, provide strong superficial anchorage, while Leguminous plants, although offering less root density, enhance soil cohesion through both mechanical and biological mechanisms, such as organic bonding (Olinic et al., 2024). This diversity allows vegetation to be adapted to the functional requirements of different dam zones for instance, fibrous species on the upstream face to resist surface erosion, and deep-rooted species on the downstream shoulder to counteract slope instability.

2.2.3 Integration with reinforced dam structures

In reinforced soil dams, the presence of vegetation modifies the stress distribution within the shell by interacting with geosynthetic or granular reinforcement elements. Experimental and numerical investigations have shown that root reinforcement synergy enhances the composite strength of the upper dam layers, particularly under variable moisture conditions (Cazzuffi et al., 2014; Olinic et al., 2024). Roots can interlock with geogrid apertures and other surface geosynthetics (e.g., erosion-control mats), improving frictional resistance and reducing the likelihood of surface slippage. This synergy is most effective during the vegetation establishment phase, after which the mechanical contribution of roots becomes dominant.

However, as later discussed in Section 2.5.1, this beneficial interaction can turn adverse if root penetration compromises the continuity of reinforcing layers or alters drainage paths. Therefore, the design of vegetated reinforced dams requires a balance between biological adaptability and structural reliability, ensuring that the depth and spread of root systems remain compatible with the dam's engineered reinforcement architecture.

2.3 Hydrological Influence of Vegetation

Vegetation influences not only the mechanical strength of soils but also their hydraulic behaviour, a factor of equal importance in the stability of reinforced soil dams. The interaction between roots, soil moisture, and pore-water pressure controls the way infiltration, evapotranspiration, and suction evolve within the dam shell, especially in the unsaturated zone. Numerous studies have shown that changes in suction and hydraulic conductivity can significantly affect the factor of safety of vegetated slopes (Löbmann et al., 2020; Wang et al., 2023).

To anchor the discussion with an authoritative hydraulics-focused government figure, see Figure 5, which shows how roots remove soil moisture and enhance near-surface drainage.

Figure 5. Roots extract soil moisture and enhance near-surface drainage. Source: USDA-NRCS, EFH Part 650 Ch. 18 Fig. 18-23 (p. ~18-37). Public Domain

2.3.1 Control of infiltration and pore pressure

Roots act as preferential flow paths during rainfall events and as water-extracting conduits during dry periods. Their presence alters both the infiltration rate and the distribution of pore pressures. Under moderate rainfall, fine roots enhance infiltration near the surface, reducing surface runoff and delaying saturation of deeper layers. However, under prolonged or intense rainfall, the same pathways can facilitate deeper percolation, potentially increasing pore pressure in the lower parts of the dam (Leung et al., 2018; Masi et al., 2021). The overall effect depends on soil type, root density, and rainfall intensity. In reinforced shells composed of granular fill, this interaction can either improve or impair drainage performance depending on how the root network intersects the geosynthetic layers (Olinic et al., 2024).

2.3.2 Root suction and evapotranspiration

One of the most stabilising hydrological effects of vegetation is the development of matric suction due to root water uptake. Transpiration reduces pore-water pressure, increasing the effective stress and thus the shear strength of the near-surface soil. This "root suction" can temporarily compensate for the absence of mechanical reinforcement in the upper dam zones during dry periods. Experimental and numerical models (Wang et al., 2023) indicate that suction may raise the factor of safety by up to 15 % in vegetated slopes. Nevertheless, this effect diminishes rapidly once soil moisture rises, for example after heavy rainfall or during seasonal saturation cycles. Therefore, while evapotranspiration provides valuable short-term stability, its contribution is transient and must not be overestimated in design.

2.3.3 Seasonal and climatic variability

Vegetation-induced hydrological effects are highly dependent on climate and season. During wet seasons, rapid infiltration through root channels can neutralise suction and lead to temporary instability. In contrast, during drought, extended drying and root shrinkage may cause desiccation cracks, which in turn become preferential infiltration routes once rainfall resumes (Deng et al., 2020). Climate-change projections suggest that increased frequency of extreme precipitation and longer dry periods could intensify this cyclical behaviour, amplifying both stabilising and destabilising phases. Such temporal variability must be incorporated into numerical simulations and monitoring programmes for reinforced dams, particularly in semi-arid or continental climates where suction fluctuations are pronounced.

2.3.4 Implications for reinforced soil dams

In reinforced soil dams, where engineered drainage and reinforcement systems coexist with vegetation, hydraulic interactions become critical. Root penetration can locally modify permeability and create zones of differential saturation around geosynthetic inclusions. Controlled vegetation can therefore enhance surface drainage and prevent erosion, while uncontrolled growth may compromise subsurface hydraulic uniformity. The design of vegetated reinforcements must balance the beneficial moisture extraction effects against the risk of preferential flow or clogging within drainage layers. Long-term stability depends on maintaining this equilibrium through proper species selection and maintenance.

2.4 Combined Vegetation-Geosynthetic Systems in Reinforced Dams

In modern dam engineering, vegetation is increasingly combined with synthetic reinforcement materials to form bio-geotechnical systems capable of delivering both structural and ecological functions. Such systems, often referred to as bio-geosynthetic or eco-reinforced structures, merge the tensile strength and durability of geosynthetics with the self-healing and hydrological regulation provided by plant root systems (Cazzuffi et al., 2014; Olinic et al., 2024). When designed correctly, this synergy can significantly improve the stability, erosion

resistance, and environmental performance of reinforced soil dams. Guidance on vegetation-based soil stabilisation and surface erosion control is consistent with the technical standards published by the Natural Resources Conservation Service, a federal agency of the United States Department of Agriculture, whose engineering manuals provide authoritative design recommendations for vegetated earth structures. To frame the dual role of vegetation in these hybrid systems, Figure 6 (USDA-NRCS) summarises reinforcement and erosion-control functions in a single conceptual representation.

Figure 6. Functional roles of vegetation in slope systems: reinforcement via roots and reduction of surface erosion. Source: USDA-NRCS, EFH Part 650, Chapter 18, Fig. 18-1. Public Domain (U.S. Government).

2.4.1 Concept and mechanism of hybrid reinforcement

Geosynthetics such as geogrids, geomaterials, and coir or jute meshes provide a continuous mechanical skeleton that confines soil deformation and distributes loads within the dam shell. Vegetation established on these surfaces adds a natural reinforcement layer over time as roots penetrate the upper fill and interlock with the geosynthetic apertures. Laboratory and pilot-scale tests have shown that root geogrid interlocking increases interface shear resistance and friction angle compared with bare geogrid soil systems (Powrie & Smethurst, 2018; Leung et al., 2015). The hybrid interface behaves as a composite shear zone in which the load transfer occurs through both tensile forces in the roots and frictional engagement with the synthetic fibres.

This dual mechanism enhances performance under variable moisture conditions. During wet periods, geosynthetics maintain mechanical stability when root strength decreases; during dry seasons, roots improve cohesion and limit desiccation cracking. The result is a dynamic, self-adjusting system that complements the limitations of each component.

2.4.2 Surface erosion control and vegetation establishment

Vegetated geomaterials and coir meshes are widely applied on the upstream faces and downstream slopes of embankments to reduce surface erosion. The synthetic matrix protects newly seeded vegetation from rainfall impact and runoff until roots are sufficiently developed to take over reinforcement duties (Cazzuffi et al., 2014). Studies on vegetated geocells have also demonstrated improved resistance against hydraulic shear and shallow slides under cyclic wetting-drying conditions. Once vegetation matures, the system transitions from an engineered barrier to a bio-stabilised surface, effectively extending the service life of the reinforcement layer. To show an applied hybrid solution, Figure 7. presents an NRCS case with geocell-reinforced fill and a vegetated finish at the slope toe.

Figure 7. Bio-geosynthetic slope: geocell-reinforced fill with vegetated surface. Source: USDA-NRCS, NEH Part 654 TS14A Fig. TS14A-13 (pp. 13-14). Public Domain.

2.4.3 Design and sustainability considerations

The design of bio-geosynthetic systems requires balancing mechanical performance, hydraulic behaviour, and biological compatibility. Material selection must account for the expected vegetation type, root strength, and environmental exposure. Synthetic polymers provide long-term tensile capacity but may limit root penetration if apertures are too small, whereas biodegradable natural fibres such as jute or coir encourage root growth but gradually lose strength as decomposition progresses (Olinic et al., 2024). A layered configuration combining a durable geogrid for internal strength and a degradable mat for initial vegetation support is often the most effective solution.

From a sustainability perspective, vegetated reinforcement systems also reduce the visual and ecological impact of dams, promote biodiversity on slopes, and can contribute to carbon

sequestration. Nevertheless, their long-term efficiency depends on periodic inspection and maintenance to prevent root overgrowth, clogging of drainage layers, and damage to exposed geosynthetics.

2.4.4 Limitations and research outlook

Although numerous field applications have demonstrated the potential of hybrid systems, comprehensive design guidelines are still limited. Long-term monitoring data on the interaction between mature (uncontrolled) vegetation and synthetic materials remain scarce, particularly regarding creep behaviour, biodegradation, and the evolution of interface shear strength under cyclic loading. Further research integrating numerical modelling with full-scale experiments is needed to quantify these effects and to optimise the layout of bio-reinforced dam structures for different climates and soil types.

2.5 Experimental and Modelling Approaches

Understanding the interaction between vegetation, soil, and reinforcement materials requires both experimental investigations and numerical modelling. These approaches provide quantitative insight into how roots modify the mechanical and hydraulic response of reinforced soil dams. Laboratory tests capture the small-scale behaviour of root soil composites, while computational models allow extrapolation to full-scale structures under varying environmental conditions.

Because vegetation establishment and reinforcement installation are staged, Figure 8 from the Federal Highway Administration (FHWA) is a useful reference for defining timing assumptions and boundary conditions in the numerical models.

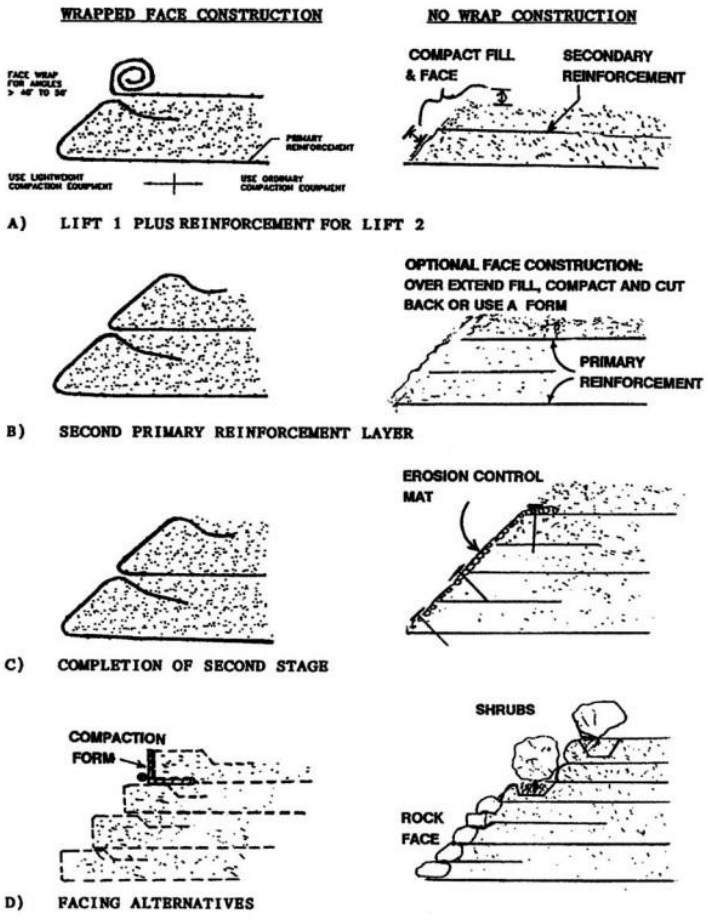

Figure 8. Construction sequence for reinforced slopes and vegetation timing. Source: FHWA, NHI-10-025 Vol. II Fig. 8-4, p. 8-12. Public Domain

2.5.1 Laboratory and field-testing techniques

Experimental work on vegetated soils has evolved substantially over the past decades. Tensile, shear, and pull-out tests are commonly used to quantify the contribution of roots to shear strength. Direct shear tests compare the stress-strain behaviour of rooted and non-rooted samples, while triaxial and unconfined compression tests evaluate the apparent cohesion and ductility induced by vegetation (Giadrossich et al., 2017; Bordoloi & Ng, 2020). Root tensile tests provide information on the maximum load-bearing capacity of individual roots, which often ranges between 5 and 80 MPa depending on species and moisture content (Leung et al., 2015).

Field investigations complement laboratory studies by capturing the natural variability of soil and vegetation conditions. Plate load tests and in situ shear-box tests on vegetated slopes have shown that the inclusion of roots can increase the shear resistance of surface layers by more than twofold compared with bare soils (Frydman & Olinic, 2000). Instrumented embankments monitored over several seasons also demonstrate the progressive improvement of stability as vegetation establishes and root density increases.

Study	Test type	Vegetation / root system	Root tensile strength (MPa)	Increase in apparent cohesion (%)	Remarks / Notes
Giadrossich et al. (2017)	Direct shear and triaxial	Mixed grass species (fibrous roots)	Oct-35	100-250	Laboratory tests on sandy-silt soils; higher cohesion under moist conditions.
Leung et al. (2015)	Pull-out and tensile tests	Vetiver grass (deep, stiff roots)	30-80	120-300	Demonstrated strong tensile resistance and enhanced interface friction.
Bordoloi & Ng (2020)	Direct shear and root soil pull-out	Shrubs and turf grasses	25-Aug	80-180	Quantified apparent cohesion and ductility; effects of water content analysed.
Frydman & Olinic (2000)	Field plate-load and in situ shear-box	Natural vegetation on slopes	20-May	50-100	Field data confirm that vegetation doubles surface shear resistance.

Table 2. Summary of laboratory and field studies on vegetated reinforced soils. Data synthesised from Giadrossich et al. (2017); Bordoloi & Ng (2020); Frydman & Olinic (2000); Leung et al. (2015).

2.5.2 Numerical and analytical modelling

Physically based models are essential to interpret and generalise experimental observations. Analytical frameworks derived from the Mohr Coulomb criterion incorporate a root-induced apparent cohesion term (c_a) to estimate the overall shear strength of vegetated soil. More advanced numerical tools, such as finite-element or limit-equilibrium models, allow coupling between mechanical and hydrological processes.

Recent developments include three-dimensional probabilistic approaches (Cislaghi et al., 2017), which simulate the spatial variability of root reinforcement using Monte Carlo techniques. These models calculate the factor of safety as a function of root cohesion, root geometry, and soil saturation, enabling probabilistic assessment of slope failure risk. Other models, such as MD-STAB and PLAXIS-based frameworks, incorporate both lateral and basal root reinforcement, providing realistic representations of shallow slide mechanisms under transient rainfall (Leung et al., 2018; Wang et al., 2023).

In the context of reinforced soil dams, numerical simulations are used to assess how root systems interact with geosynthetic inclusions. Finite-element analyses (Olinic et al., 2024) demonstrate that the combined presence of vegetation and reinforcement can improve the safety factor by up to 25 % compared with either component alone. However, these models also indicate that local stress concentrations may develop near the reinforcement interface if roots penetrate or disturb the geosynthetic layers.

2.5.3 Potential adverse effects of root penetration

While vegetation is frequently introduced for erosion control and near-surface reinforcement, its interaction with engineered inclusions can also create unfavourable conditions in reinforced-soil embankment dams, particularly when roots extend into drainage or reinforcement zones. Root systems may alter local hydraulic and mechanical conditions by (i) opening preferential flow paths along interfaces, (ii) obstructing or intruding into drainage elements, and (iii) disrupting the continuity of geosynthetic layers that contribute to stability.

Evidence from field exhumations of geosynthetic systems shows that roots can reach and occupy drainage components. For example, in a monitored composite cover, roots were found within the geonet component of a geosynthetic drainage composite drain, together with a light coating of fines, although severe clogging was not observed (Benson et al., 2010). Even where hydraulic capacity remains acceptable in the short term, the presence of roots within geosynthetic drainage pathways confirms the potential for bio-intrusion into engineered layers whenever moist, oxygenated conditions are available. Complementary experimental work on levee drainage systems indicates that geosynthetics such as geotextiles and geosynthetic drainage composites may be insufficient as root-exclusion measures, as neither type was able to prevent root encroachment into drainage areas under bench-top testing (Ito, 2010). These findings are directly relevant to reinforced embankment dams, where internal drains, filters, and reinforcement interfaces must remain functional throughout the service life.

Where barrier elements (e.g., geomembranes for waterproofing or seepage control) are present within an embankment system, root and rhizome penetration can represent an additional long-term concern. Controlled tests on waterproofing membranes showed that rhizomes (rather than fine roots) were responsible for puncturing some polymeric membranes, with penetration more likely in softer or thinner products (Tanaka et al., 2008). For dam applications, this supports the practical recommendation that any lining/support structure intended to preserve barrier integrity should be protected from biological intrusion and kept free of vegetation at the interface (CFG, 2017), especially in zones where loss of watertightness could modify seepage and pore-pressure distributions.

2.5.4 Integration of experiments and models

Combining experimental and modelling approaches provides a robust basis for design. Laboratory testing supplies empirical parameters such as tensile strength, root cohesion, and suction characteristics while numerical models translate these into system-level predictions. This integration enables engineers to optimise the location, density, and allowable depth of vegetation, ensuring that biological reinforcement enhances rather than compromises structural safety. The synergy between experimental validation and computational modelling is therefore fundamental to the future development of reliable, sustainable, and environmentally compatible reinforced soil dam designs.

2.6 Environmental and Climatic Considerations

The long-term performance of vegetation on reinforced soil dams is strongly influenced by environmental and climatic conditions. Temperature fluctuations, precipitation patterns, and seasonal variations in moisture availability all affect the growth, strength, and hydraulic function of root systems. Because vegetation acts as a living component within an engineered structure, its reinforcing capacity is dynamic rather than constant. Understanding how environmental factors alter the biological and mechanical response of vegetated reinforcements is therefore essential for reliable dam design and maintenance.

To keep the focus on structural safety checks that remain mandatory regardless of vegetation, Figure 9. summarises the standard reinforced-slope failure modes per FHWA.

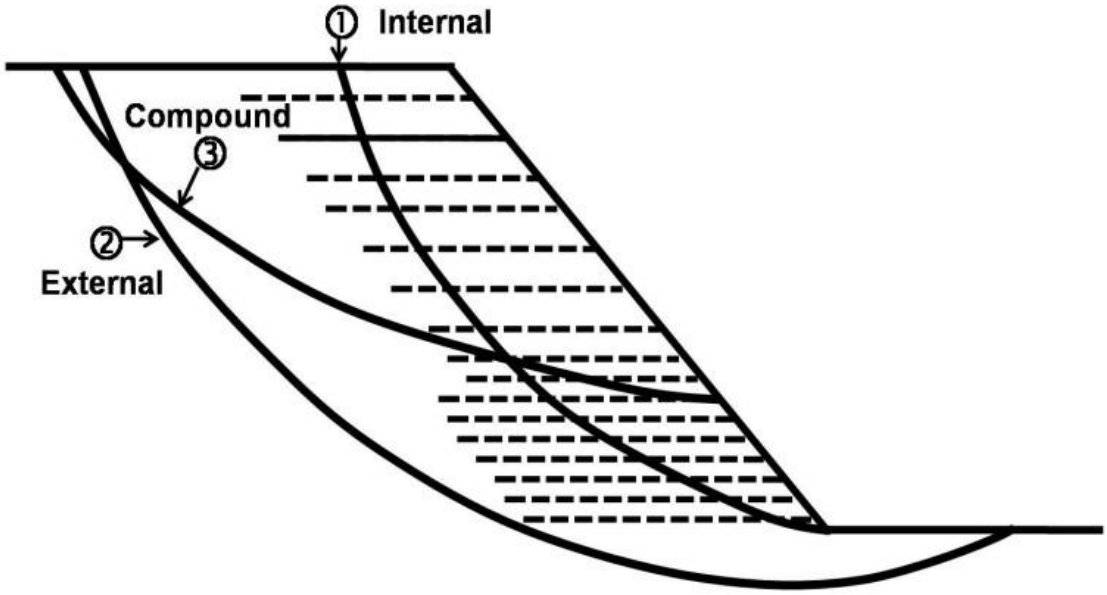

Figure 9. Failure modes in vegetated reinforced slopes. Source: FHWA, NHI-10-025 Vol. II Fig. 8-1 (pp. 8-3-8-4). Public Domain.

2.6.1 Temperature and moisture variations

Temperature and soil moisture regulate root activity and tensile strength. Under moderate temperatures and adequate moisture, roots maintain elasticity and bonding with the surrounding soil, sustaining the apparent cohesion that supports stability (Löbmann et al., 2020). However, during extended dry periods, water stress causes desiccation and shrinkage, leading to partial loss of root-soil contact. This reduces shear strength and may induce the formation of desiccation cracks that later serve as preferential infiltration paths once rainfall resumes (Deng et al., 2020). Conversely, in cold or saturated conditions, oxygen deficiency and frost heave can damage fine roots, weakening their mechanical function. These cycles of dehydration and rehydration contribute to temporal variability in the stabilising effects of vegetation.

2.6.2 Seasonal root growth and decay

Vegetation follows a biological cycle of growth, dormancy, and decay. During active growth phases, new fine roots expand the reinforced zone and enhance the ductility of the soil mass. Over time, however, older roots decay, particularly in the absence of aeration or under prolonged saturation. Research by Ziemer (1981) and Wu (1976) demonstrated that, following vegetation removal or dieback, the tensile contribution of roots may decline by more than 50 % within a few years, substantially lowering slope safety factors. In dam structures, similar effects can occur naturally as vegetation matures and renews. Maintaining long-term reinforcement therefore requires continuous vegetation management to ensure that new root systems replace decaying ones at a sufficient rate to preserve mechanical continuity.

2.6.3 Influence of extreme weather and climate change

The increasing frequency of extreme climatic events presents additional challenges. Intense rainfall can rapidly neutralise root-induced suction and generate transient pore pressure peaks within the dam shell, while prolonged drought may desiccate soils and trigger surface cracking. Modelling studies (Wang et al., 2023; Masi et al., 2021) have shown that both effects can reduce the factor of safety by up to 20 % compared with average climatic conditions. Climate change projections suggest that these alternating wet-dry cycles will intensify, making it essential to incorporate temporal variability into the design and analysis of vegetated reinforcements. Adaptive strategies such as mixed-species planting, drought-resistant

vegetation, and flexible maintenance schedules are increasingly recommended for dams located in climates with pronounced seasonal contrasts.

2.6.4 Implications for maintenance and design

Environmental and climatic factors highlight the need for an integrated management approach. Regular monitoring of vegetation health, root depth, and moisture regimes can prevent the decline of reinforcement capacity. Irrigation or drainage control may be necessary during extreme dry or wet periods to preserve optimal root function. Selection of species suited to local climatic conditions ensures that vegetation continues to perform as an effective natural reinforcement without excessive maintenance requirements. In the long term, integrating climate-responsive vegetation management into dam operation protocols enhances resilience, extends service life, and aligns structural safety with environmental sustainability goals.

2.7 Implications for Dam Engineering Practice

The integration of vegetation into reinforced soil dam design represents both an opportunity and a challenge for geotechnical engineers. When properly managed, vegetation contributes to the long-term stability, erosion control, and environmental compatibility of dam structures. However, if not adequately planned or maintained, it can compromise the integrity of reinforcement layers and drainage systems. Translating the findings from experimental and modelling research into practical engineering applications therefore requires a systematic design and maintenance framework.

To standardise detailing for the vegetated face and drainage continuity, Figure 10. provides a USDA-NRCS joint-planting geometry that aligns with reinforced slope practice.

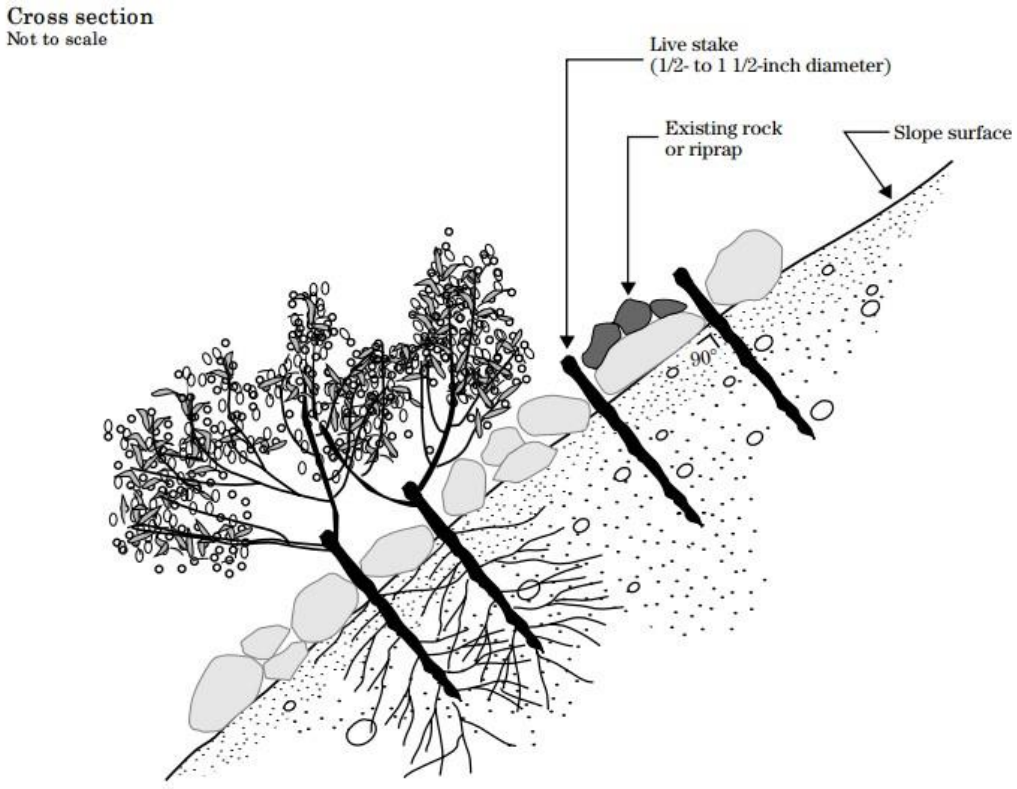

Figure 10. Joint planting geometry for slope face reinforcement and drainage. Source: USDA-NRCS, EFH Part 650 Ch. 18 Fig. 18-24. Public Domain.

2.7.1 Design integration

The design of vegetated reinforced dams should begin with a clear definition of functional zones areas intended for mechanical reinforcement, hydraulic control, and ecological stabilisation. Each zone demands specific vegetation characteristics. For instance, shallow-rooted herbaceous species may be suited for the upstream face to minimise hydraulic erosion, while deeper-rooted shrubs or grasses can stabilise the downstream shell (Olinic et al., 2024; Cazzuffi et al., 2014).

Root penetration depth must be coordinated with the location of geosynthetic inclusions and drainage layers to avoid damage or clogging. Numerical analyses show that the factor of safety decreases when roots disturb reinforcement continuity; therefore, proper separation distances between biological and synthetic elements are essential. Using geotextile barriers or transition layers can control root penetration without impeding water drainage.

Vegetation also affects the hydrological performance of dams. Engineers must account for seasonal suction changes and evapotranspiration when evaluating slope stability under unsaturated conditions. Coupled hydro-mechanical models that include vegetation parameters are now recommended as standard tools for design verification.

2.7.2 Construction and establishment

The construction phase is critical for ensuring successful vegetation establishment. Surfaces intended for bio-reinforcement must provide sufficient soil cover and nutrient availability to support root growth. Temporary protective layers such as biodegradable erosion-control blankets or coir mats can prevent erosion during the initial vegetation phase, gradually transferring reinforcement duties to roots as they mature (Powrie & Smethurst, 2018). Seeding or planting should be scheduled in accordance with local climatic conditions to maximise survival rates and root penetration before extreme weather events.

2.7.3 Monitoring and maintenance

Because vegetation is a living component, its behaviour and effectiveness evolve over time. Regular monitoring of vegetation coverage, root depth, and overall slope condition is necessary to detect early signs of deterioration. Remote sensing, ground-penetrating radar, and fibre-optic monitoring can provide non-destructive assessment of vegetated slopes. Maintenance activities include controlled trimming, reseeding of bare zones, and removal of invasive species whose root systems might compromise reinforcement or drainage layers (Ziemer, 1981). A well-defined maintenance schedule ensures that the stabilising effects of vegetation remain consistent throughout the dam's service life.

2.7.4 Sustainability and policy considerations

The adoption of vegetated reinforcements aligns with global trends toward sustainable and nature-based engineering solutions. Beyond mechanical stability, such systems contribute to biodiversity enhancement, improved aesthetics, and reduced carbon footprint compared with conventional concrete facings. However, the implementation of vegetation-based strategies requires clear regulatory guidance and interdisciplinary collaboration among civil engineers, hydrologists, and ecologists. Establishing standards for vegetation type selection, allowable root depth, and inspection frequency can bridge the gap between environmental objectives and safety requirements. Integrating these principles into dam design codes and maintenance manuals would ensure that vegetation contributes positively to both structural performance and environmental sustainability.

Chapter 3

Modelling Strategy and LEM Analysis

3.1 Modelling Procedure and Scenario Definition

3.1.1 Overview of "Slide2" software

The stability analyses presented in this thesis were performed using Slide2 software, a two-dimensional slope-stability program developed by Rocscience, and its modelling workflow and analysis options are described in the official Slide2 user documentation (Rocscience Inc., 2022). Slide2 is a limit equilibrium method (LEM) based tool for evaluating the factor of safety and, when probabilistic inputs are defined, the probability of failure, for both circular and non-circular slip surfaces in soil or rock slopes (Rocscience Inc., 2022).

Slide2 evaluates potential failure mechanisms using limit equilibrium formulations based on both vertical-slice and non-vertical-slice approaches. It provides several analysis options, including widely used methods such as Bishop, Janbu, Spencer, and Sarma, and includes automated search procedures to locate the critical slip surface for both circular and non-circular failure mechanisms (Rocscience Inc., 2022).

A key capability of Slide2 is the modelling of groundwater and pore pressure conditions using different approaches, including finite element seepage analysis for steady state and transient conditions. These pore pressure distributions can then be incorporated directly into the LEM stability calculations. In addition, Slide2 provides probabilistic analysis tools in which input parameters can be treated as random variables, allowing computation of a probability of failure and associated measures (e.g., reliability index), together with sensitivity analysis (Rocscience Inc., 2022).

In this research, Slide2 was used to perform a systematic set of two-dimensional limit-equilibrium analyses for reinforced embankment dam configurations under different hydraulic and loading scenarios. For consistency across all simulations, stability was evaluated using three analysis methods available in Slide2: Janbu's Simplified, Janbu's Corrected, and Bishop's Simplified (Rocscience Inc., 2022).

3.1.2 Numerical model overview

All simulations were performed in Slide2 as two-dimensional limit-equilibrium analyses. For each scenario, the critical slip surface was identified using the automated search procedure, and stability was quantified in terms of the factor of safety using Bishop's Simplified and Janbu's methods. Pore-water pressures were defined using two alternative groundwater representations, depending on the scenario. In the impermeable cases, hydraulic conditions were prescribed using the Water Surfaces method, which defines the phreatic level without modelling seepage through the embankment. In the seepage cases, pore-water pressures were obtained from a coupled finite-element groundwater analysis (steady-state seepage), in which the finite-element mesh and hydraulic boundary conditions were defined within Slide2, and the computed pore-pressure field was subsequently transferred to the slope-stability calculations. A parametric approach was adopted. Starting from a single reference geometry, the influence of reservoir level, seepage condition, reinforcement spacing, vegetation assumptions, and wave loading was examined by varying one factor at a time while keeping the remaining inputs unchanged. Vegetation was incorporated as a modelling assumption applied consistently across the scenario set. In vegetated configurations, vegetation was assumed to extend over the dam

surface from the crest to the downstream face, and root influence was represented by a near-surface root-affected zone with an average penetration depth of 1.0 m. To explore a conservative root-intrusion condition for reinforced embankments, an additional configuration was defined in which geosynthetic reinforcement was omitted within the root-affected zone. This assumption does not imply that reinforcement would be fully absent in practice; rather, it represents a bounding case in which root growth and associated disturbance may reduce the continuity or effectiveness of engineered inclusions and interfaces. The baseline (reinforced) and root-affected configurations were otherwise analysed using the same geometry, material properties, groundwater representation, and loading assumptions so that differences in stability response could be attributed to the near-surface discontinuity in reinforcement. This conservative idealisation is consistent with published observations that roots can intrude into geosynthetic drainage layers (Benson et al., 2010) and that common geosynthetic components may not function as reliable root barriers (Ito, 2010). Accordingly, vegetation on reinforced embankment dams should be managed through appropriate zoning, species selection, and detailing of reinforcement and drainage layouts so that the beneficial effects of vegetation are retained while limiting the likelihood of root intrusion into critical engineered layers (CFG, 2017).

3.1.3 Scenario development and input parameters

A parametric approach was adopted to evaluate how reservoir level, seepage condition, reinforcement spacing, vegetation assumptions, and wave loading affect embankment stability, while keeping the reference geometry constant. All scenarios were defined using the same geometric and material properties, and each parameter was varied independently to isolate its effect on the computed stability response.

3.1.4 Rationale for the selected embankment configuration

The numerical study adopts a simplified zoned embankment-dam geometry representative of small-to-medium earth structures frequently used in mountainous and alpine regions, where valleys constrain the footprint and locally available soils/rock materials make embankment solutions practical. The trapezoidal cross-section provides a standard and widely applicable baseline that allows systematic comparison of hydraulic conditions (water level and seepage), internal reinforcement layouts, and vegetation-related assumptions without introducing geometry-driven bias. This choice supports the main objective of the thesis: assessing how hydraulic loading and bio-mechanical effects influence the stability of reinforced embankment slopes.

3.1.5 General dam parameters

The modelled embankment dam was defined with a trapezoidal cross-section having a total height of 11 m, a crest width of 4 m, and side slopes inclined at 65°. The embankment body was assumed to be homogeneous and represented as a compacted frictional cohesive soil, characterised by a friction angle of 34°, a cohesion of 17 kPa, and a unit weight of 20 kN/m³. The foundation was modelled as a frictional cohesive soil with slightly lower friction but higher cohesion ($\Phi = 30°$, $c = 20$ kPa), and the same unit weight (20 kN/m³). Two hydraulic conditions were considered: an impermeable (non-seepage) case and a seepage case, in which the hydraulic conductivity was set to 1×10^{-8} m/s for the dam body and 1×10^{-12} m/s for the foundation. In all base configurations, the freeboard defined as the vertical distance between the dam crest and the reservoir water level was fixed at 1.5 m.

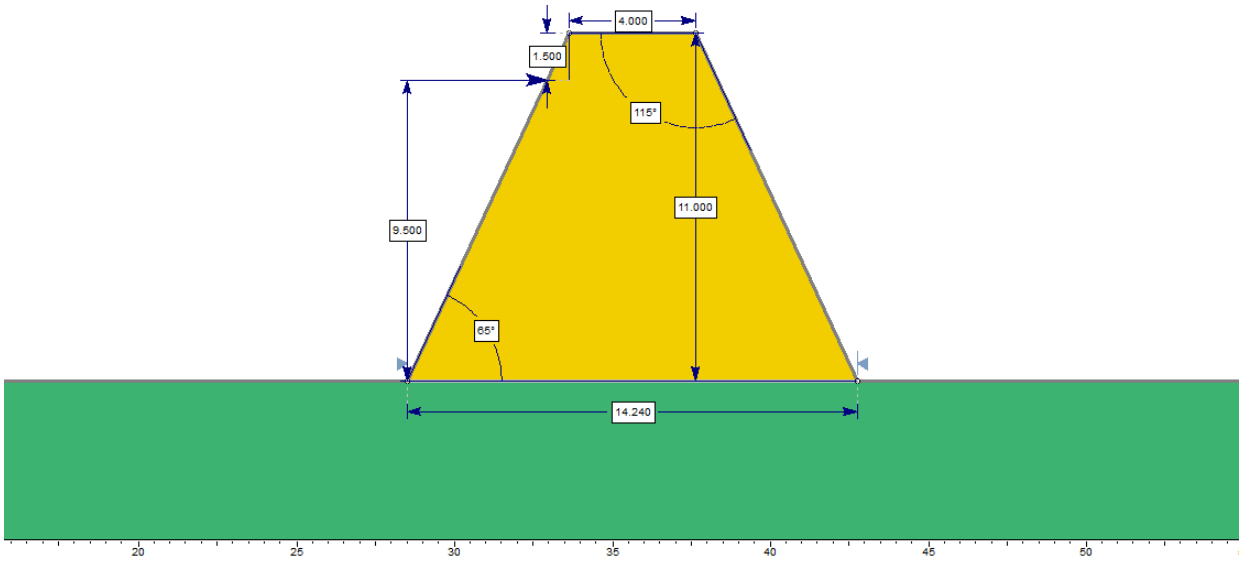

Figure 11. Reference embankment dam cross-section adopted for the analyses, including the embankment body and the foundation layer. The section is trapezoidal (H =11 m, crest width =4 m, side slopes =65°) and includes a freeboard of 1.5m.

Figure 11 presents the reference cross-section adopted for all analyses. This reference layout is maintained in all simulations, while individual parameters (water level, seepage condition, reinforcement spacing, vegetation, and wave loading) are varied one at a time to isolate their effect on stability.

3.1.6 Support conditions

Geosynthetic reinforcement was included in selected simulations to evaluate its contribution to embankment stability. Two main configurations were therefore considered: reinforced and unreinforced models. In all reinforced cases, the same reinforcement type was adopted, with an Ultimate Tensile Strength (UTS) of 30 kN/m and Long-Term Design Strength (LTDS) of 19 kN/m. The reinforcement layout was varied only in terms of vertical spacing between successive layers, which was set to 0.60 m, 0.90 m, and 1.20 m in the reinforced scenarios. A reference configuration without reinforcement was also analysed for comparison.

3.1.7 Water level conditions

Five reservoir water levels were modelled to represent empty to full storage conditions. The empty-reservoir case corresponds to a water height of 0.00 m (dry condition). Partial filling conditions were represented by water heights of 2.38 m (25% of the maximum level ($H_{p.Max}$=9.5m)), 4.75 m (50%), and 7.13 m (75%). The fully filled condition corresponds to a maximum water height of 9.50 m (100%).

3.1.8 Wave height scenarios

To evaluate the influence of surface waves on dam stability, additional loading scenarios were defined by introducing wave action at the reservoir surface. Wave elevations were applied only within limits that did not exceed the dam crest, thereby maintaining physically realistic boundary conditions. The wave heights considered in the analyses were 0.5 m, 1.0 m, 1.5 m, 2.0 m, 2.5 m, 3.0 m, 3.5 m, and 4.0 m.

3.1.9 Wave computation method

The wave action analysed in this thesis is generated by an impulse wave produced by a subaerial granular slide, i.e., a mass movement initiating above the reservoir water level that impacts the water body and generates a wave train. This description is consistent with the impulse-wave framework adopted as reference, where the impacting mass is treated as a slide with granular/debris-like behaviour during motion and impact (Heller, Hager and Minor, 2009). Conceptually, the phenomenon can be described in three stages: wave generation at the impact zone, wave propagation through the reservoir, and wave run-up/loading at the dam (Heller, Hager and Minor, 2009).

In this work, the hydrodynamic stages of generation and propagation are not simulated in a time-dependent way. Instead, the analysis adopts wave conditions at the dam (defined through scenarios) and focuses on converting them into equivalent loads suitable for limit-equilibrium stability modelling.

Although the wave is generated as an impulse wave, the loading at the dam face was estimated by assuming full reflection at the upstream boundary. Under this assumption, the near-wall free-surface motion can be represented using a standing-wave (fully reflected) pressure model, which provides a practical way to compute equivalent wave-induced pressures for stability calculations (Heller, Hager and Minor, 2009).

For each reservoir condition, the still-water depth at the upstream face is denoted by (h). The wave at the dam is characterised by a wave height (H) and wavelength (L). The geometric meaning of (H), (Δh) and (h), and the corresponding pressure distribution used to define P_1 and P_2, are shown in Figure 12. (Heller, Hager and Minor, 2009).

In the parametric study, wavelength values were assigned through a scenario rule:

$$L = n\,H$$

where (n) is a scenario coefficient used only for wavelength assignment in this thesis. The computations adopted ρ_w=1000 kg/m^3, g = 9.81 m/s^2, and n = 8.

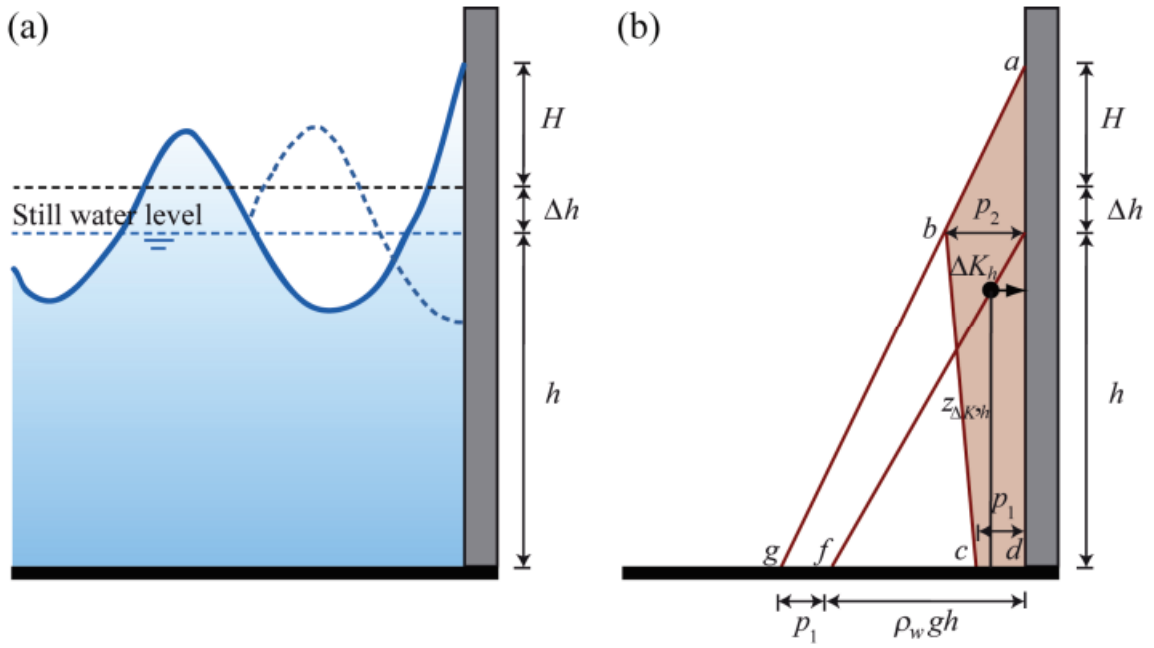

Figure 12. Standing-wave representation of wave run-up and dam-face pressure distribution: (a) definition of wave height (H), still-water depth (h), and equivalent mean water-level rise (Δh); (b) corresponding pressure diagram on the upstream face showing the wave-induced pressures P_1 (at the foundation) and P_2 (at the still-water level) used to compute equivalent loads (Heller, Hager and Minor, 2009).

Following the procedure in (Heller, Hager and Minor, 2009), wave loading at the dam is described through:

- (Δh): equivalent mean water-level rise above the still-water level,
- P_1: wave-induced pressure contribution at the dam foundation,
- P_2: wave-induced pressure contribution at the still-water level.

The mean level rise and wave-induced pressures were obtained from the following equations as functions of (h), (H), and (L) (Heller, Hager and Minor, 2009):

1. Foundation pressure contribution:

$$P_1 = \frac{\rho_w g H}{\cos h\left(\frac{2\pi h}{L}\right)}$$

2. Equivalent mean water-level rise:

$$\Delta h = \frac{\pi H^2}{L} \cot h\left(\frac{2\pi h}{L}\right)$$

3. Still-water level pressure contribution:

$$P_2 = \frac{(\rho_w g h + P_1)(\Delta h + H)}{h + \Delta h + H}$$

For the limit-equilibrium analyses, the computed pressures were converted into equivalent pressure heads (m of water):

$$PH_1 = \frac{P_1}{\rho_w g}$$

$$PH_2 = \frac{P_2}{\rho_w g}$$

To implement wave action in the numerical models, two head quantities were defined:

Segment A (submerged zone): a total head combining still-water depth, the equivalent mean water-level rise, and the wave contribution at the base:

$$H_A = h + \Delta h + PH_1$$

Segment B (run-up zone): a wave contribution expressed as a pressure head near the still-water level:

$$H_B = PH_2$$

Two embankment configurations were analysed: permeable and impermeable. In the permeable case (Figure 13), the upstream face was divided into the two segments above to represent both seepage and wave impact. Below the still-water level (Segment A), a Total Head boundary was applied to reproduce the hydrostatic interaction with the reservoir and to allow infiltration and pore-pressure development within the embankment. Above the still-water level (Segment B), a Pressure Head boundary was applied to represent intermittent wave impact within the run-up zone without imposing a permanent raised reservoir level, which would

otherwise overestimate seepage. The resulting pore-pressure field from the seepage analysis was then used in the subsequent limit-equilibrium stability calculations.

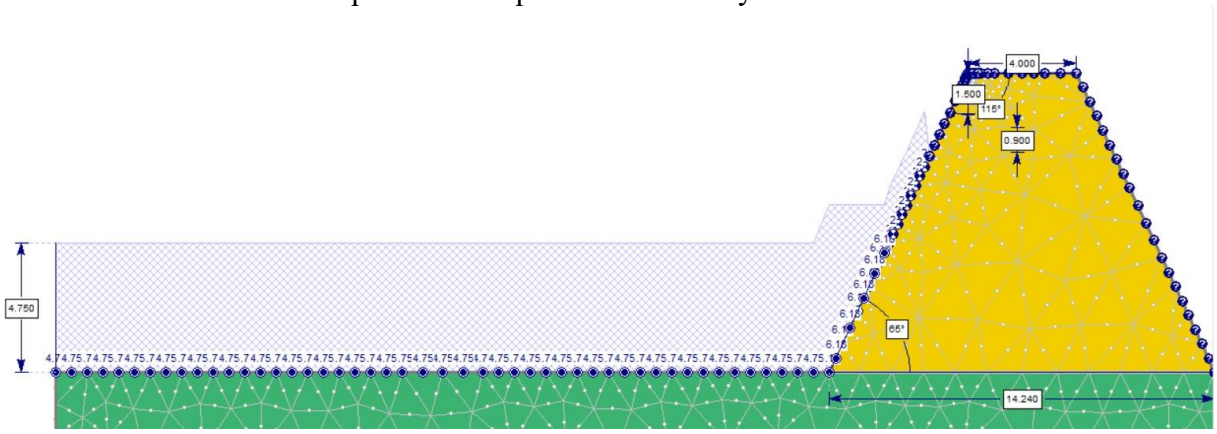

Figure 13. Permeable embankment: pond level h = 4.75 m (50%) and wave height H = 2.5 m, without vegetation.

In the impermeable case (Figure 14), seepage through the dam body was not allowed; therefore, wave action was modelled purely as an external hydraulic load acting on the upstream face. The face was again divided into two zones: in the submerged zone (toe to still-water level) the computed base pressure contribution P_1 was applied, while in the run-up zone above the still-water level the impact pressure contribution *P2* was applied. This ensured that wave forces were distributed realistically along the upstream slope while maintaining impermeable structural behaviour (Heller, Hager and Minor, 2009).

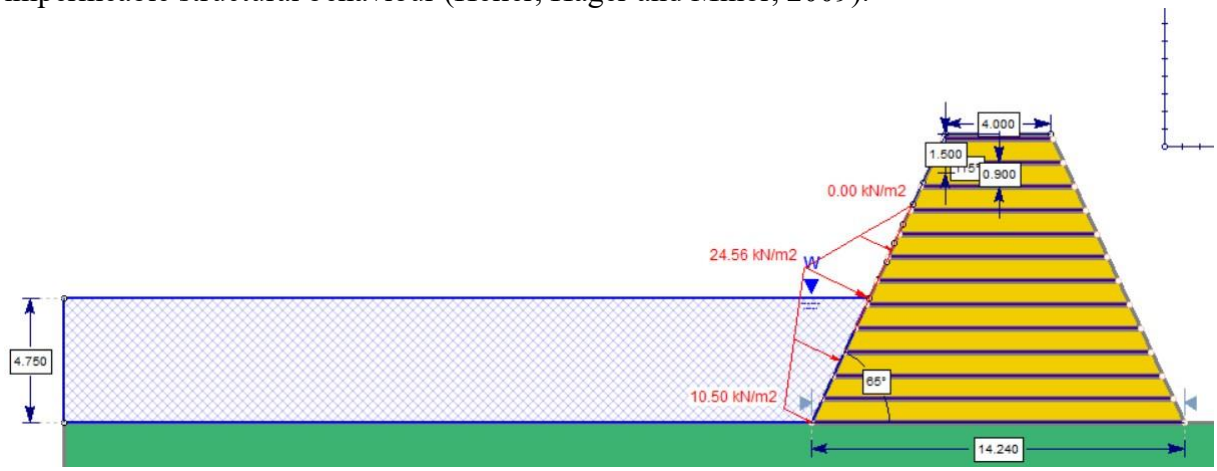

Figure 14. Impermeable embankment: pond level h = 4.75 m (50%) and wave height H = 2.5 m, without vegetation.

These wave-induced boundary conditions were subsequently used as input in the limit-equilibrium analyses presented in the following sections.

3.1.10 Vegetation conditions

Vegetation effects were evaluated under two alternative modelling conditions, which were applied consistently across all scenarios (including variations in reinforcement spacing, permeability condition, reservoir level, and wave height). In the vegetated configuration, vegetation was assumed to extend from the dam crest to the downstream face, with roots penetrating to an average depth of 1 m. Within this root-affected zone, geosynthetic reinforcement was not included, in order to represent a conservative case in which reinforcement continuity is locally absent in the vegetated layer. In the non-vegetated configuration, no vegetation effects were modelled and the reinforcement layers, when present, were assumed to extend continuously through the dam body.

This scenario framework enabled a systematic assessment of how hydraulic loading conditions and bio-mechanical assumptions, together with reinforcement layout, influence the stability response of the embankment dam within the limit-equilibrium analyses performed in Slide2.

3.2 Limit Equilibrium Method (LEM) Analysis

3.2.1 Model setup and preliminary configuration

This section describes the step-by-step procedure used to build, configure, and analyse the slope stability models in Slide2. All simulations were performed within the LEM framework described in Section 3.1, using the parameters and scenarios defined previously.

The modelling process began in the main Slide2 environment, where the geometry and boundary conditions of the dam were defined through various menu options. Before constructing the model, several project settings were adjusted through the menu path: Analysis → Project Settings (figure15).

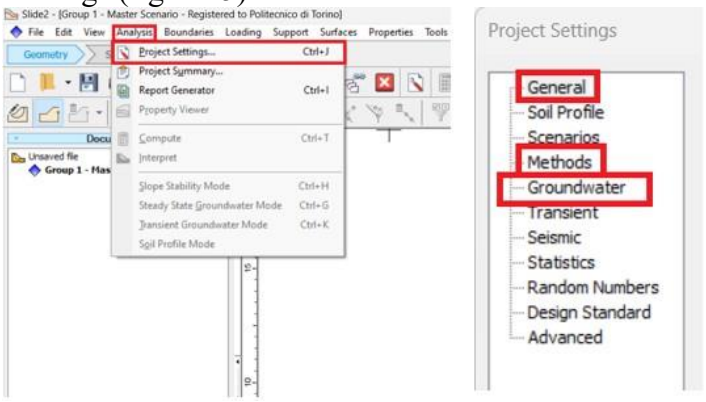

Figure 15. Model Setup and Preliminary Configuration

In the General tab (figure16), the analysis direction was configured to perform calculations from left to right and from right to left, to ensure a complete evaluation of potential failure mechanisms.

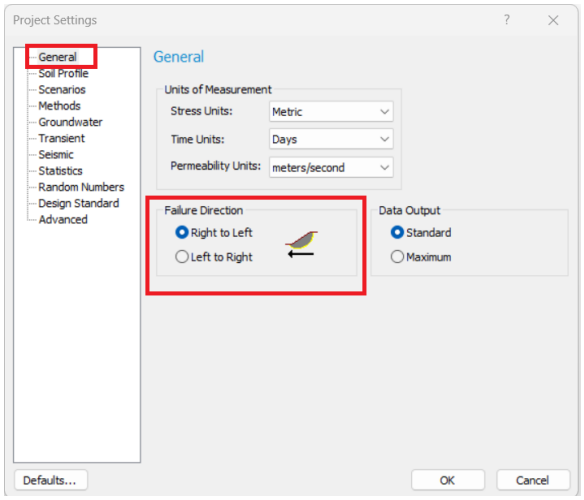

Figure 16. General tab

In the Methods tab (figure17), three analysis methods were selected: Bishop's Simplified, Janbu's Simplified, and Janbu's Corrected.

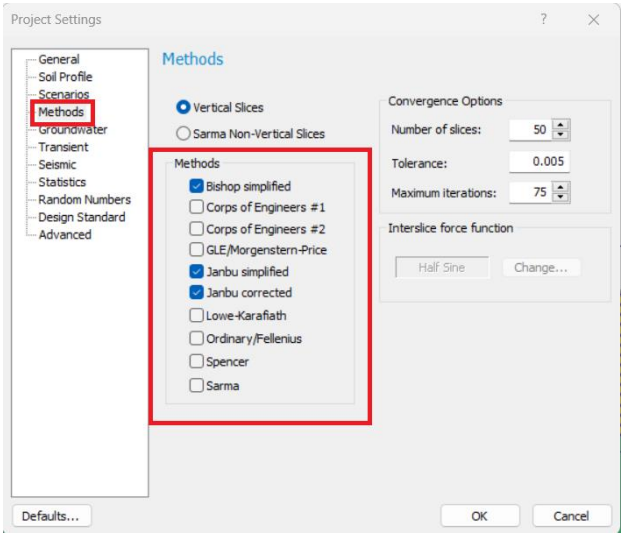

Figure 17. Methods tab

In the Groundwater tab (figure18), two different configurations were defined depending on the permeability condition of the scenario:

Water Surfaces option for impermeable (non-seepage) models.

Steady State option for permeable (seepage) models.

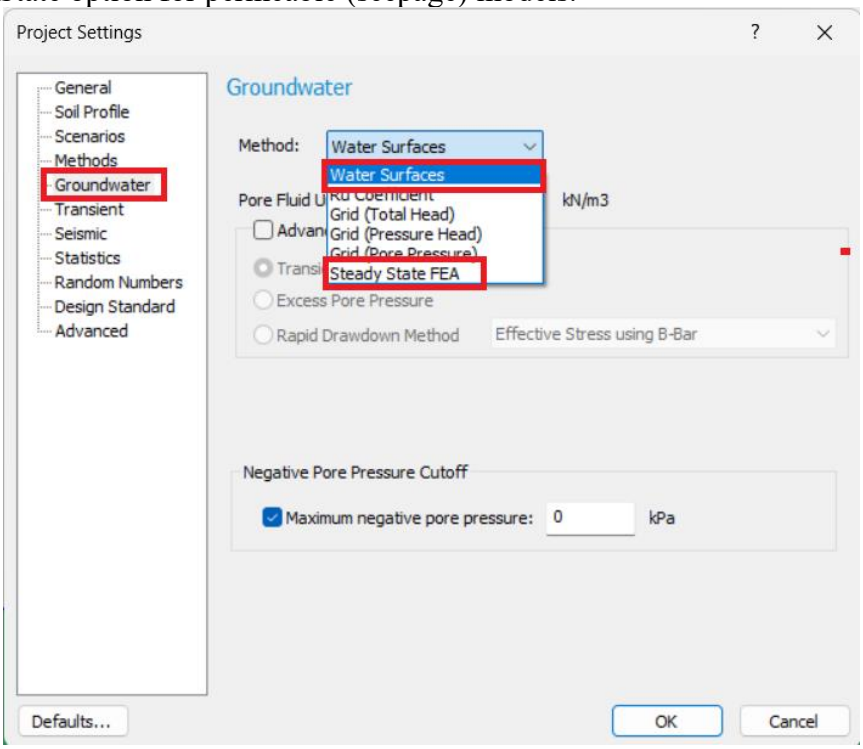

Figure 18. Groundwater tab

After the appropriate settings were selected, the configuration was confirmed by clicking OK, saving all adjustments.

3.2.2 Geometry definition and material assignment

The model geometry was created using the command path:
Boundaries → Add External Boundary (figure19).

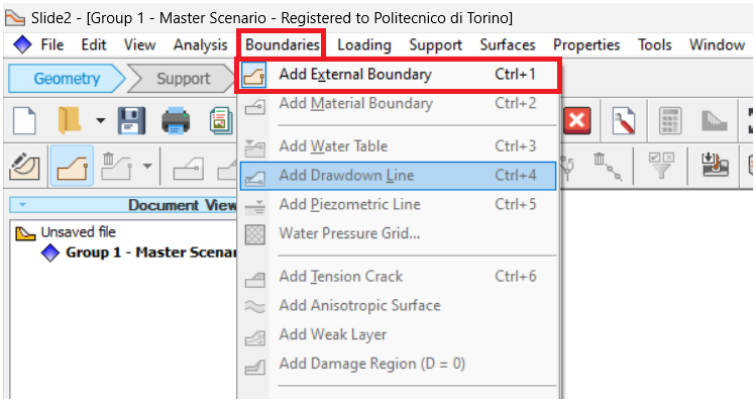

Figure 19. Geometry Definition

The reference dam geometry adopted in all simulations is defined in Section 3.1.5 and illustrated in Figure 11. Both the embankment body and the foundation layer were modelled (figure 20), resulting in a complete cross-sectional representation of the dam foundation system.

Figure 20. Geometry Definition

Subsequently, the Add Material Boundary option was used to separate the dam body from its foundation.

The material properties were then assigned through the menu:
Properties → Define Materials (figure 21).

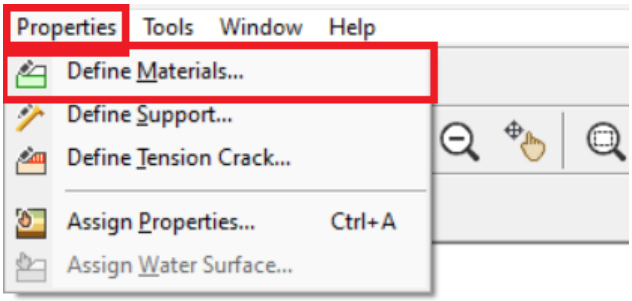

Figure 21. Material Assignment

where the parameters of the dam (figure 22), and foundation (figure 23) were entered as previously specified.

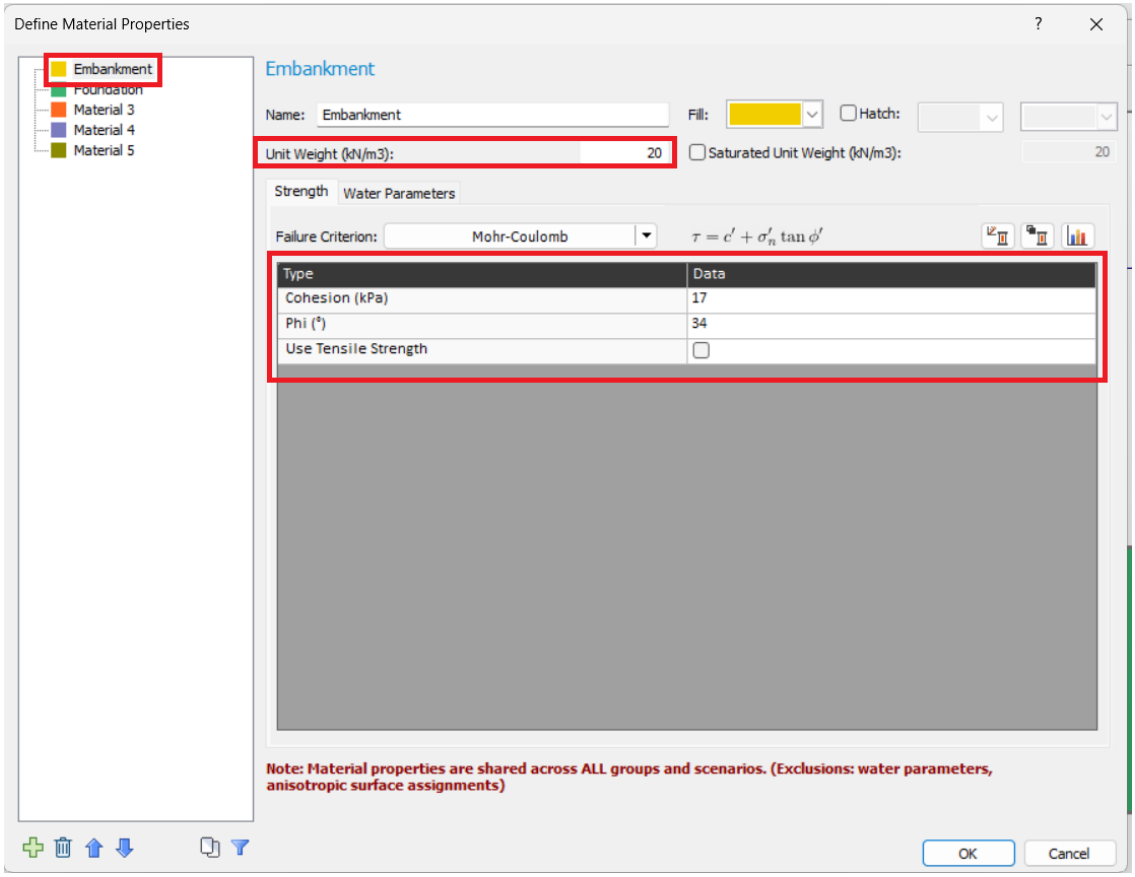

Figure 22. Embankment properties

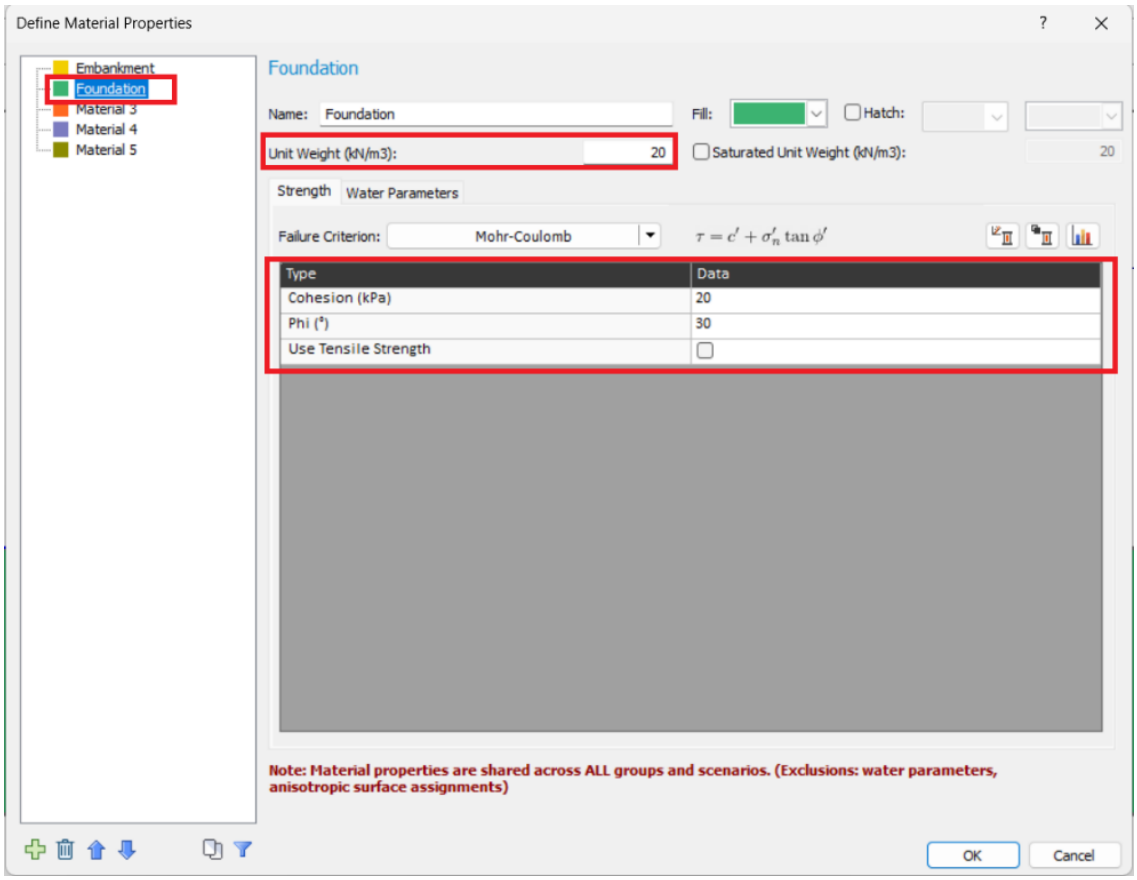

Figure 23. Foundation properties

3.2.3 Failure surface generation

To prepare for slope stability analysis, the failure surface search parameters were set via: Surfaces → Surface Options.

The Grid Search method was selected as the default searching algorithm. Then, using Surfaces → Auto Grid, the software automatically generated the grid of potential slip surfaces across the slope (figure 24).

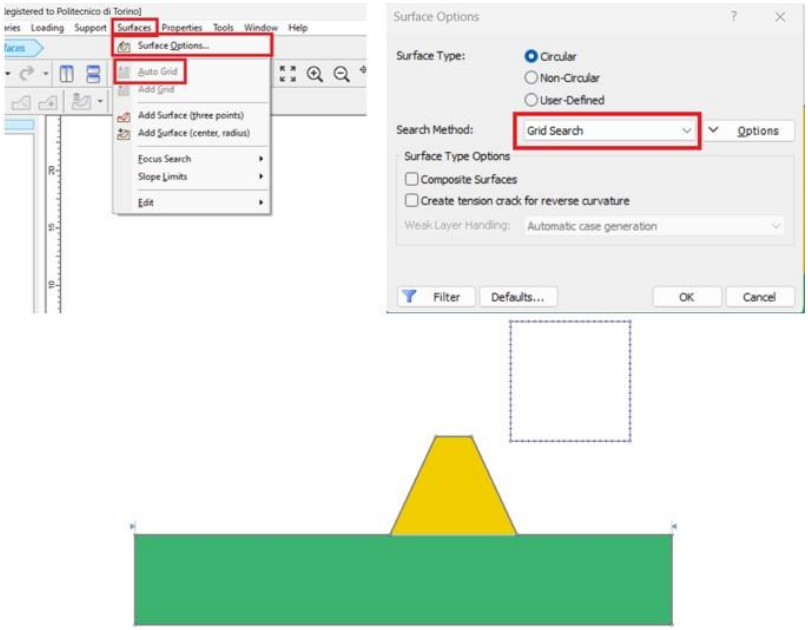

Figure 24. Failure Surface Generation

3.2.4 Definition of reinforcements (supports)

Geosynthetic reinforcement elements were defined to simulate the stabilizing effect of internal supports (figure 25). The properties were entered via:
Properties → Define Support

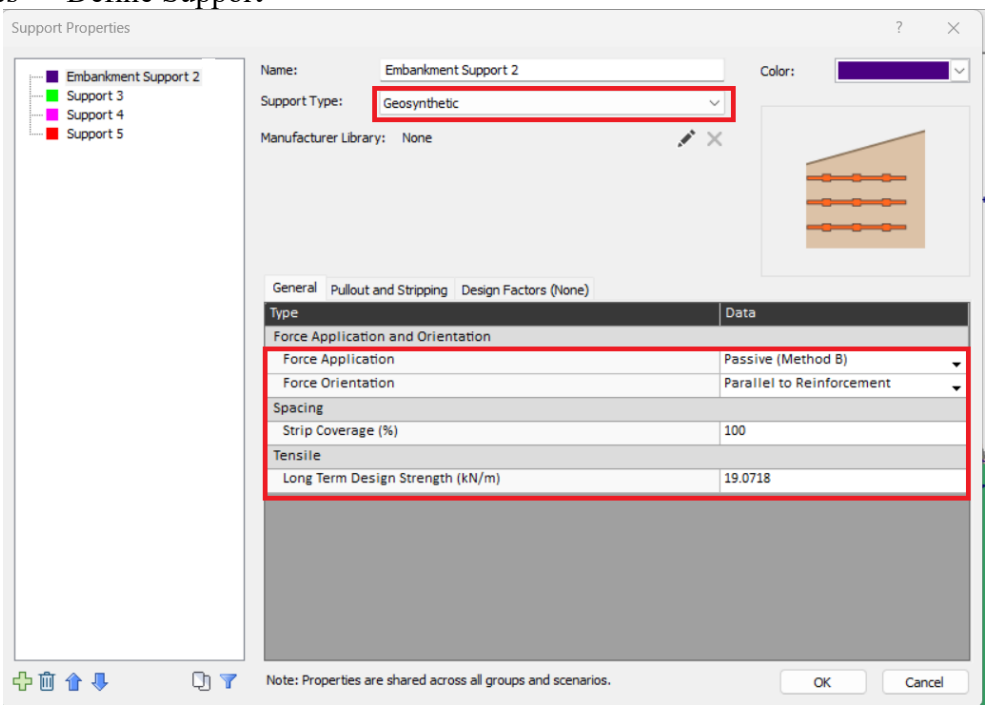

Figure 25. Support properties

where the Geosynthetic characteristics specified in Section 3.1.6 (UTS = 30 kN/m, LTDS = 19 kN/m) were assigned.

After defining the reinforcement type, the layout was generated using: Support → Add Support Pattern (figure 26).

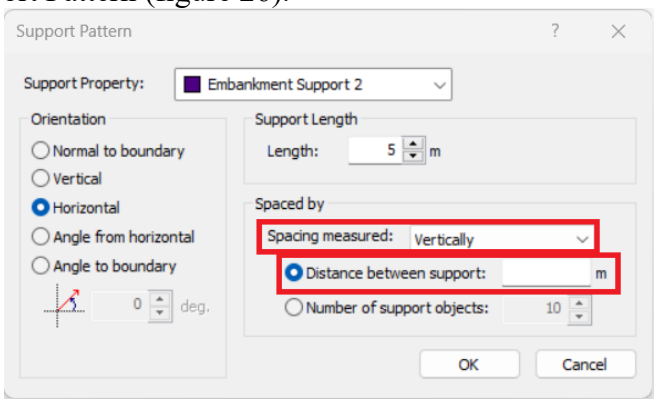

Figure 26. Support Pattern

The spacing between reinforcement layers was set according to the scenario (0.60 m, 0.90 m, 1.20 m, or none). The reinforcements were drawn from the downstream toe to the crest of the dam using the mouse cursor. The length of each reinforcement element was then individually adjusted with the "Move To" command to ensure correct alignment and distribution along the slope (figure 27).

In models representing the presence of vegetation, the uppermost 1 m layer (from the crest to the downstream face) was modelled as a vegetated zone. Within this region, no geosynthetic reinforcement was included, simulating the natural root-dominated layer. In contrast, in non-vegetated scenarios, reinforcements extended continuously without modification.

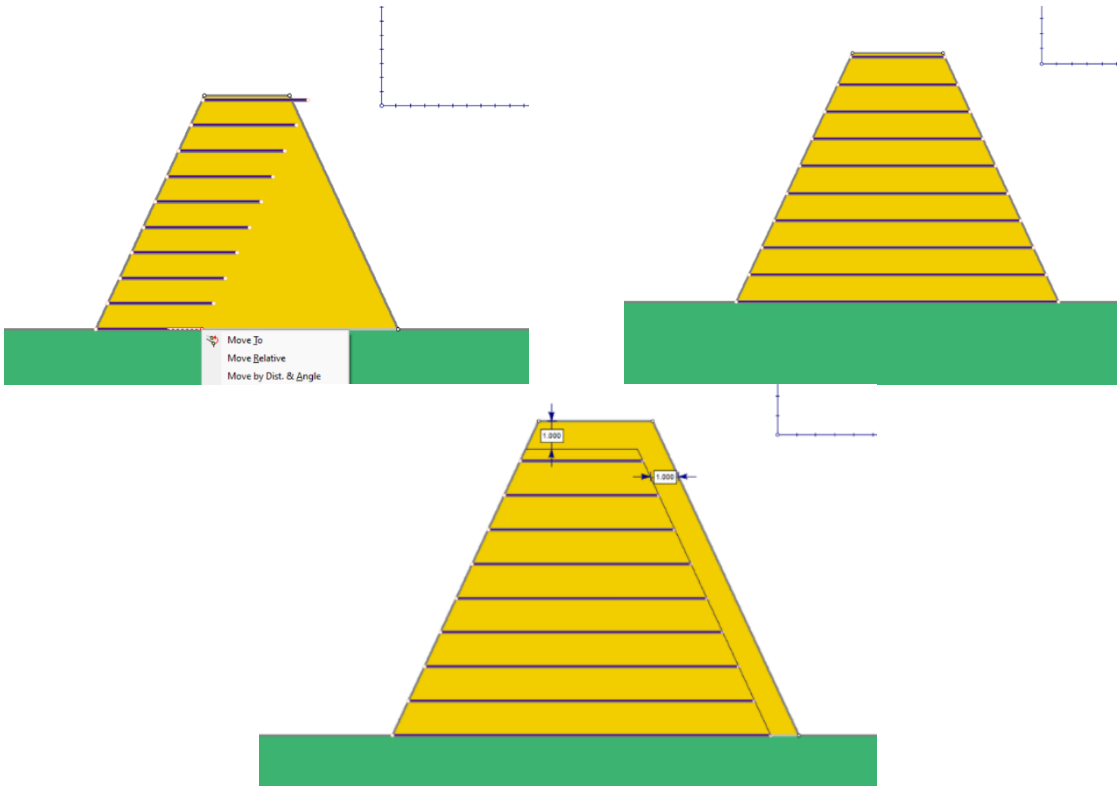

Figure 27. Adding Support Pattern steps

3.2.5 Groundwater and seepage conditions

Two hydraulic configurations were considered, as defined in Section 3.1.5: an impermeable (no-seepage) case and a finite-element seepage case. Their implementation in Slide2 is described below.

(A) Non-seepage (Impermeable) Scenarios (figure 28): For impermeable models, the Water Surfaces option was selected in the Groundwater menu. The reservoir water level was then drawn using: Boundaries → Add Water Table, adjusted according to the predefined levels (e.g., 2.38 m for 25% full reservoir).

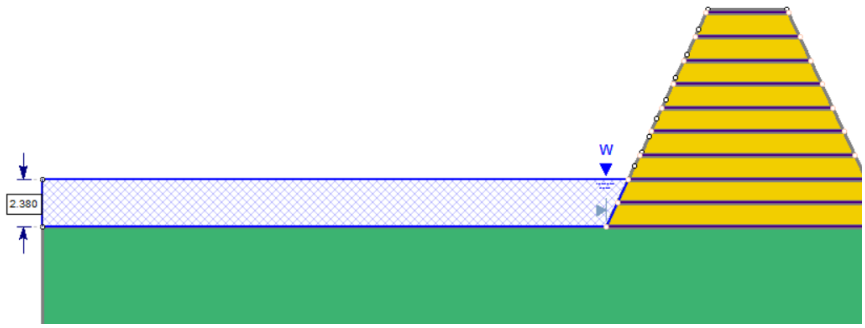

Figure 28. Non-seepage (Impermeable) Scenarios

(B) Seepage Scenarios: For scenarios considering seepage, the Steady State condition was selected in the Groundwater tab. This automatically activated a new Groundwater tab on the main interface. The hydraulic properties were entered via:
Properties → Define Hydraulic Properties (figure 29).

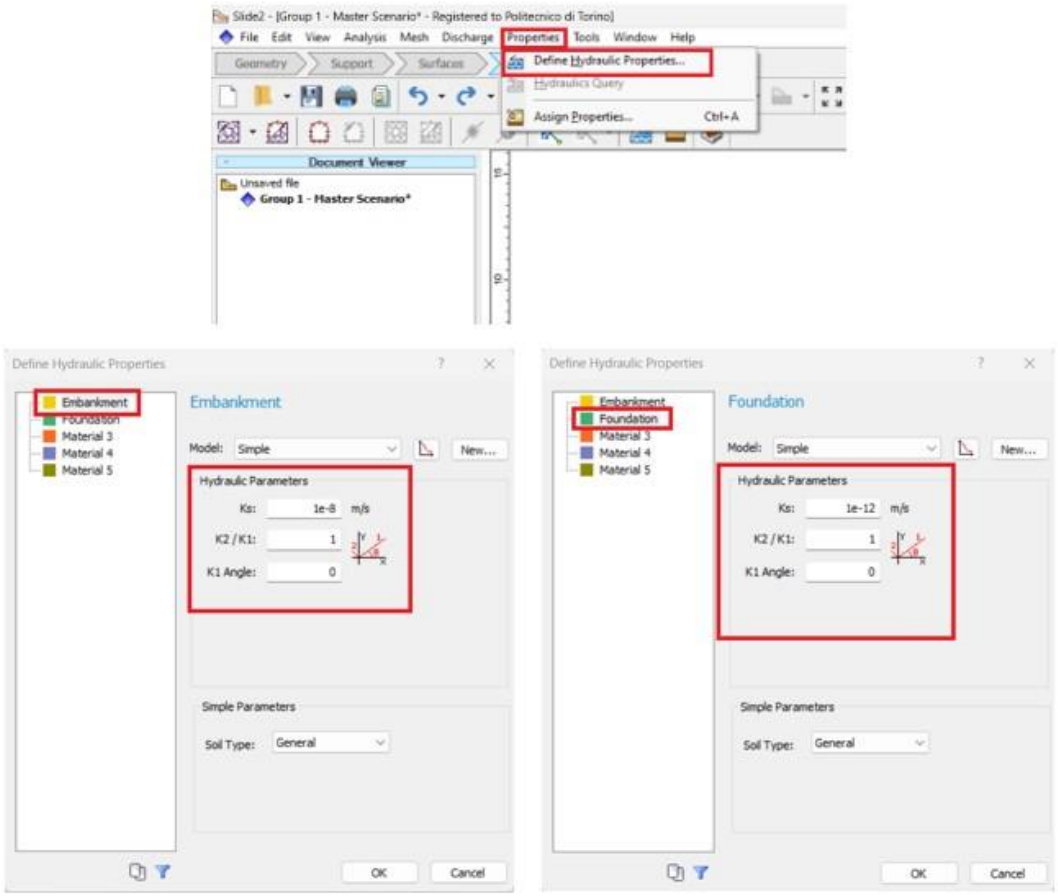

Figure 29. Seepage Hydraulic Properties

where the following permeability values were specified:

Dam body: $K = 1 \times 10^{-8}\ m/s$
Foundation: $K = 1 \times 10^{-12}\ m/s$

The computational mesh was then generated through:
Mesh → Mesh Setup (figure 30).

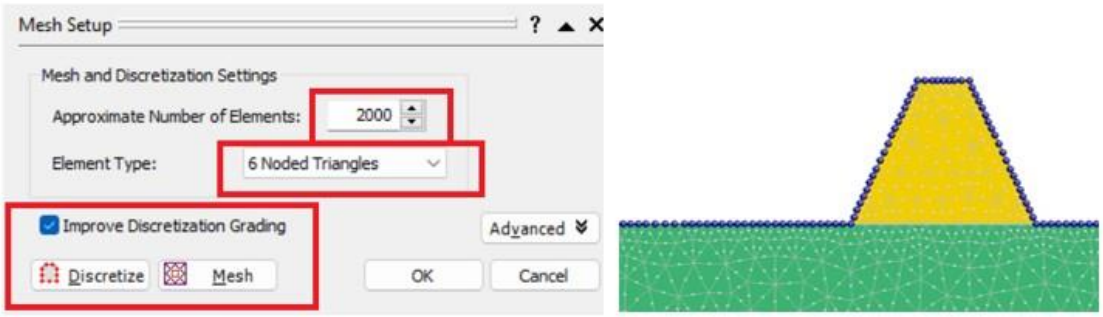

Figure 30. Mesh Setup

and the corresponding boundary conditions were defined using:
Mesh → Set Boundary Conditions (figure 31).

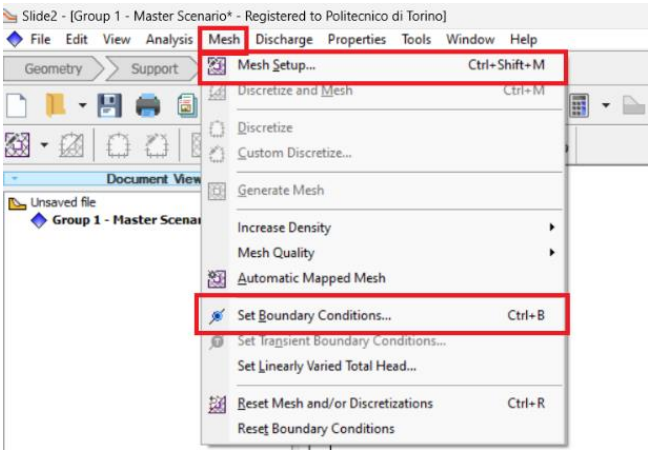

Figure 31. Boundary Conditions

Figure 32 illustrates the reservoir surface corresponding to the 25% fill condition (2.38 m water height).

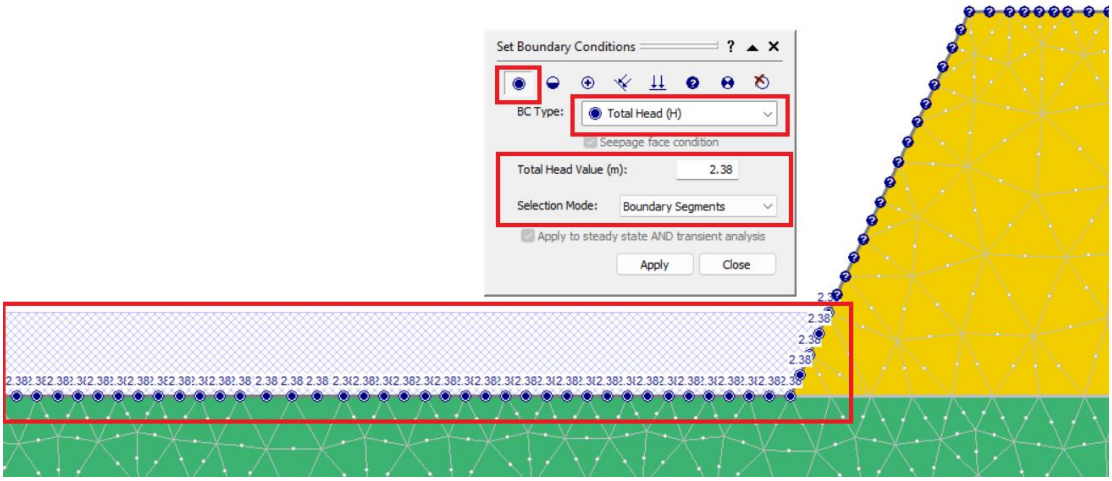

Figure 32. seepage 2.38 m water height

3.2.6 Wave loading

(A) Non-seepage Scenarios: For models without seepage, wave forces were applied as distributed surface loads. After calculating the hydrodynamic wave pressure and the water level difference (Δh), the loads were defined using:
Loading → Add Distributed Load (figure 33).

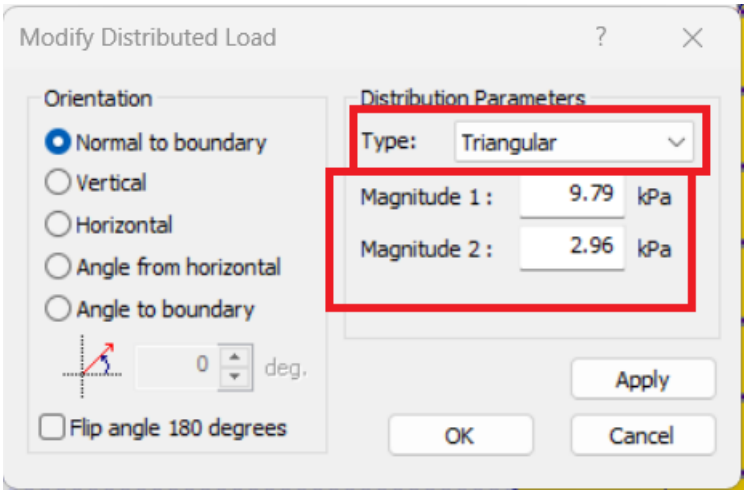

Figure 33. Wave Loading (impermeable).1

The Triangular load type was selected, and the pressure distribution was applied along the corresponding height according to each wave condition (e.g., 1.0 m wave height at 25% reservoir level (figure 34)).

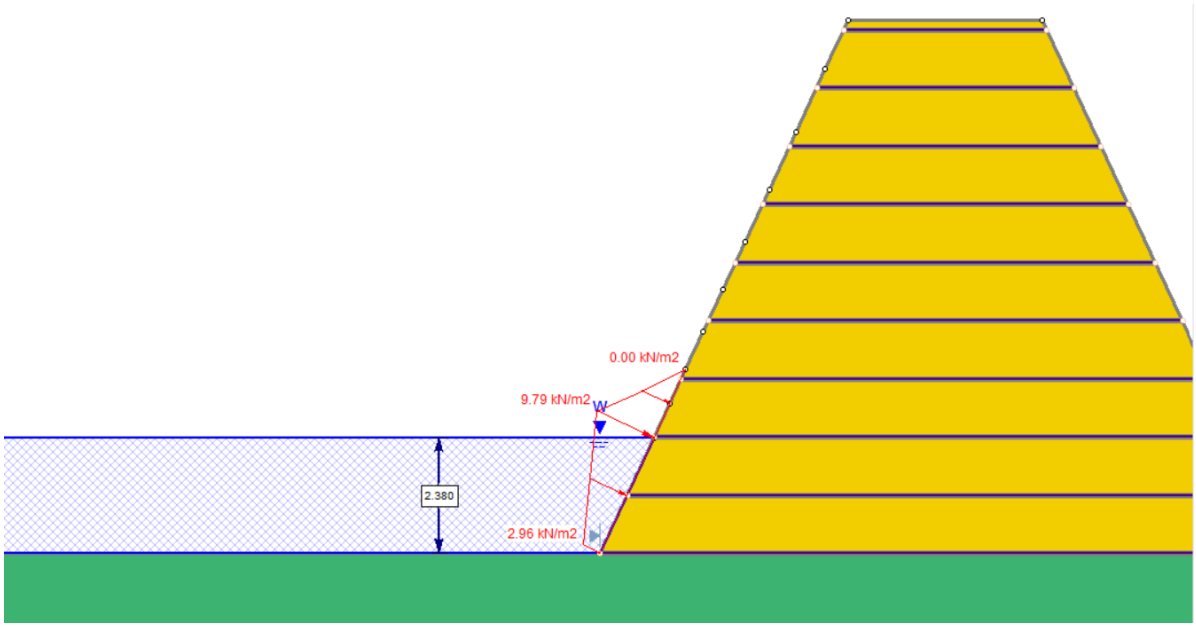

Figure 34. Wave Loading (impermeable).2

(B) Seepage Scenarios: In seepage models, both hydrostatic and hydrodynamic pressures were considered. Within the Groundwater tab, using Mesh → Set Boundary Conditions. The total head was applied from the bottom of the reservoir up to the steady-state water level (e.g., 2.38 m), while the pressure head was applied from the water surface to the maximum wave crest level (figure 35).
This approach ensured that both the static water pressure and the dynamic wave impact were correctly simulated.

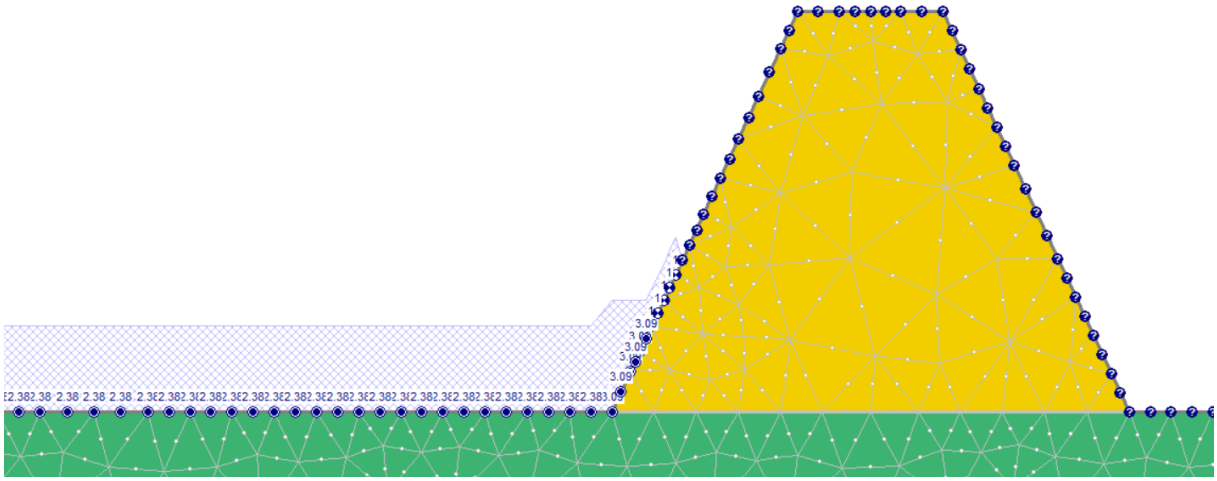

Figure 35. Wave Loading (seepage)

3.2.7 Computation and interpretation

After completing all geometric, hydraulic, and loading definitions, the model was ready for computation. The final analysis was performed by selecting Compute, followed by Interpret.

The software then calculated the Safety Factor corresponding to each selected method (Bishop, Janbu Simplified, Janbu Corrected) under the defined scenario conditions (figure 36).

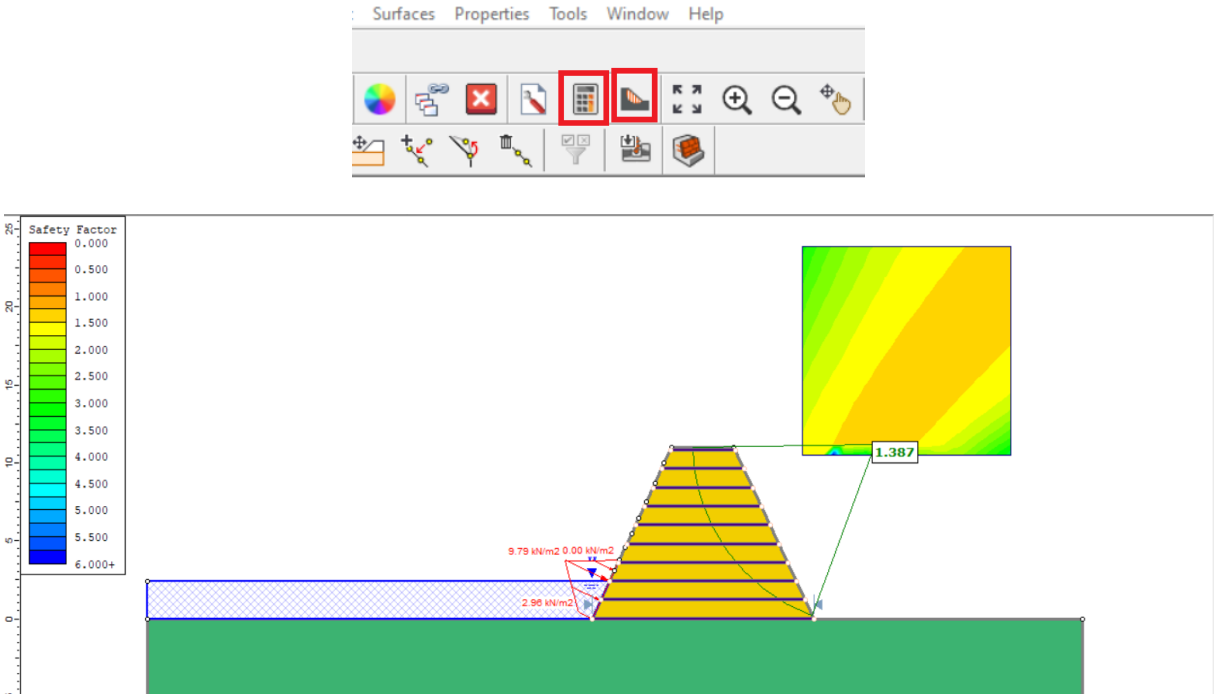

Figure 36. Computation and Interpretation

The results obtained from these computations are discussed in detail in the next Chapter (4), where the influence of each parameter on the stability of the embankment is interpreted.

Chapter 4

Results of LEM analyses

4.1 Introduction

This chapter presents and discusses the results obtained from the limit equilibrium analyses conducted using Slide2, as described in Chapter 3. The outcomes correspond directly to the modelling framework, scenario definitions, and input parameters previously established, ensuring consistency across all simulations.

The objective of this chapter is to evaluate the influence of permeability conditions, reinforcement spacing, reservoir water level, wave height, and vegetation on the stability of the embankment dam. All results reported herein are derived from the systematic variation of these parameters, while maintaining identical geometric and material properties, as outlined in Section 3.1.

4.2 Modelling Scenarios and Result Framework

Based on the scenarios described in Section 3.1.3, the analyses were performed under two fundamental permeability conditions:

1. Impermeable dam, representing dry conditions without seepage.
2. Seepage condition, in which constant hydraulic parameters were assigned to both the dam body and the foundation.

For each permeability condition, four reinforcement configurations were considered, as defined in Section 3.1.6:

1. Reinforcement spacing of 0.60 m (figure 38).
2. Reinforcement spacing of 0.90 m (figure 39).
3. Reinforcement spacing of 1.20 m (figure 40).
4. Reference model without reinforcement (figure 37).

These configurations form the basis for all subsequent comparisons presented in this chapter.

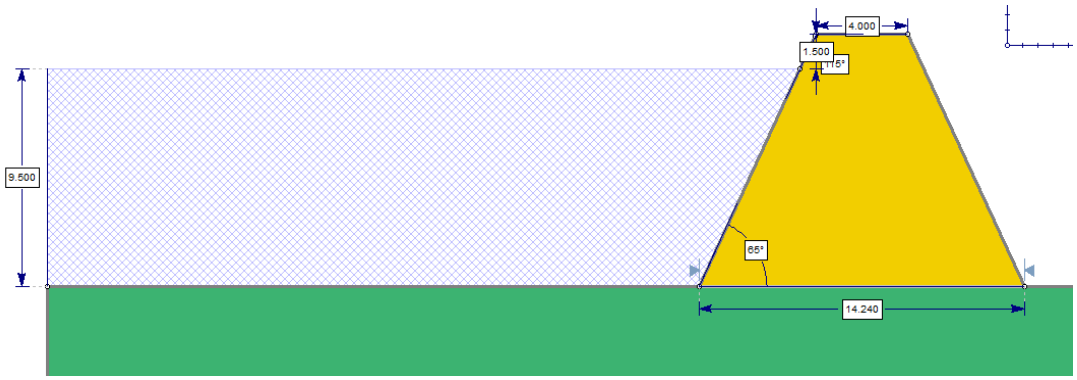

Figure 37. Reference model without reinforcement

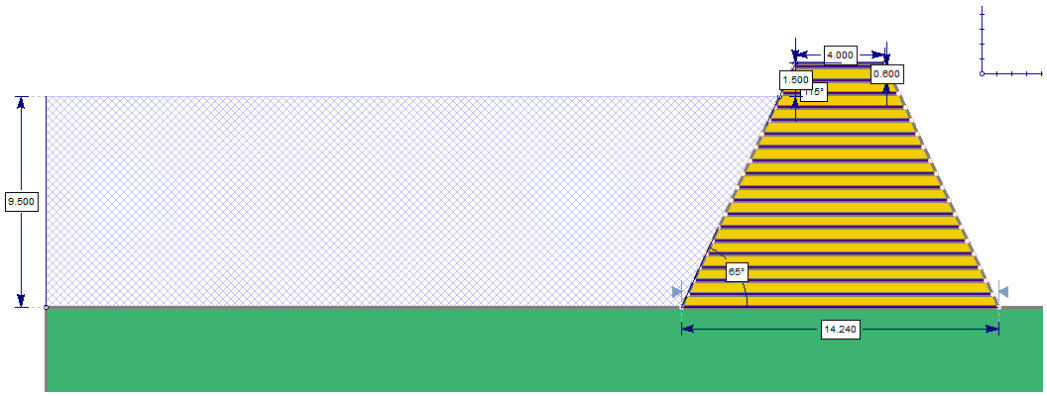

Figure 38. Reinforcement spacing of 0.60 m

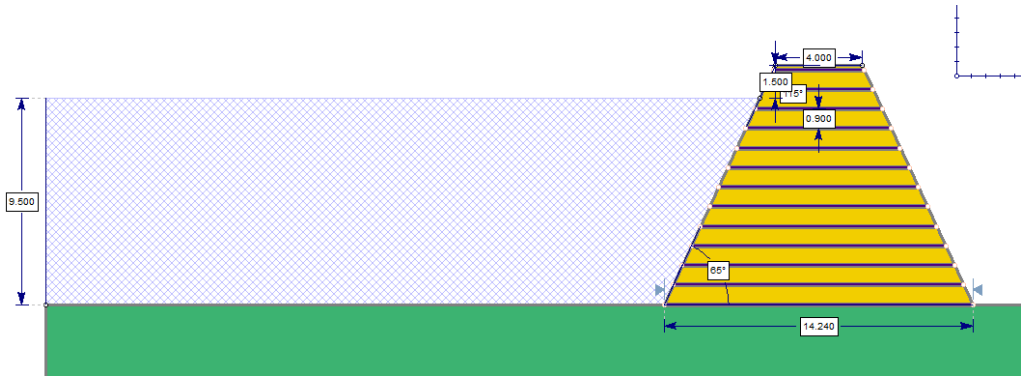

Figure 39. Reinforcement spacing of 0.90 m

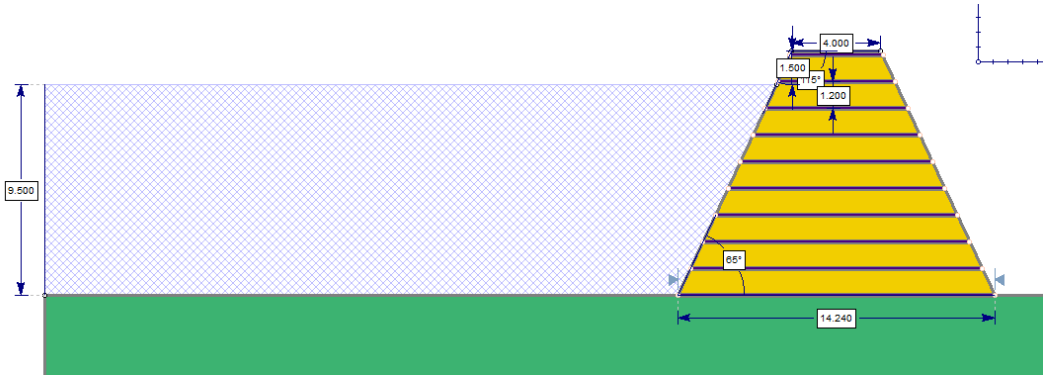

Figure 40. Reinforcement spacing of 1.20 m

4.2.1 Effect of wave loading

In the next stage of the analyses, the models corresponding to different reinforcement spacings were further examined by considering the presence and absence of wave-induced forces. The wave height scenarios followed exactly the range defined in Section 3.1.8 and were applied only up to elevations that did not exceed the dam crest which defined in Section 3.1.9, ensuring physically realistic loading conditions.

This approach allows for a direct assessment of the incremental effect of wave action on slope stability under varying structural and hydraulic conditions.

4.2.2 Influence of vegetation

For all modelling scenarios including variations in permeability, reinforcement spacing, reservoir water level, and wave height two vegetation conditions were analysed, as described in Section 3.1.10:

Presence of vegetation on the downstream slope, extending from the crest to the toe with a root penetration depth of 1 m, and without reinforcement within the vegetated zone.

Absence of vegetation, where no vegetation effects were included, and reinforcement layers extended continuously throughout the dam body.

This distinction enables the evaluation of vegetation effects both independently and in combination with structural reinforcement and hydraulic loading.

4.2.3 General model configuration

A general overview of the different modelling configurations considered in this study is presented in the following section, providing a reference framework for the detailed results discussed subsequently. To simplify the visual presentation of the modelling configurations, all models shown in the following figures (figures 41-48) are illustrated using the full-tank (100% reservoir level) condition, regardless of the water level considered in the corresponding analyses

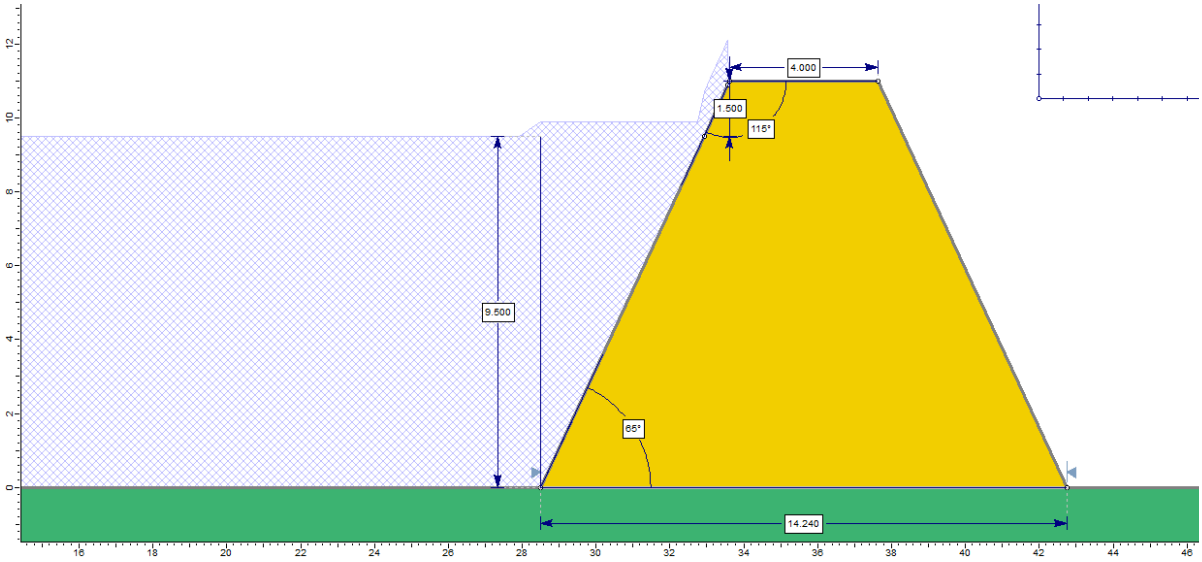

Figure 41. Wave Loading and Vegetation Influence (Reference model without reinforcement) (seepage)

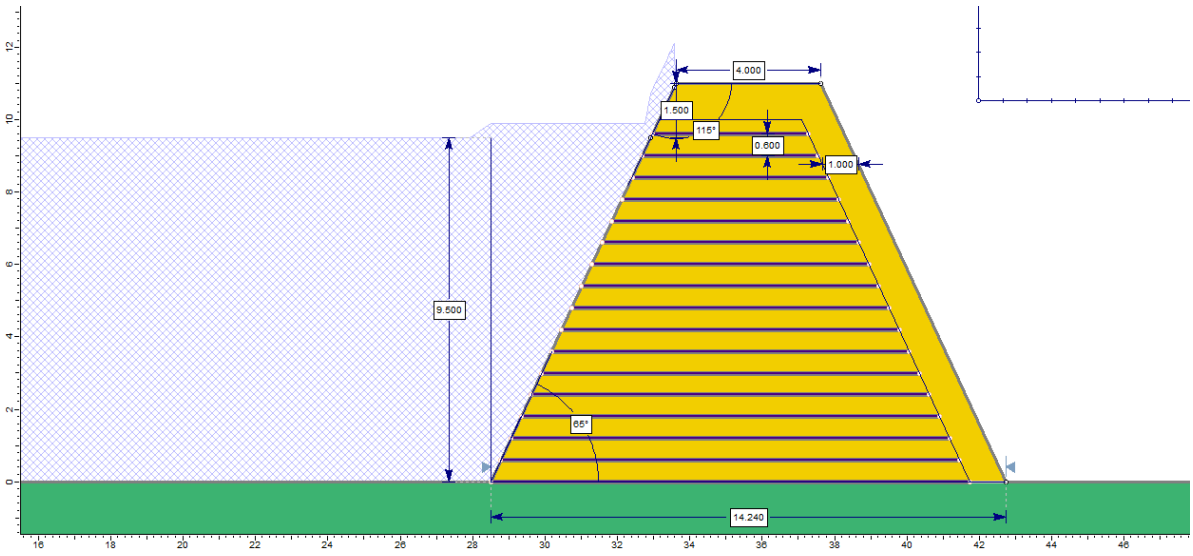

Figure 42. Wave Loading and Vegetation Influence (spacing 0.6m) (seepage)

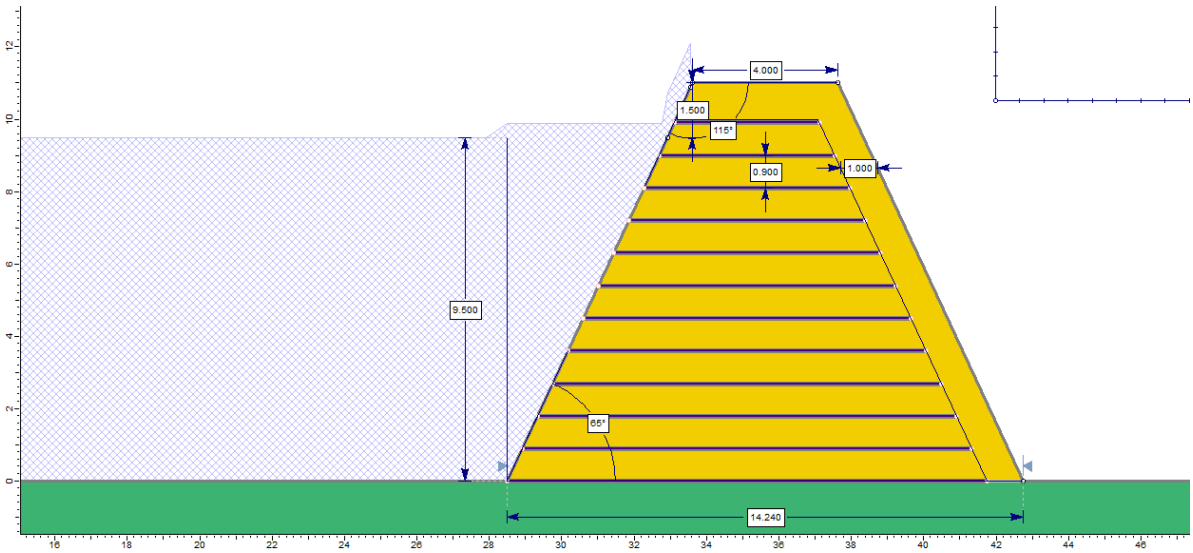

Figure 43. Wave Loading and Vegetation Influence (spacing 0.9m) (seepage)

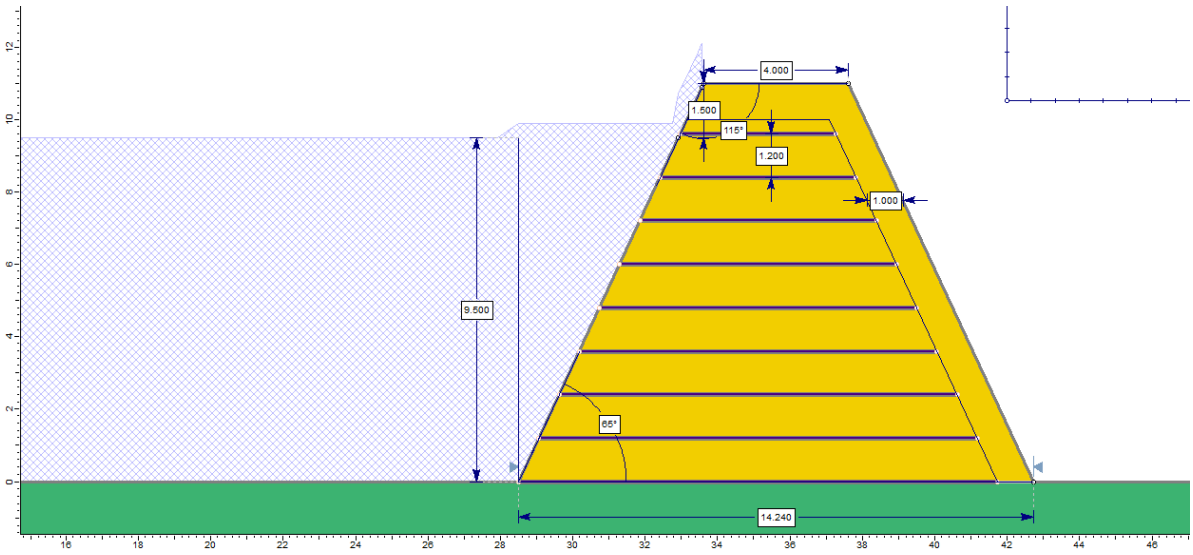

Figure 44. Wave Loading and Vegetation Influence (spacing 1.2m) (seepage)

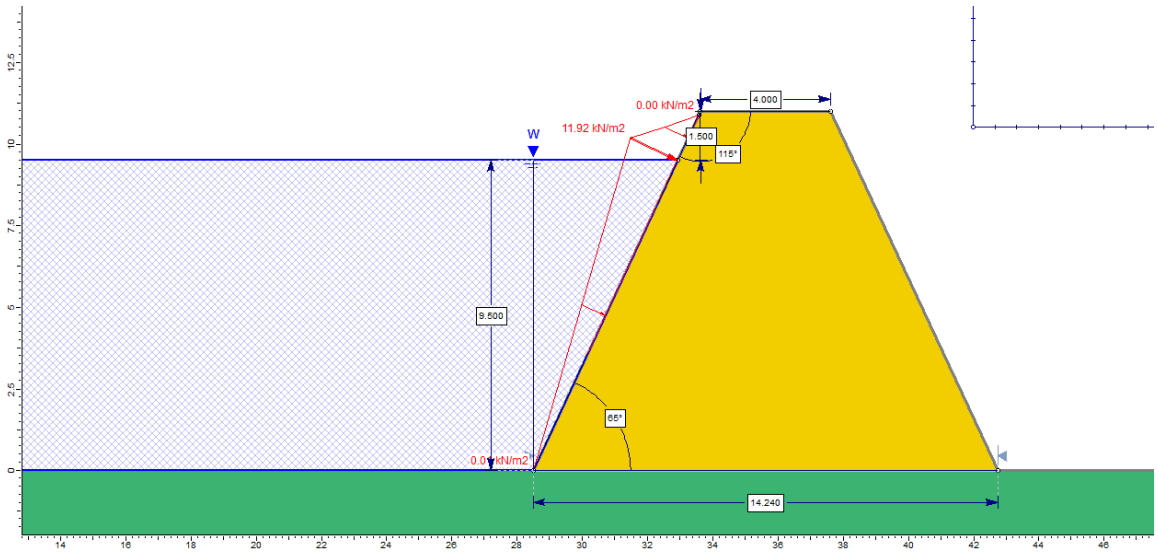

Figure 45. Wave Loading and Vegetation Influence (without reinforcement) (Impermeable)

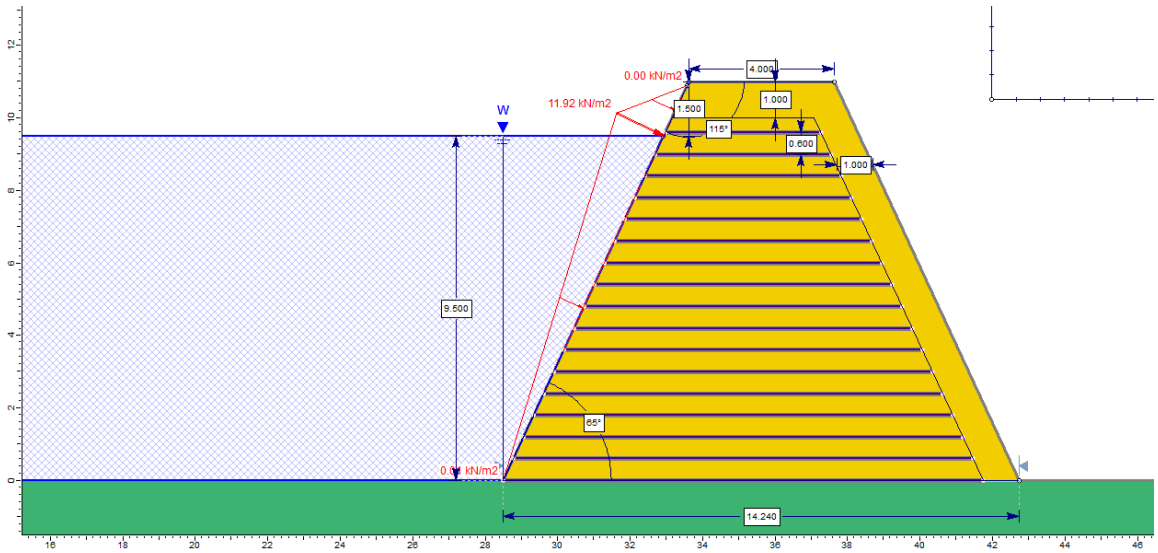

Figure 46. Wave Loading and Vegetation Influence (spacing 0.6m) (Impermeable)

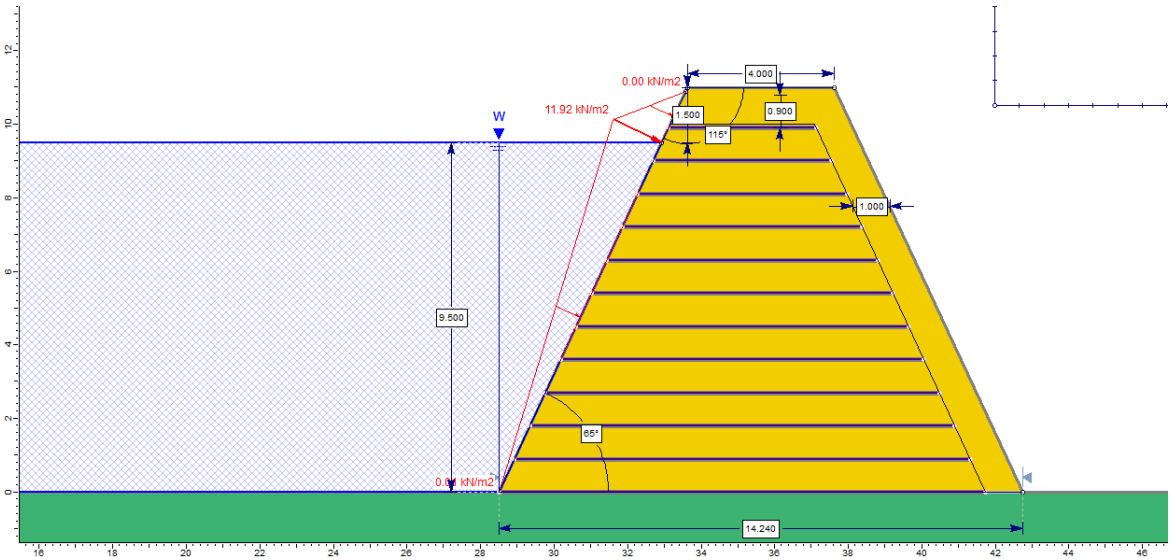

Figure 47. Wave Loading and Vegetation Influence (spacing 0.9m) (Impermeable)

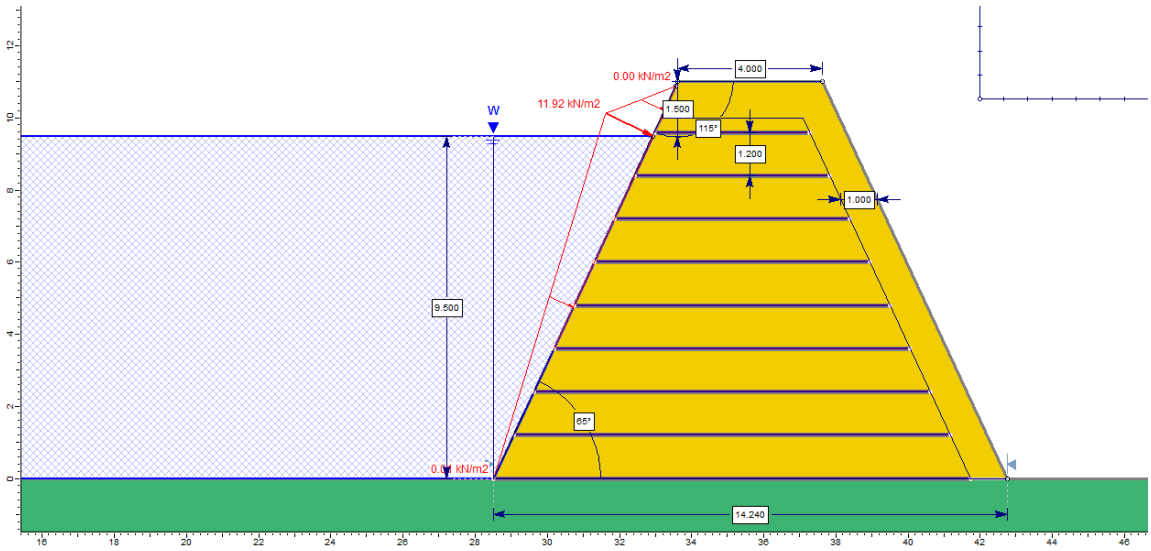

Figure 48. Wave Loading and Vegetation Influence (spacing 1.2m) (Impermeable)

4.3 Presentation of Results

In this section, the results obtained from each modelling scenario are presented.

4.3.1 Results for wave-included analyses

As stated earlier, four reservoir water levels were considered for all models:

$$H_{P.Max} = 9.5m$$

- 25% H_P (2.38 m)
- 50% H_P (4.75 m)
- 75% H_P (7.13 m)
- 100% H_P (9.5 m)

The results presented in the following section correspond to dam models in which wave effects on the slope are included. For the reservoir water levels listed above, the outcomes compare permeable and impermeable conditions under the applied wave loading. The influence of vegetation is also assessed through paired simulations with and without vegetative cover. The computed factors of safety are summarised in (Tables 3-34) and illustrated in (Figures 49-64), organised by reservoir water level and reinforcement-layer spacing.

The results are presented in two stages: first the numerical results, followed by the corresponding graphs.

♣ Spacing Between Supports (0.6 m), (Tables 3-10) and (Figures 49-52):

Pond level: **2.38m(25%)** Wave effect		Water surface (No Permeability) (factors of safety)	
		With vegetation	Without vegetation
Scenario number	Wave height (H) (m)	Left to Right	Left to Right
1	0.5	1.581	1.626
2	1	1.581	1.626
3	1.5	1.581	1.626
4	2	1.581	1.626
5	2.5	1.581	1.626
6	3	1.581	1.626
7	3.5	1.581	1.626
8	4	1.581	1.626

Table 3. Wave-Included Analyses (spacing0.6m-pond level 25%) (impermeable)

Pond level: **2.38m(25%)** Wave effect		Steady state (Seepage) (factors of safety)	
		With vegetation	Without vegetation
Scenario number	Wave height (H) (m)	Left to Right	Left to Right
1	0.5	1.573	1.62
2	1	1.562	1.611
3	1.5	1.538	1.583
4	2	1.502	1.549
5	2.5	1.454	1.502
6	3	1.364	1.373
7	3.5	1.203	1.222
8	4	1.09	1.115

Table 4. Wave-Included Analyses (spacing0.6m-pond level 25%) (permeable)

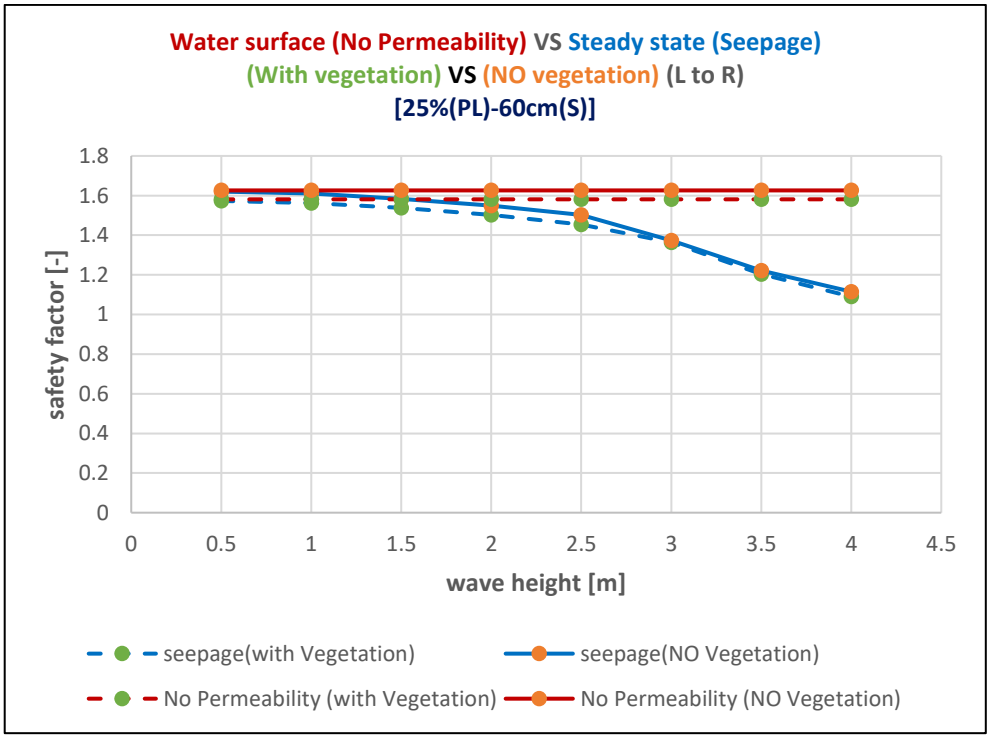

Figure 49. Wave-Included Analyses (spacing0.6m-pond level 25% comparison)

Pond level: **4.75m(50%)** Wave effect		Water surface (No Permeability) (factors of safety)	
		With vegetation	Without vegetation
Scenario number	Wave height (H) (m)	Left to Right	Left to Right
1	0.5	1.581	1.626
2	1	1.581	1.626
3	1.5	1.581	1.626
4	2	1.581	1.626
5	2.5	1.581	1.626
6	3	1.581	1.626
7	3.5	1.581	1.626
8	4	1.581	1.618

Table 5. Wave-Included Analyses (spacing0.6m-pond level 50%) (impermeable)

Pond level: **4.75m(50%)** Wave effect		Steady state (Seepage) (factors of safety)	
		With vegetation	Without vegetation
Scenario number	Wave height (H) (m)	Left to Right	Left to Right
1	0.5	1.526	1.569
2	1	1.502	1.548
3	1.5	1.472	1.52
4	2	1.428	1.476
5	2.5	1.36	1.373
6	3	1.261	1.28
7	3.5	1.175	1.197
8	4	1.091	1.117

Table 6. Wave-Included Analyses (spacing0.6m-pond level 50%) (permeable)

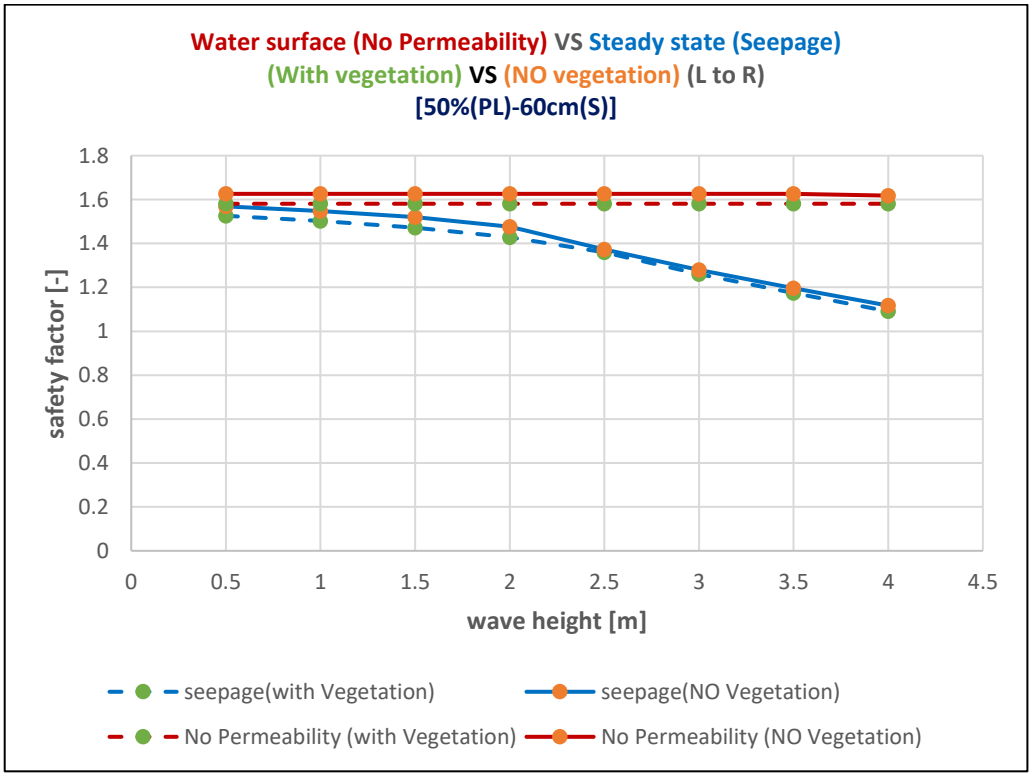

Figure 50. Wave-Included Analyses (spacing0.6m-pond level 50% comparison)

Pond level: **7.13m(75%)** Wave effect		Water surface (No Permeability) (factors of safety)	
		With vegetation	Without vegetation
Scenario number	Wave height (H) (m)	Left to Right	Left to Right
1	0.5	1.581	1.626
2	1	1.581	1.626
3	1.5	1.581	1.626
4	2	1.581	1.626
5	2.5	1.581	1.622

Table 7. Wave-Included Analyses (spacing0.6m-pond level 75%) (impermeable)

Pond level: **7.13m(75%)** Wave effect		Steady state (Seepage) (factors of safety)	
		With vegetation	Without vegetation
Scenario number	Wave height (H) (m)	Left to Right	Left to Right
1	0.5	1.423	1.471
2	1	1.393	1.437
3	1.5	1.351	1.376
4	2	1.305	1.323
5	2.5	1.25	1.265

Table 8. Wave-Included Analyses (spacing0.6m-pond level 75%) (permeable)

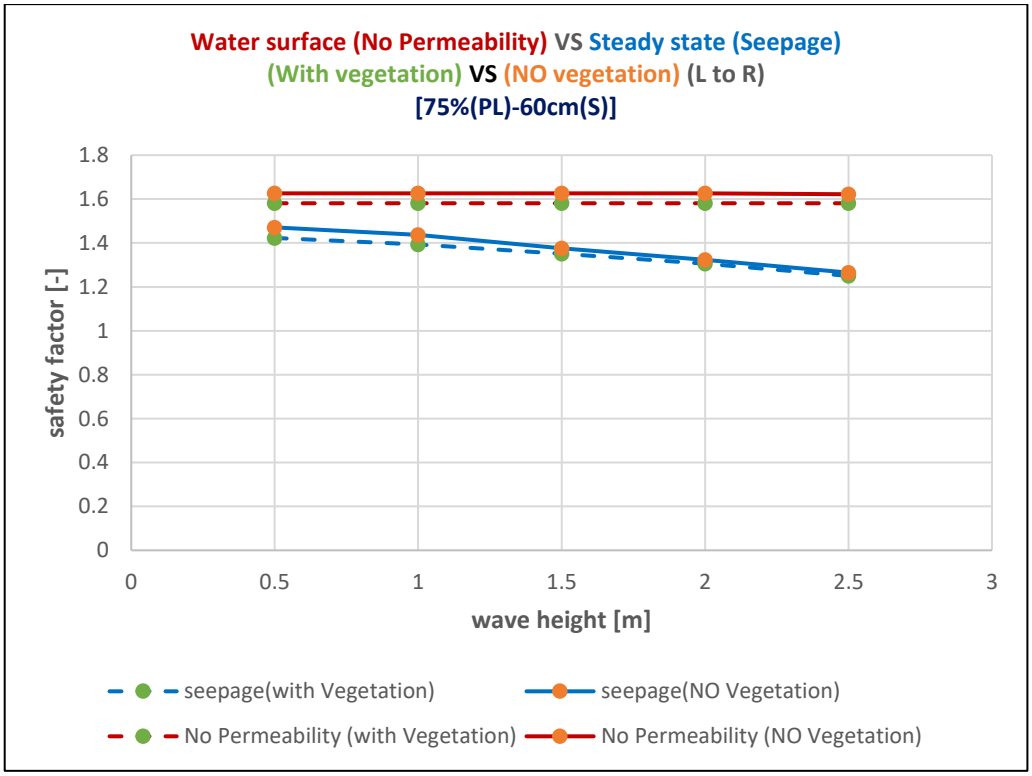

Figure 51. Wave-Included Analyses (spacing0.6m-pond level 75% comparison)

Pond level: **9.5m(100%)** Wave effect		Water surface (No Permeability) (factors of safety)	
		With vegetation	Without vegetation
Scenario number	Wave height (H) (m)	Left to Right	Left to Right
1	0.5	1.581	1.626
2	1	1.581	1.613

Table 9. Wave-Included Analyses (spacing0.6m-pond level 100%) (impermeable)

Pond level: **9.5m(100%)** Wave effect		Steady state (Seepage) (factors of safety)	
		With vegetation	Without vegetation
Scenario number	Wave height (H) (m)	Left to Right	Left to Right
1	0.5	1.292	1.319
2	1	1.266	1.292

Table 10. Wave-Included Analyses (spacing0.6m-pond level 100%) (permeable)

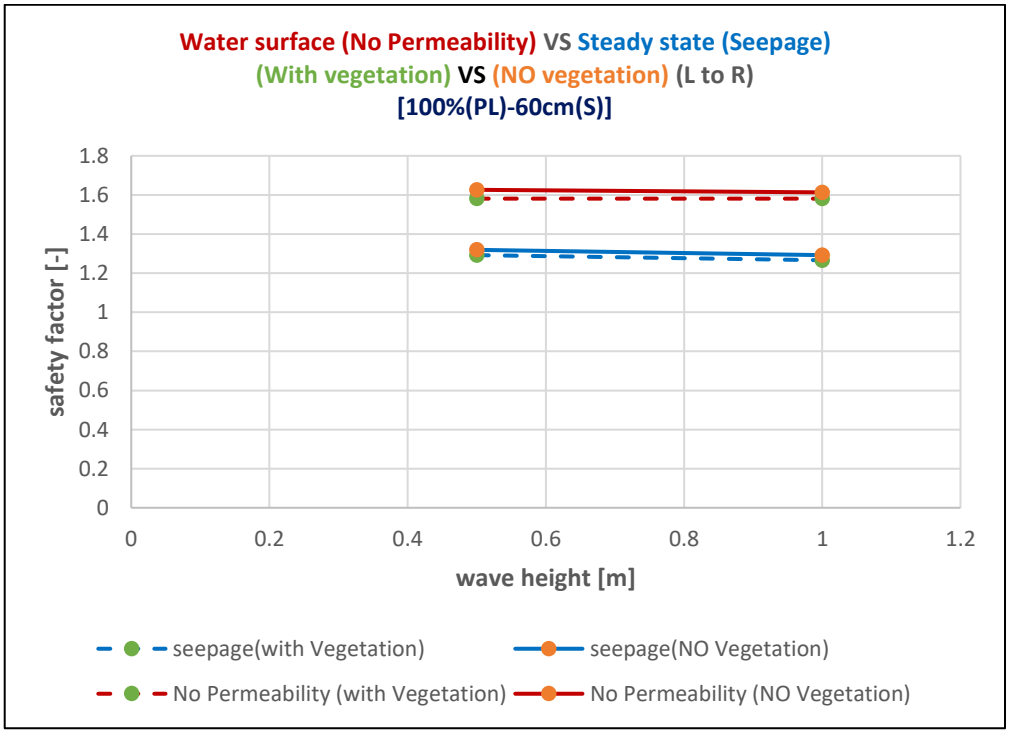

Figure 52. Wave-Included Analyses (spacing0.6m-pond level 100% comparison)

Impermeable cases are nearly insensitive to wave height, while seepage cases show a clear decrease in factor of safety as wave height increases, especially at higher pond levels. Vegetation produces only a minor additional reduction.

♣ Spacing Between Supports (0.9 m), (Tables 11-18) and (Figures 53-56):

Pond level: **2.38m(25%)** Wave effect		Water surface (No Permeability) (factors of safety)	
		With vegetation	Without vegetation
Scenario number	Wave height (H) (m)	Left to Right	Left to Right
1	0.5	1.438	1.474
2	1	1.438	1.474
3	1.5	1.438	1.474
4	2	1.438	1.474
5	2.5	1.438	1.474
6	3	1.438	1.474
7	3.5	1.438	1.474
8	4	1.438	1.474

Table 11. Wave-Included Analyses (spacing0.9m-pond level 25%) (impermeable)

Pond level: **2.38m(25%)** Wave effect		Steady state (Seepage) (factors of safety)	
		With vegetation	Without vegetation
Scenario number	Wave height (H) (m)	Left to Right	Left to Right
1	0.5	1.433	1.469
2	1	1.424	1.457
3	1.5	1.401	1.431
4	2	1.371	1.397
5	2.5	1.329	1.351
6	3	1.24	1.274
7	3.5	1.069	1.097
8	4	0.961	0.984

Table 12. Wave-Included Analyses (spacing0.9m-pond level 25%) (permeable)

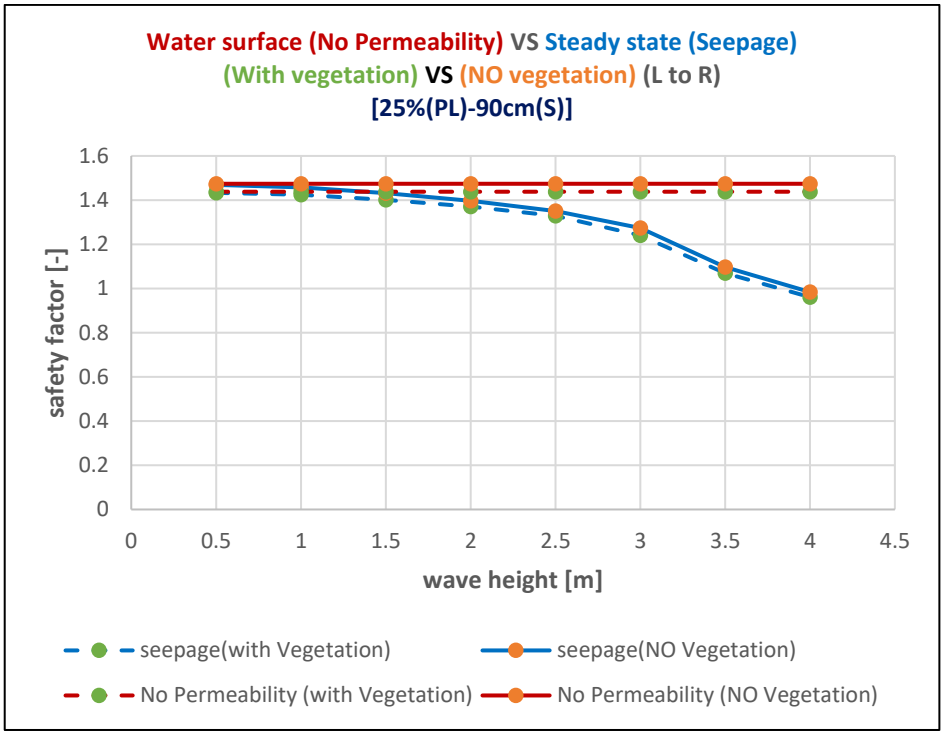

Figure 53. Wave-Included Analyses (spacing0.9m-pond level 25% comparison)

Pond level: **4.75m(50%)** Wave effect		Water surface (No Permeability) (factors of safety)	
		With vegetation	Without vegetation
Scenario number	Wave height (H) (m)	Left to Right	Left to Right
1	0.5	1.438	1.474
2	1	1.438	1.474
3	1.5	1.438	1.474
4	2	1.438	1.474
5	2.5	1.438	1.474
6	3	1.438	1.474
7	3.5	1.438	1.474
8	4	1.438	1.474

Table 13. Wave-Included Analyses (spacing0.9m-pond level 50%) (impermeable)

Pond level: **4.75m(50%)** Wave effect		Steady state (Seepage) (factors of safety)	
		With vegetation	Without vegetation
Scenario number	Wave height (H) (m)	Left to Right	Left to Right
1	0.5	1.39	1.419
2	1	1.371	1.396
3	1.5	1.346	1.368
4	2	1.305	1.325
5	2.5	1.233	1.267
6	3	1.127	1.159
7	3.5	1.041	1.065
8	4	0.964	0.986

Table 14. Wave-Included Analyses (spacing0.9m-pond level 50%) (permeable)

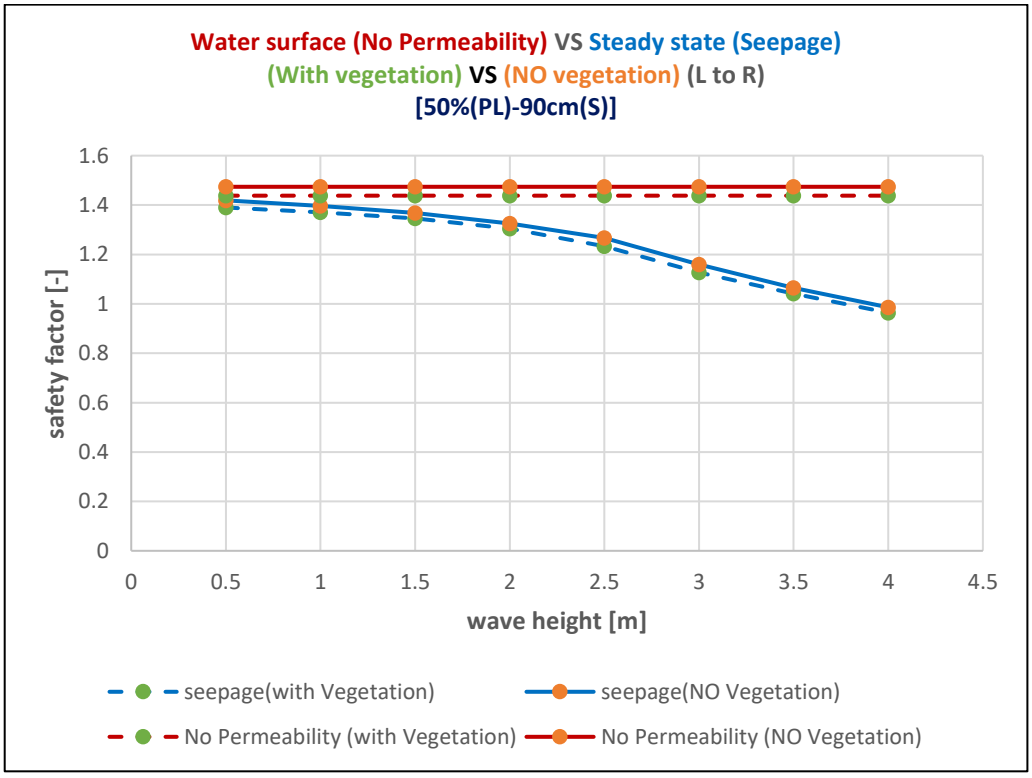

Figure 54. Wave-Included Analyses (spacing0.9m-pond level 50% comparison)

Pond level: **7.13m(75%)** Wave effect		Water surface (No Permeability) (factors of safety)	
		With vegetation	Without vegetation
Scenario number	Wave height (H) (m)	Left to Right	Left to Right
1	0.5	1.438	1.474
2	1	1.438	1.474
3	1.5	1.438	1.474
4	2	1.438	1.474
5	2.5	1.438	1.474

Table 15. Wave-Included Analyses (spacing0.9m-pond level 75%) (impermeable)

Pond level: **7.13m(75%)** Wave effect		Steady state (Seepage) (factors of safety)	
		With vegetation	Without vegetation
Scenario number	Wave height (H) (m)	Left to Right	Left to Right
1	0.5	1.302	1.321
2	1	1.275	1.292
3	1.5	1.224	1.257
4	2	1.161	1.198
5	2.5	1.103	1.138

Table 16. Wave-Included Analyses (spacing0.9m-pond level 75%) (permeable)

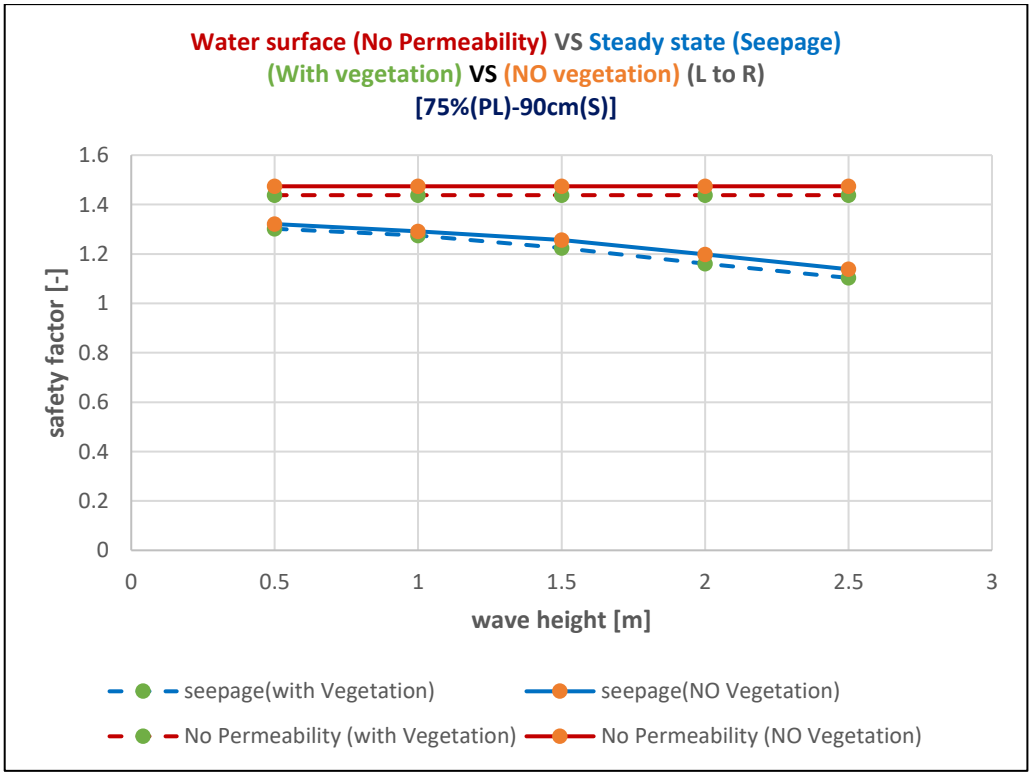

Figure 55. Wave-Included Analyses (spacing0.9m-pond level 75% comparison)

Pond level: **9.5m(100%)** Wave effect		Water surface (No Permeability) (factors of safety)	
		With vegetation	Without vegetation
Scenario number	Wave height (H) (m)	Left to Right	Left to Right
1	0.5	1.438	1.474
2	1	1.438	1.474

Table 17. Wave-Included Analyses (spacing0.9m-pond level 100%) (impermeable)

Pond level: **9.5m(100%)** Wave effect		Steady state (Seepage) (factors of safety)	
		With vegetation	Without vegetation
Scenario number	Wave height (H) (m)	Left to Right	Left to Right
1	0.5	1.164	1.192
2	1	1.133	1.165

Table 18. Wave-Included Analyses (spacing0.9m-pond level 100%) (permeable)

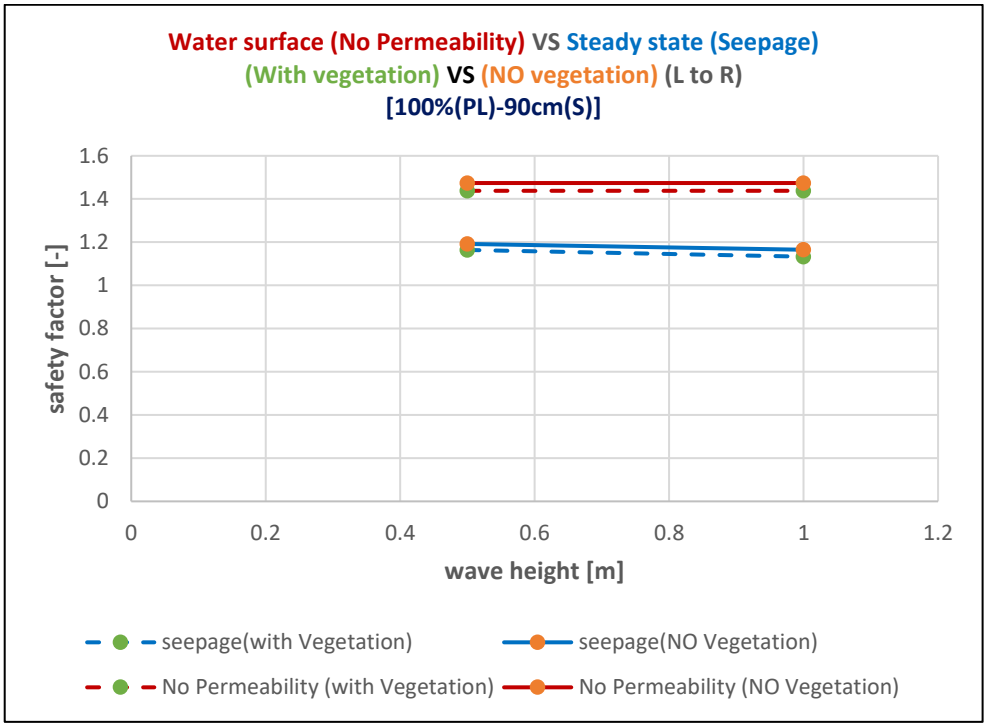

Figure 56. Wave-Included Analyses (spacing0.9m-pond level 100% comparison)

The same pattern is observed: flat response with wave height for impermeable conditions and monotonic reduction for seepage conditions. Compared with 0.6 m spacing, safety factors are generally lower, indicating reduced reinforcement effectiveness.

♣ Spacing Between Supports (1.2 m), (Tables 19-26) and (Figures 57-60):

Pond level: **2.38m(25%)** Wave effect		Water surface (No Permeability) (factors of safety)	
		With vegetation	Without vegetation
Scenario number	Wave height (H) (m)	Left to Right	Left to Right
1	0.5	1.373	1.387
2	1	1.373	1.387
3	1.5	1.373	1.387
4	2	1.373	1.387
5	2.5	1.373	1.387
6	3	1.373	1.387
7	3.5	1.373	1.387
8	4	1.373	1.387

Table 19. Wave-Included Analyses (spacing1.2m-pond level 25%) (impermeable)

Pond level: **2.38m(25%)** Wave effect		Steady state (Seepage) (factors of safety)	
		With vegetation	Without vegetation
Scenario number	Wave height (H) (m)	Left to Right	Left to Right
1	0.5	1.371	1.38
2	1	1.367	1.37
3	1.5	1.345	1.346
4	2	1.312	1.313
5	2.5	1.265	1.266
6	3	1.198	1.198
7	3.5	1.016	1.035
8	4	0.882	0.924

Table 20. Wave-Included Analyses (spacing1.2m-pond level 25%) (permeable)

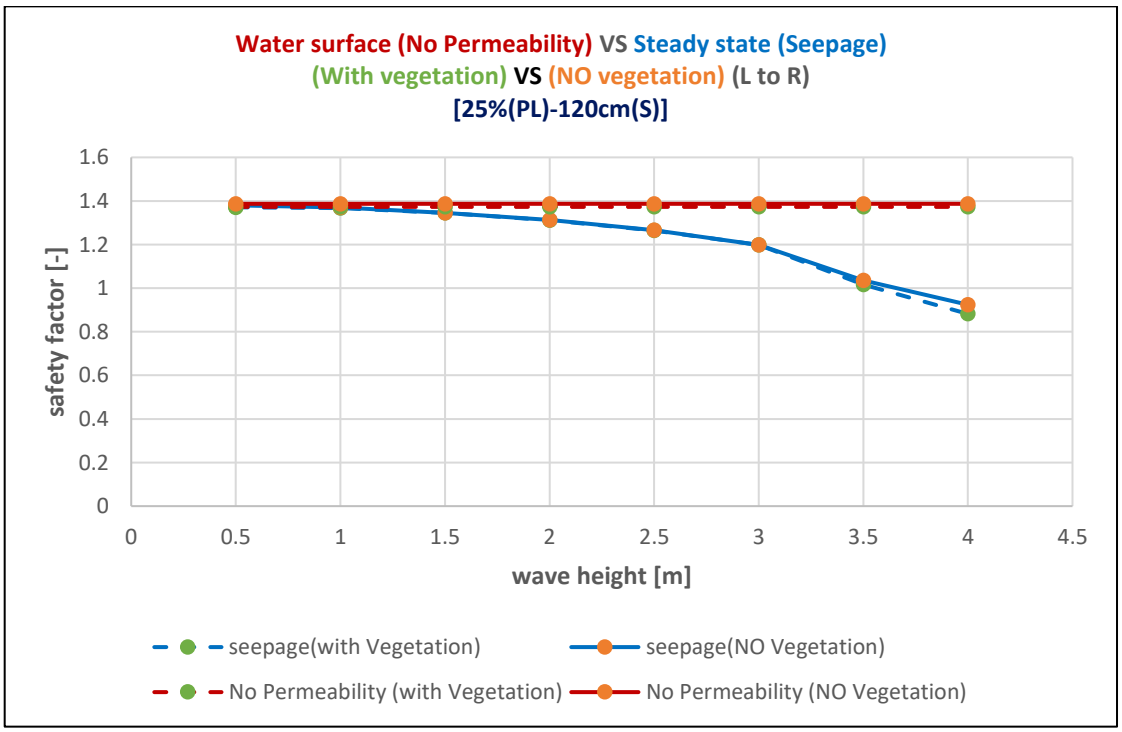

Figure 57. Wave-Included Analyses (spacing1.2m-pond level 25% comparison)

Pond level: **4.75m(50%)** Wave effect		Water surface (No Permeability) (factors of safety)	
		With vegetation	Without vegetation
Scenario number	Wave height (H) (m)	Left to Right	Left to Right
1	0.5	1.373	1.387
2	1	1.373	1.387
3	1.5	1.373	1.387
4	2	1.373	1.387
5	2.5	1.373	1.387
6	3	1.373	1.387
7	3.5	1.373	1.387
8	4	1.368	1.387

Table 21. Wave-Included Analyses (spacing1.2m-pond level 50%) (impermeable)

Pond level: **4.75m(50%)** Wave effect		Steady state (Seepage) (factors of safety)	
		With vegetation	Without vegetation
Scenario number	Wave height (H) (m)	Left to Right	Left to Right
1	0.5	1.333	1.334
2	1	1.312	1.312
3	1.5	1.283	1.284
4	2	1.241	1.242
5	2.5	1.19	1.191
6	3	1.059	1.086
7	3.5	0.962	1.002
8	4	0.881	0.923

Table 22. Wave-Included Analyses (spacing1.2m-pond level 50%) (permeable)

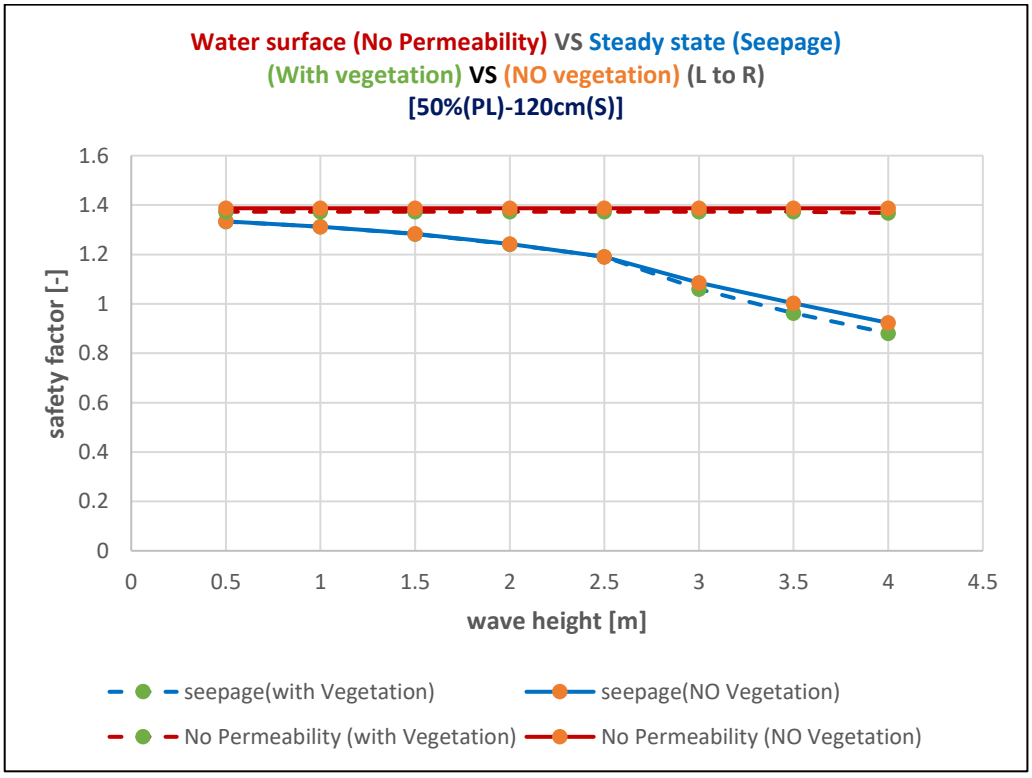

Figure 58. Wave-Included Analyses (spacing1.2m-pond level 50% comparison)

Pond level: **7.13m(75%)** Wave effect		Water surface (No Permeability) (factors of safety)	
		With vegetation	Without vegetation
Scenario number	Wave height (H) (m)	Left to Right	Left to Right
1	0.5	1.373	1.387
2	1	1.373	1.387
3	1.5	1.373	1.387
4	2	1.373	1.387
5	2.5	1.371	1.387

Table 23. Wave-Included Analyses (spacing1.2m-pond level 75%) (impermeable)

Pond level: **7.13m(75%)** Wave effect		Steady state (Seepage) (factors of safety)	
		With vegetation	Without vegetation
Scenario number	Wave height (H) (m)	Left to Right	Left to Right
1	0.5	1.237	1.237
2	1	1.207	1.208
3	1.5	1.174	1.174
4	2	1.097	1.119
5	2.5	1.032	1.063

Table 24. Wave-Included Analyses (spacing1.2m-pond level 75%) (permeable)

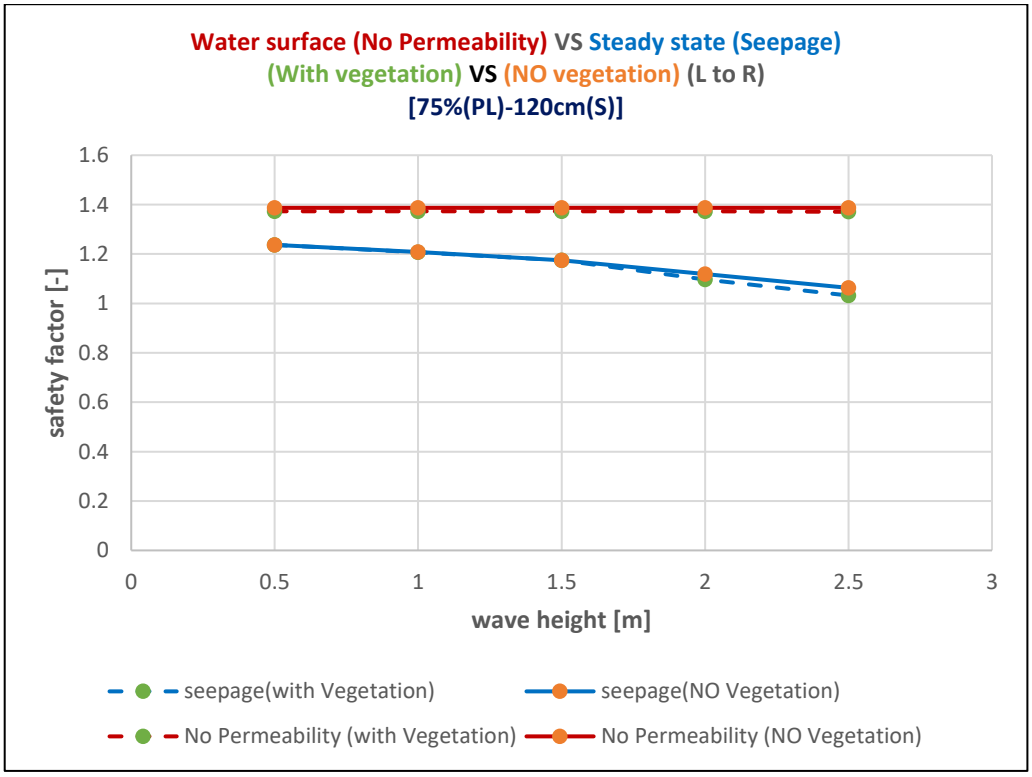

Figure 59. Wave-Included Analyses (spacing1.2m-pond level 75% comparison)

Pond level: **9.5m(100%)** Wave effect		Water surface (No Permeability) (factors of safety)	
		With vegetation	Without vegetation
Scenario number	Wave height (H) (m)	Left to Right	Left to Right
1	0.5	1.373	1.387
2	1	1.364	1.387

Table 25. Wave-Included Analyses (spacing1.2m-pond level 100%) (impermeable)

Pond level: **9.5m(100%)** Wave effect		Steady state (Seepage) (factors of safety)	
		With vegetation	Without vegetation
Scenario number	Wave height (H) (m)	Left to Right	Left to Right
1	0.5	1.108	1.109
2	1	1.074	1.085

Table 26. Wave-Included Analyses (spacing1.2m-pond level 100%) (permeable)

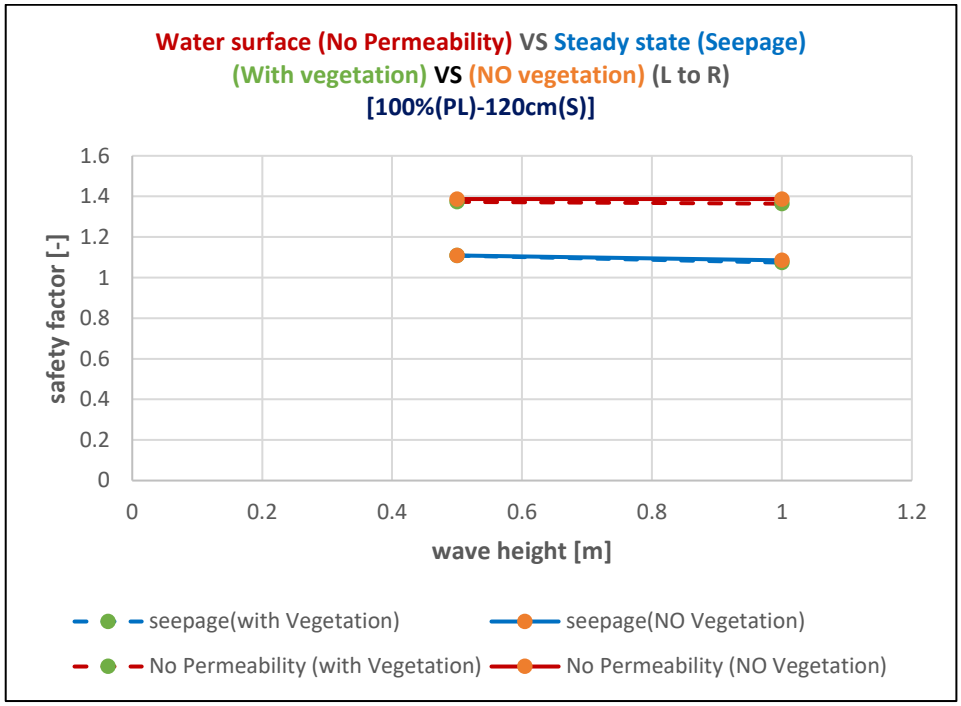

Figure 60. Wave-Included Analyses (spacing1.2m-pond level 100% comparison)

With the widest spacing, seepage results show the largest sensitivity to wave height and pond level, whereas impermeable cases remain almost constant. Vegetation effects remain secondary.

♣ Reference model (without reinforcement), (Tables 27-34) and (Figures 61-64):

Pond level: **2.38m(25%)** Wave effect		Water surface (No Permeability) (factors of safety) With & Without vegetation
Scenario number	Wave height (H) (m)	Left to Right
1	0.5	1.104
2	1	1.104
3	1.5	1.104
4	2	1.104
5	2.5	1.104
6	3	1.104
7	3.5	1.104
8	4	1.104

Table 27. Wave-Included Analyses (No geogrid-pond level 25%) (impermeable)

Pond level: **2.38m(25%)** Wave effect		Steady state (Seepage) (factors of safety) With & Without vegetation
Scenario number	Wave height (H) (m)	Left to Right
1	0.5	1.099
2	1	1.091
3	1.5	1.068
4	2	1.037
5	2.5	0.996
6	3	0.924
7	3.5	0.817
8	4	0.648

Table 28. Wave-Included Analyses (No geogrid-pond level 25%) (permeable)

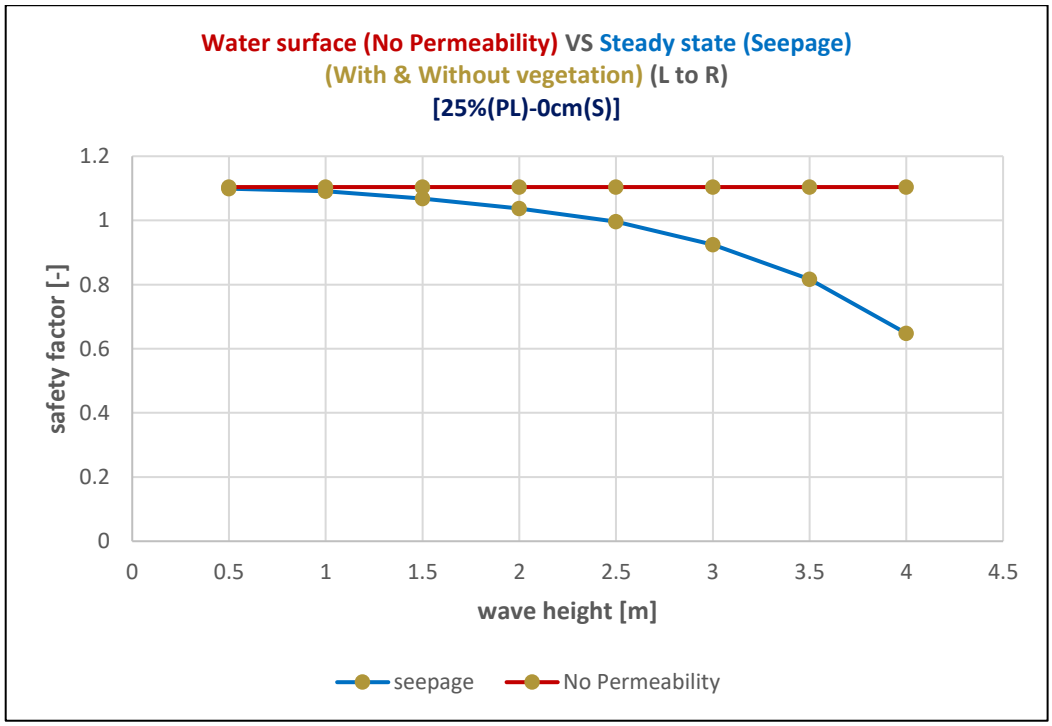

Figure 61. Wave-Included Analyses (No geogrid-pond level 25% comparison)

Pond level: **4.75m(50%)** Wave effect		Water surface (No Permeability) (factors of safety) With & Without vegetation
Scenario number	Wave height (H) (m)	Left to Right
1	0.5	1.104
2	1	1.104
3	1.5	1.104
4	2	1.104
5	2.5	1.104
6	3	1.104
7	3.5	1.104
8	4	1.104

Table 29. Wave-Included Analyses (No geogrid-pond level 50%) (impermeable)

Pond level: **4.75m(50%)** Wave effect		Steady state (Seepage) (factors of safety) With & Without vegetation
Scenario number	Wave height (H) (m)	Left to Right
1	0.5	1.057
2	1	1.036
3	1.5	1.005
4	2	0.966
5	2.5	0.917
6	3	0.846
7	3.5	0.731
8	4	0.641

Table 30. Wave-Included Analyses (No geogrid-pond level 50%) (permeable)

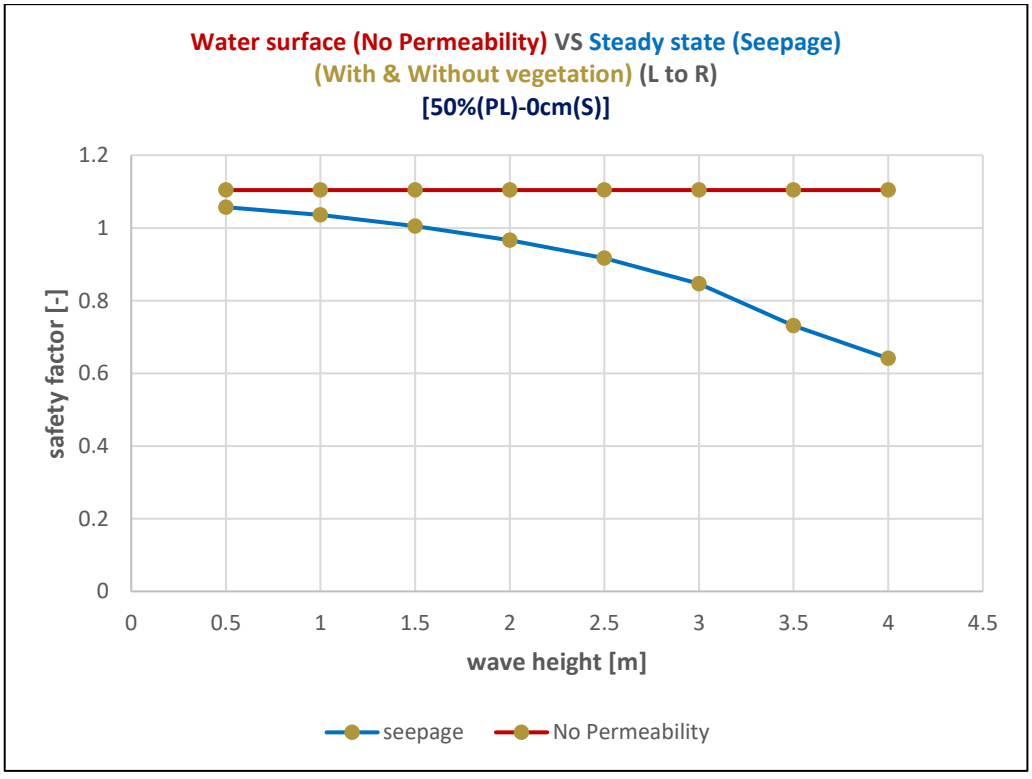

Figure 62. Wave-Included Analyses (No geogrid-pond level 50% comparison)

Pond level: **7.13m(75%)** Wave effect		Water surface (No Permeability) (factors of safety) With & Without vegetation
Scenario number	Wave height (H) (m)	Left to Right
1	0.5	1.104
2	1	1.104
3	1.5	1.104
4	2	1.104
5	2.5	1.104

Table 31. Wave-Included Analyses (No geogrid-pond level 75%) (impermeable)

Pond level: **7.13m(75%)** Wave effect		Steady state (Seepage) (factors of safety) With & Without vegetation
Scenario number	Wave height (H) (m)	Left to Right
1	0.5	0.962
2	1	0.933
3	1.5	0.9
4	2	0.861
5	2.5	0.795

Table 32. Wave-Included Analyses (No geogrid-pond level 75%) (permeable)

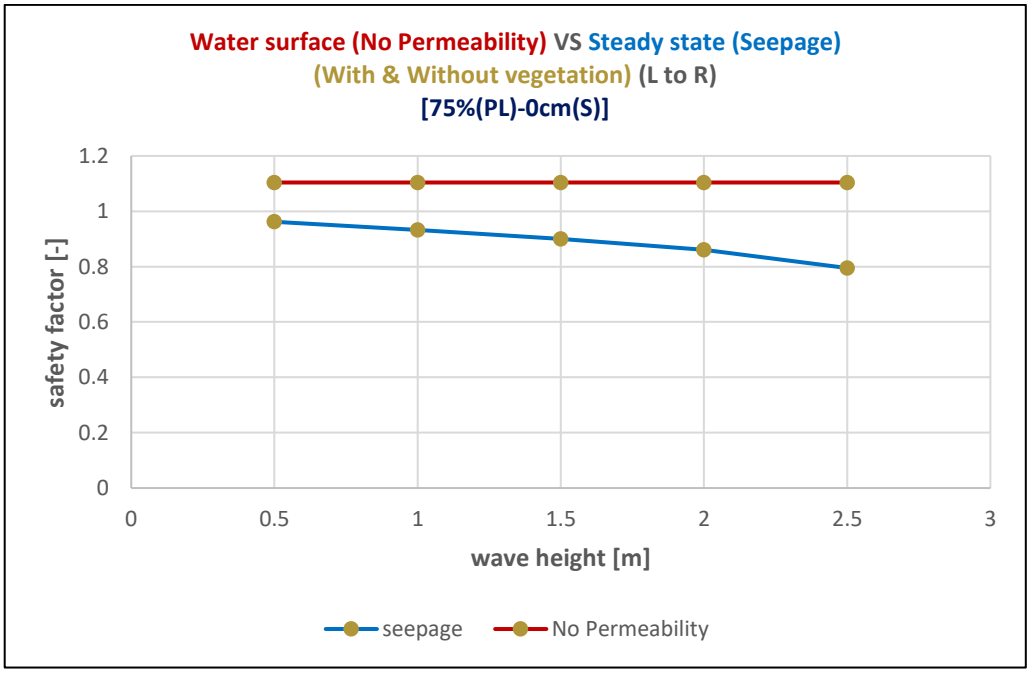

Figure 63. Wave-Included Analyses (No geogrid-pond level 75% comparison)

Pond level: **9.5m(100%)** Wave effect		Water surface (No Permeability) (factors of safety)
		With & Without vegetation
Scenario number	Wave height (H) (m)	Left to Right
1	0.5	1.104
2	1	1.104

Table 33. Wave-Included Analyses (No geogrid-pond level 100%) (impermeable)

Pond level: **9.5m(100%)** Wave effect		Steady state (Seepage) (factors of safety)
		With & Without vegetation
Scenario number	Wave height (H) (m)	Left to Right
1	0.5	0.834
2	1	0.812

Table 34. Wave-Included Analyses (No geogrid-pond level 100%) (permeable)

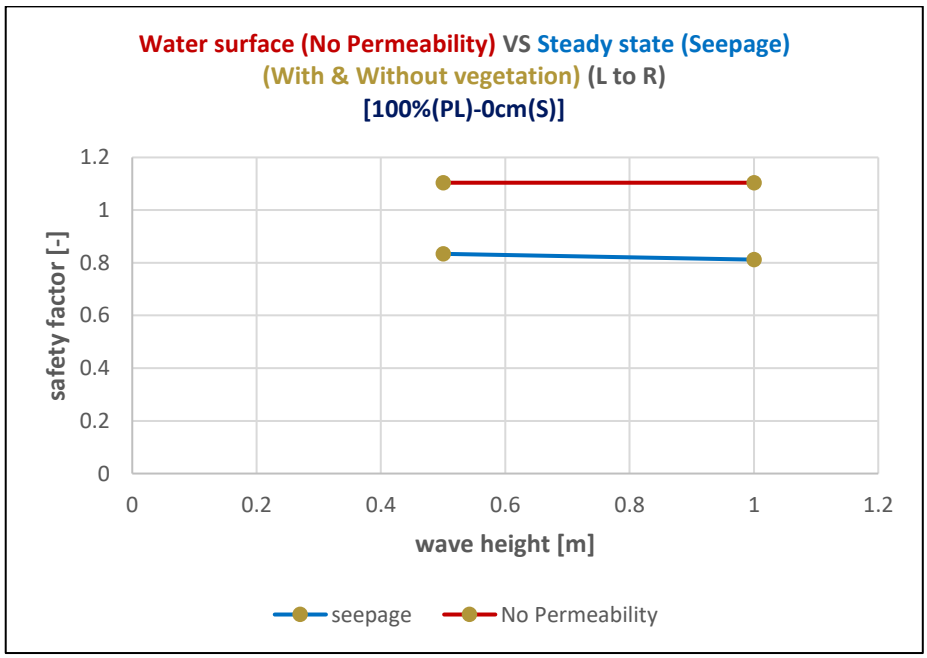

Figure 64. Wave-Included Analyses (No geogrid-pond level 100% comparison)

This configuration gives the lowest stability, particularly under seepage where factor of safety drops rapidly with increasing wave height. Impermeable cases remain nearly constant but at a lower baseline than reinforced models.

Interpretation of Wave-Included Results

The given results (Tables 3-34 and Figures 49-64) provide a clear separation between the impermeable condition, reported in the outputs as "Water surface (No Permeability)," and the steady-state seepage condition. Under the impermeable (Water surface) representation, the factor of safety is essentially insensitive to wave height for a fixed pond level and remains constant across the wave-height series shown in the tables. This behaviour is consistent across reinforcement spacings and pond levels, indicating that within the selected modelling assumption, the wave-height variation does not alter the computed stability response for the impermeable condition.

In contrast, under steady-state seepage, the factor of safety decreases systematically as wave height increases, demonstrating that wave loading acts as an additional destabilising mechanism when pore-water pressures are allowed to develop. This pattern is evident for all reinforcement spacings and becomes most critical in the no-geogrid reference case. For example, at pond level 25% (2.38 m), the seepage results show a progressive reduction with increasing wave height, reaching 1.09 at H = 4 m for the 0.60 m spacing vegetated case (Table 4), 0.961 at H = 4 m for the 0.90 m spacing vegetated case (Table 12), and 0.882 at H = 4 m for the 1.20 m spacing vegetated case (Table 20). The no-geogrid seepage case reaches 0.648 at H = 4 m (Table 28), highlighting that the absence of reinforcement produces the most critical stability envelope under combined seepage and wave loading.

The influence of reinforcement spacing is consistent across the wave-included scenarios. For both hydraulic conditions, closer reinforcement spacing yields higher stability, but its benefit becomes particularly important under seepage where wave-induced reductions can be significant. At the maximum wave height available for pond level 25%, the seepage results show that the reinforced cases remain clearly above the no-geogrid reference case, confirming that reinforcement spacing is a primary mechanical parameter controlling stability even when hydraulic loading is adverse.

Pond level also influences the admissible wave-loading combinations and the overall stability trend. The tables show that as pond level increases to 75% and 100%, fewer wave heights are included in the scenario sets, reflecting the requirement that wave elevation must not exceed the dam crest. This constraint is visible in the reported maximum wave heights, where pond level 75% is limited to H = 2.5 m and pond level 100% is limited to H = 1.0 m across the wave tables. This modelling choice supports the physical realism of the comparisons, while also indicating that at higher reservoir levels, even smaller waves occur under a reduced freeboard condition.

The vegetation comparison, represented by "with vegetation" versus "without vegetation" columns, shows that the "without vegetation" results are typically slightly higher than the corresponding "with vegetation" results for reinforced models. This difference is consistent with the adopted vegetation modelling assumption, in which reinforcement is excluded within the upper 1 m for vegetated cases. Although the vegetation-related differences remain present across spacings and pond levels, they are generally smaller than the reductions caused by seepage and increasing wave height, indicating that hydraulic condition and wave loading dominate the critical response under the wave-included seepage scenarios.

4.3.2 Results for static-water analyses

In the following section, the results correspond to dam models without wave effects, where only static reservoir water levels were considered. The results compare the influence of reinforcement-layer spacing under permeable and impermeable conditions and evaluate the effect of vegetation, through paired simulations with and without vegetative cover. The computed factors of safety are summarised in (Tables 35-42) and illustrated in (Figures 65-68).

The results are presented in two stages: first the numerical results, followed by the corresponding graphs.

- **Spacing Between Supports (0.6 m), (Tables 35-36) and (Figures 65-68):**

Pond Level(m) ↓	Without wave-affected scenarios		
	Support:60 cm	Water surface (No Permeability) (factors of safety)	
	Pond Level ($\%H_{P.\,Max}$) ↓	With vegetation	Without vegetation
		Left to Right	Left to Right
0m	0	1.581	1.626
2.38m	25	1.581	1.626
4.75m	50	1.581	1.626
7.13m	75	1.581	1.626
9.5m	100	1.581	1.626

Table 35. Support:60 cm (impermeable-vegetated & non vegetated)

Pond Level(m) ↓	Without wave-affected scenarios		
	Support:60 cm	Steady state (Seepage) (factors of safety)	
	Pond Level ($\%H_{P.\,Max}$) ↓	With vegetation	Without vegetation
		Left to Right	Left to Right
0m	0	1.581	1.626
2.38m	25	1.577	1.624
4.75m	50	1.539	1.584
7.13m	75	1.447	1.495
9.5m	100	1.317	1.346

Table 36. Support:60 cm (permeable-vegetated & non vegetated)

These tables provide the baseline (no-wave) factor of safety for the closest reinforcement spacing under impermeable (Table35) and seepage conditions (Table36). The paired "with/without vegetation" columns quantify the small vegetation-related shift under the same hydraulic boundary conditions.

♣ Spacing Between Supports (0.9 m), (Tables 37-38) and (Figures 65-68):

Pond Level(m) ↓	Without wave-affected scenarios		
	Support:90 cm	Water surface (No Permeability) (factors of safety)	
	Pond Level ($\%H_{P.\,Max}$) ↓	With vegetation	Without vegetation
		Left to Right	Left to Right
0m	0	1.438	1.474
2.38m	25	1.438	1.474
4.75m	50	1.438	1.474
7.13m	75	1.438	1.474
9.5m	100	1.438	1.474

Table 37. Support:90 cm (impermeable-vegetated & non vegetated)

Pond Level(m) ↓	Without wave-affected scenarios		
	Support:90 cm	Steady state (Seepage) (factors of safety)	
	Pond Level ($\%H_{P.\,Max}$) ↓	With vegetation	Without vegetation
		Left to Right	Left to Right
0m	0	1.438	1.474
2.38m	25	1.436	1.473
4.75m	50	1.403	1.433
7.13m	75	1.324	1.344
9.5m	100	1.195	1.215

Table 38. Support:90 cm (permeable-vegetated & non vegetated)

This spacing represents an intermediate reinforcement layout and is included to show how the stability level changes when reinforcement is less frequent, under the same static reservoir levels. The results are reported in the same impermeable (Table37) vs seepage (Table38) format to keep comparisons consistent across the chapter.

♣ Spacing Between Supports (1.2 m), (Tables 39-40) and (Figures 65-68):

Pond Level(m) ↓	Without wave-affected scenarios		
	Support:120 cm	Water surface (No Permeability) (factors of safety)	
	Pond Level ($\%H_{P.\,Max}$) ↓	With vegetation	Without vegetation
		Left to Right	Left to Right
0m	0	1.373	1.387
2.38m	25	1.373	1.387
4.75m	50	1.373	1.387
7.13m	75	1.373	1.387
9.5m	100	1.373	1.387

Table 39. Support:120 cm (impermeable-vegetated & non vegetated)

Pond Level(m) ↓	Without wave-affected scenarios		
	Support:120 cm	Steady state (Seepage) (factors of safety)	
	Pond Level ($\%H_{P.\ Max}$) ↓	With vegetation	Without vegetation
		Left to Right	Left to Right
0m	0	1.373	1.387
2.38m	25	1.372	1.384
4.75m	50	1.346	1.347
7.13m	75	1.259	1.259
9.5m	100	1.131	1.132

Table 40. Support:120 cm (permeable-vegetated & non vegetated)

These results provide the response for the widest reinforcement spacing (Tables 39-40), supporting direct comparison with the tighter spacing configurations. They are particularly useful for identifying the spacing-dependent stability margin at the highest reservoir levels.

♣ Reference model (without reinforcement), (Tables 41-42) and (Figures 65-68):

Pond Level(m) ↓	Without wave-affected scenarios		
	No Geogrid	Water surface (No Permeability) (factors of safety)	
	Pond Level ($\%H_{P.\ Max}$) ↓	With vegetation	Without vegetation
		Left to Right	Left to Right
0m	0	1.104	1.104
2.38m	25	1.104	1.104
4.75m	50	1.104	1.104
7.13m	75	1.104	1.104
9.5m	100	1.104	1.104

Table 41. No geogrid (impermeable-vegetated & non vegetated)

Pond Level(m) ↓	Without wave-affected scenarios		
	No Geogrid	Steady state (Seepage) (factors of safety)	
	Pond Level ($\%H_{P.\ Max}$) ↓	With vegetation	Without vegetation
		Left to Right	Left to Right
0m	0	1.104	1.104
2.38m	25	1.102	1.102
4.75m	50	1.07	1.07
7.13m	75	0.989	0.989
9.5m	100	0.858	0.858

Table 42. No geogrid (permeable-vegetated & non vegetated)

This case is presented as the reference model without reinforcement, forming the lower-bound baseline for the static-water condition. It is used to quantify the net benefit of reinforcement at each reservoir level before introducing additional wave loading.

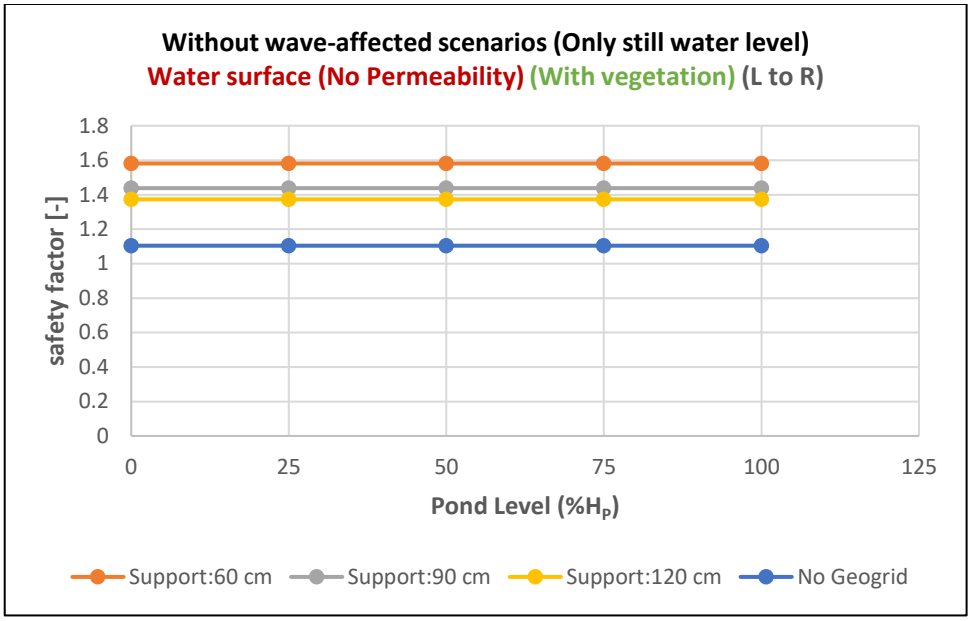

Figure 65. Static-Water Analyses (impermeable-vegetated)

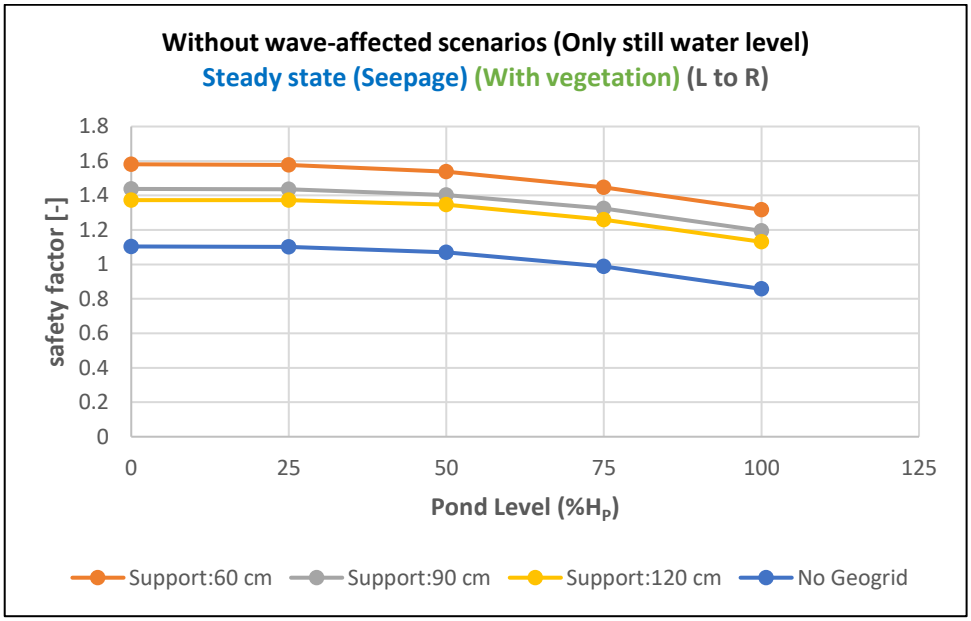

Figure 66. Static-Water Analyses (permeable-vegetated)

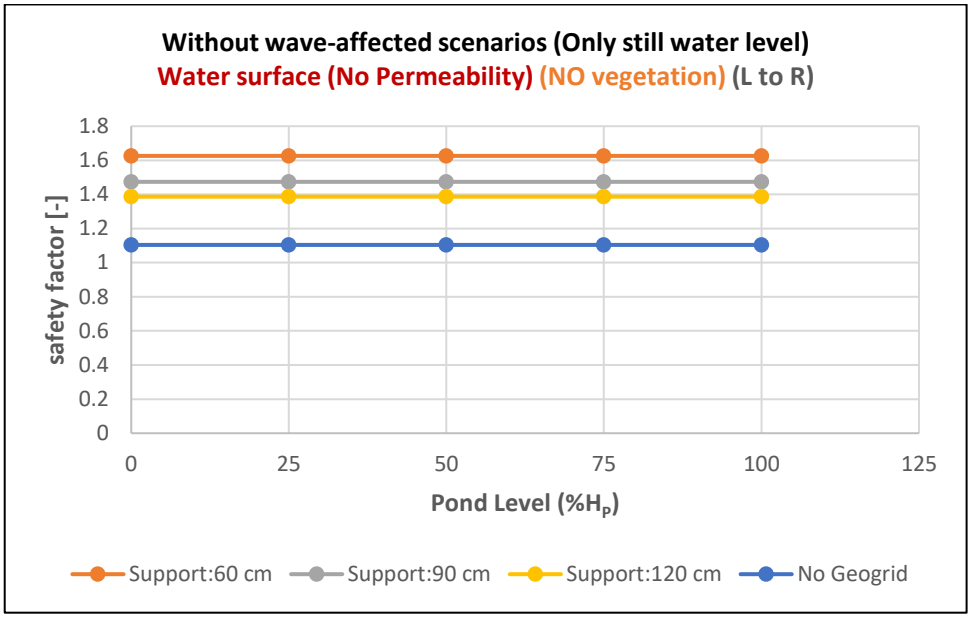

Figure 67. Static-Water Analyses (impermeable-non vegetated)

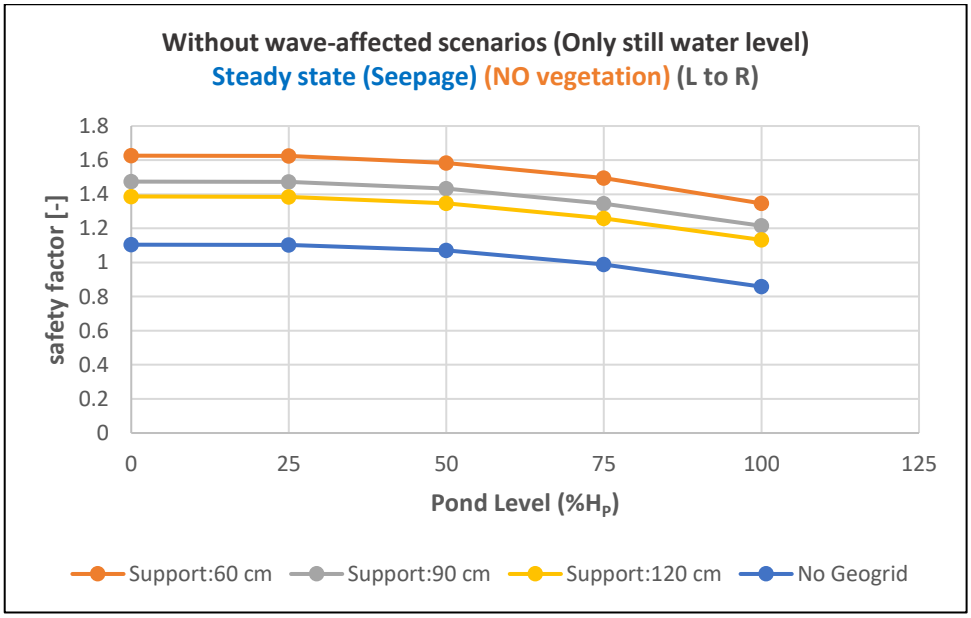

Figure 68. Static-Water Analyses (permeable-non vegetated)

Interpretation of Static-Water Results

The static-water results (Tables 35-42 and Figures 65-68) further emphasise the dominant role of seepage in controlling stability response under rising reservoir levels. Under the impermeable condition reported as "Water surface (No Permeability)," the factor of safety remains constant across pond levels for each reinforcement configuration. For example, Support 0.60 m remains 1.581 (with vegetation) and 1.626 (without vegetation) from 0 m through 9.5 m (Table 35), and the same constant behaviour appears for Support 0.90 m (Table 37), Support 1.20 m (Table 39), and the no-geogrid reference model (Table 41). This indicates that within the impermeable representation used in these simulations, increasing the reservoir level does not change the computed stability response.

In steady-state seepage conditions, however, the results show a consistent reduction in factor of safety as pond level increases, demonstrating that rising reservoir level becomes destabilising once seepage is enabled. This trend is evident across all reinforcement spacings and is most pronounced at higher reservoir levels. For instance, Support 0.60 m decreases from 1.577 at 25% (2.38 m) to 1.317 at 100% (9.5 m) in the vegetated case (Table 36), while Support 0.90 m decreases from 1.436 to 1.195 (Table 38), and Support 1.20 m decreases from 1.372 to 1.131 (Table 40). The no-geogrid seepage case decreases from 1.102 at 25% to 0.858 at 100% (Table 42), forming the lowest stability envelope among the static-water scenarios. These results confirm that pore-pressure effects associated with seepage control the sensitivity of stability to reservoir level.

Reinforcement spacing continues to show a clear mechanical influence in the static-water seepage results. Although all seepage cases decrease with increasing pond level, closer reinforcement spacing maintains higher safety factors and preserves a larger stability margin at high reservoir levels compared with wider spacing and especially compared with the unreinforced model. This is consistent with the overall stability ranking observed across the chapter and supports the interpretation that reinforcement spacing is a key design parameter under adverse hydraulic conditions.

The vegetation effect in static-water scenarios follows the same pattern observed in wave-included results. For reinforced models, "without vegetation" typically yields slightly higher factors of safety than "with vegetation," which is consistent with the modelling assumption that excludes reinforcement within the upper 1 m in vegetated scenarios. However, as reservoir level rises under seepage, the magnitude of seepage-induced reduction becomes substantially larger than the vegetation-related differences, again highlighting that hydraulic condition dominates the critical response.

4.3.3 Additional scenario to examine potential adverse vegetation effects

Following the analyses, an additional scenario was defined to verify whether removing reinforcement layers within the upper 1 m (as assumed in vegetation scenarios) is, by itself, sufficient to produce a meaningful effect in the calculations.

For this purpose, a scenario was considered in which, in addition to removing the reinforcement layer within the upper 1 m, the soil strength parameters were also reduced to:

- Friction angle: 34° → 27°
- Cohesion: 17 kPa → 11 kPa

This modification was introduced to enable a clearer comparison. To better isolate and understand the influence of these changes, they were applied to the most critical case, namely the dam model without reinforcement layers. The corresponding results for the factor of safety are presented in (Tables 43-50) and (Figures 69-72) in the following section.

Pond level: **2.38m(25%)** Wave effect		Water surface (No Permeability) (Factor of safety)	
		No change in properties	New properties
Scenario number	Wave height (H) (m)	Left to Right	Left to Right
1	0.5	1.104	1.056
2	1	1.104	1.056
3	1.5	1.104	1.056
4	2	1.104	1.056
5	2.5	1.104	1.056
6	3	1.104	1.056
7	3.5	1.104	1.056
8	4	1.104	1.056

Table 43. Verification Scenario for Vegetation (impermeable (PL:25%)-old properties vs new properties)

Pond level: **2.38m(25%)** Wave effect		Steady state (Seepage) (Factor of safety)	
		No change in properties	New properties
Scenario number	Wave height (H) (m)	Left to Right	Left to Right
1	0.5	1.099	1.053
2	1	1.091	1.045
3	1.5	1.068	1.026
4	2	1.037	0.998
5	2.5	0.996	0.947
6	3	0.924	0.885
7	3.5	0.817	0.803
8	4	0.648	0.635

Table 44. Verification Scenario for Vegetation (permeable (PL:25%)-old properties vs new properties)

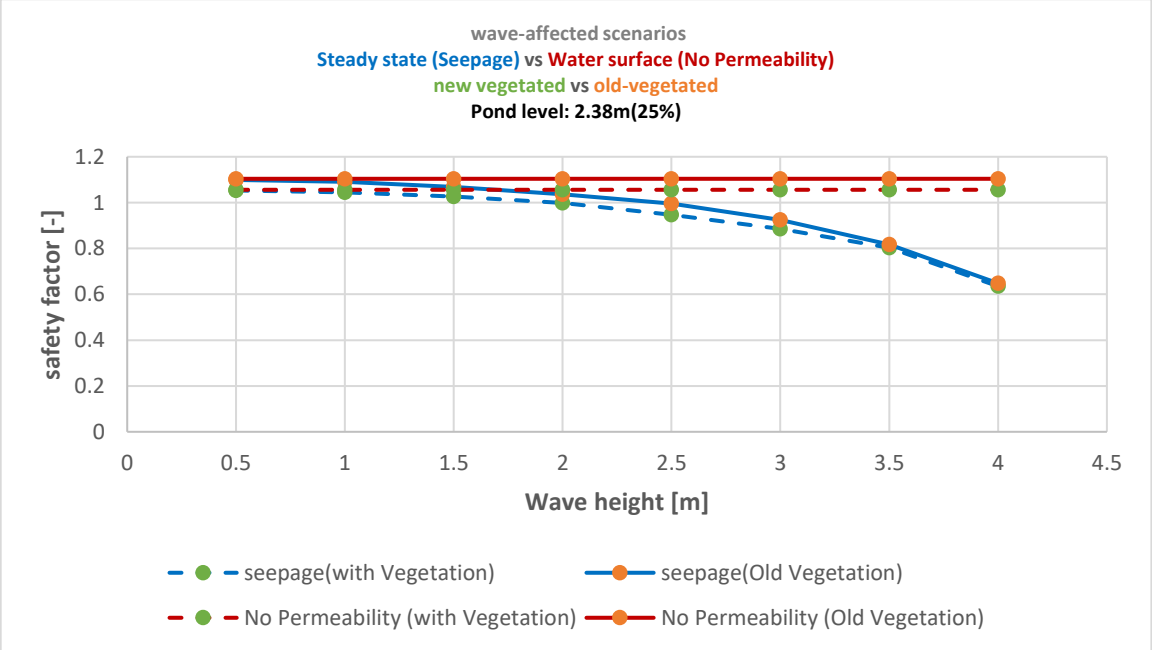

Figure 69. Verification Scenario for Vegetation (No geogrid-pond level 25% comparison)

Pond level: **4.75m(50%)** Wave effect		Water surface (No Permeability) (Factor of safety)	
		No change in properties	New properties
Scenario number	Wave height (H) (m)	Left to Right	Left to Right
1	0.5	1.104	1.056
2	1	1.104	1.056
3	1.5	1.104	1.056
4	2	1.104	1.056
5	2.5	1.104	1.056
6	3	1.104	1.056
7	3.5	1.104	1.056
8	4	1.104	1.056

Table 45. Verification Scenario for Vegetation (impermeable (PL:50%)-old properties vs new properties)

Pond level: **4.75m(50%)** Wave effect		Steady state (Seepage) (Factor of safety)	
		No change in properties	New properties
Scenario number	Wave height (H) (m)	Left to Right	Left to Right
1	0.5	1.057	1.012
2	1	1.036	0.997
3	1.5	1.005	0.966
4	2	0.966	0.927
5	2.5	0.917	0.878
6	3	0.846	0.823
7	3.5	0.731	0.712
8	4	0.641	0.612

Table 46. Verification Scenario for Vegetation (permeable (PL:50%)-old properties vs new properties)

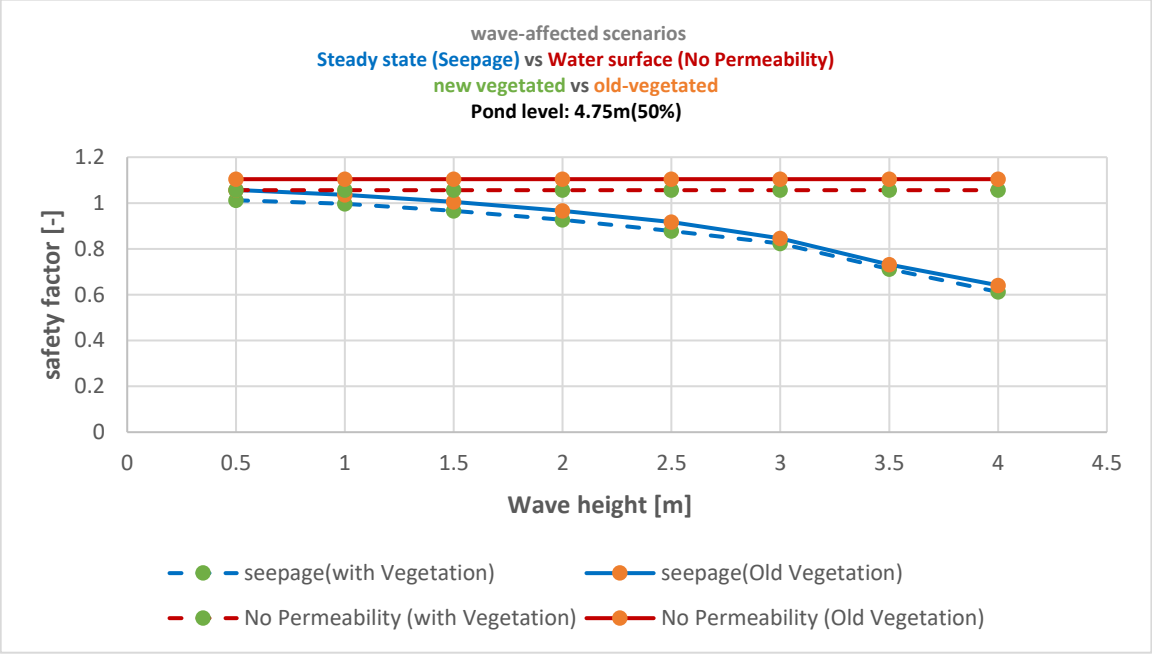

Figure 70. Verification Scenario for Vegetation (No geogrid-pond level 50% comparison)

Pond level: **7.13m(75%)** Wave effect		Water surface (No Permeability) (Factor of safety)	
		No change in properties	New properties
Scenario number	Wave height (H) (m)	Left to Right	Left to Right
1	0.5	1.104	1.056
2	1	1.104	1.056
3	1.5	1.104	1.056
4	2	1.104	1.056
5	2.5	1.104	1.056

Table 47. Verification Scenario for Vegetation (impermeable (PL:75%)-old properties vs new properties)

Pond level: **7.13m(75%)** Wave effect		Steady state (Seepage) (Factor of safety)	
		No change in properties	New properties
Scenario number	Wave height (H) (m)	Left to Right	Left to Right
1	0.5	0.962	0.922
2	1	0.933	0.894
3	1.5	0.9	0.861
4	2	0.861	0.824
5	2.5	0.795	0.763

Table 48. Verification Scenario for Vegetation (permeable (PL:75%)-old properties vs new properties)

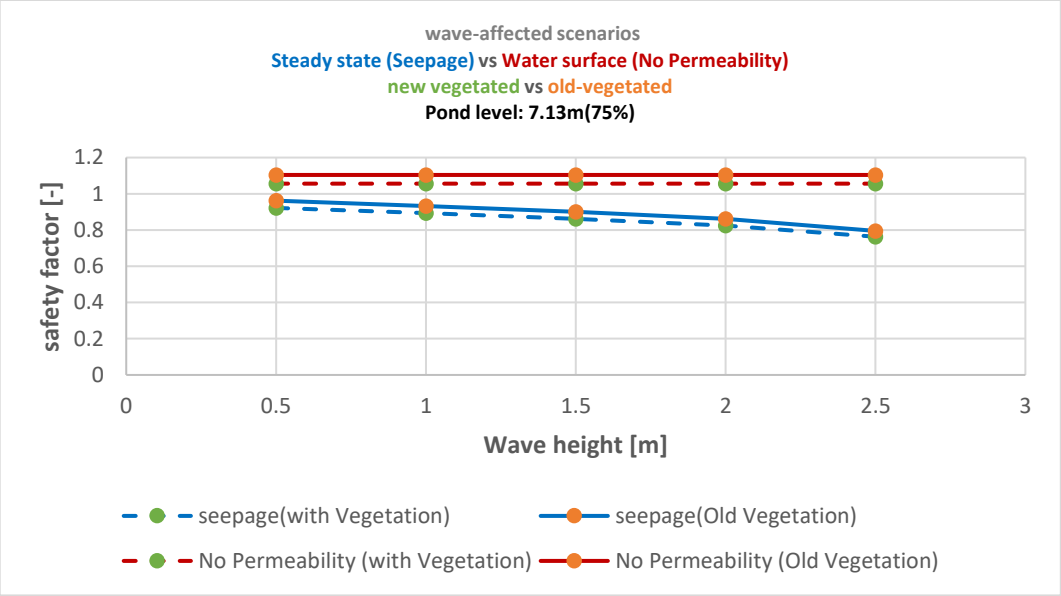

Figure 71. Verification Scenario for Vegetation (No geogrid-pond level 75% comparison)

Pond level: **9.5m(100%)** Wave effect		Water surface (No Permeability) (Factor of safety)	
		No change in properties	New properties
Scenario number	Wave height (H) (m)	Left to Right	Left to Right
1	0.5	1.104	1.056
2	1	1.104	1.056

Table 49. Verification Scenario for Vegetation (impermeable (PL:100%)-old properties vs new properties)

Pond level: **9.5m(100%)** Wave effect		Steady state (Seepage) (Factor of safety)	
		No change in properties	New properties
Scenario number	Wave height (H) (m)	Left to Right	Left to Right
1	0.5	0.834	0.799
2	1	0.812	0.774

Table 50. Verification Scenario for Vegetation (permeable (PL:100%)-old properties vs new properties)

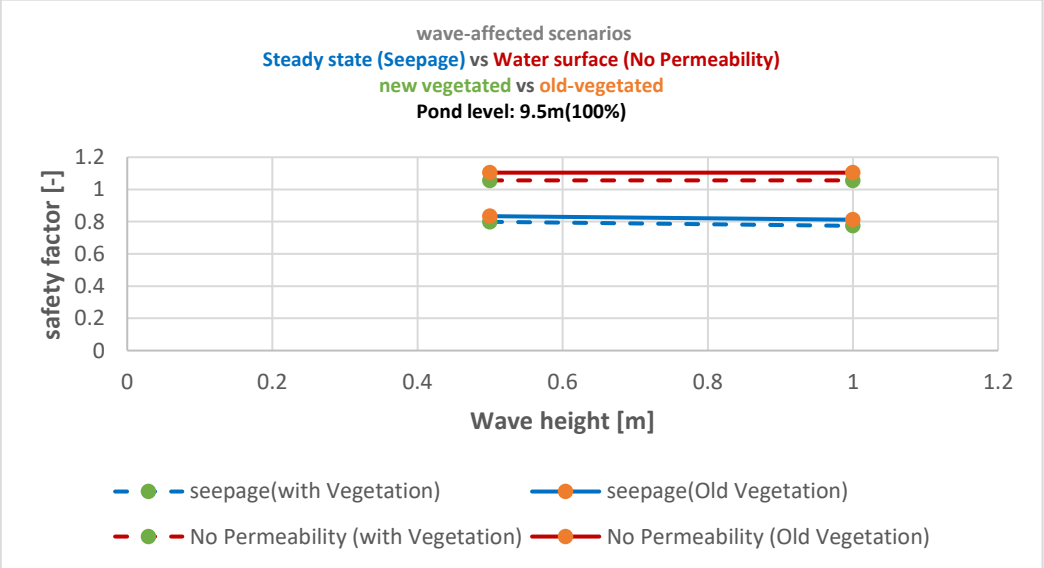

Figure 72. Verification Scenario for Vegetation (No geogrid-pond level 100% comparison)

Interpretation of the Verification Scenario

In the last set of scenarios, Verification Scenario (Tables 43-50 and Figures 69-72) was introduced to evaluate whether the vegetation modelling assumption based solely on excluding reinforcement within the upper 1 m is sufficient to represent a meaningful vegetation influence on stability. In this verification, the most critical configuration (no geogrid) was examined by comparing "no change in properties" with "new properties," where the shear-strength parameters were reduced to c = 11 kPa and $\Phi = 27°$.

The results show that under the impermeable condition reported as "Water surface (No Permeability)," the computed factors of safety remain constant across wave heights for each pond level, consistent with the broader behaviour observed throughout Chapter 4 for impermeable cases. However, the "new properties" column produces a systematically lower factor of safety compared with the baseline column. For example, at pond level 25% the baseline value of 1.104 reduces to 1.056 for the modified properties (Table 43), showing that when strength reduction is introduced, the stability margin decreases even under the impermeable representation.

Under seepage, the verification scenario demonstrates that the modified properties have a more pronounced effect under combined hydraulic loading. For pond level 25%, the seepage results reduce from 0.648 to 0.635 at H = 4 m (Table 44). For higher pond levels, the trend remains consistent, with the modified properties producing lower stability than the baseline at the same wave height and pond level, such as the reduction from 0.812 to 0.774 at pond level 100% and H = 1.0 m (Table 50). This indicates that once seepage governs the response, even relatively small reductions in strength parameters can further decrease stability.

Overall, the verification scenario confirms that excluding reinforcement within the upper 1 m captures only one component of the vegetation modelling assumption, namely a structural reduction in reinforcement contribution. When strength reduction is also considered, the stability decreases further, especially under seepage and wave loading. This supports the need to interpret vegetation effects cautiously and highlights that vegetation-related mechanisms may be better represented through combined structural and strength-based modelling assumptions when a conservative evaluation is required.

4.4 Synthesis of Results and Concluding Remarks

The results presented in Section 4.3 demonstrate that reinforcement spacing is a consistent mechanical control on slope stability across all loading cases. For both wave-included and static-water analyses, closer spacing produces higher factors of safety than wider spacing, and the no-geogrid reference model forms the lowest stability envelope. This overall ranking persists under both hydraulic representations, indicating that reinforcement layout governs baseline performance.

A clear contrast emerges between the impermeable condition and steady-state seepage. In the results tables and graphs, the impermeable condition is represented as "Water surface (No Permeability)," and under this representation the factor of safety remains essentially constant with changing reservoir level and wave height. In steady-state seepage conditions, however, the factor of safety decreases as reservoir level increases in static-water scenarios and decreases further when wave loading is included. This shows that seepage governs the sensitivity of stability to hydraulic loading, while wave effects mainly act as an amplifier when seepage is active.

Vegetation, as represented in this chapter through reinforcement exclusion within the upper 1 m, generally produces slightly lower stability than the corresponding non-vegetated cases for reinforced models, because the reinforcement remains continuous only in the "without vegetation" scenarios. While this difference is visible in both wave-included and static-water comparisons, it is typically smaller than the reductions caused by seepage and increasing wave height, particularly in the more critical hydraulic scenarios.

The verification scenario was included to assess whether the vegetation modelling assumption adopted in this study is adequately represented by excluding reinforcement only within the upper 1 m. To examine this, the most critical configuration (the no-geogrid model) was analysed in two versions: one with no change in soil strength parameters, and a second in which the reinforcement exclusion was combined with reduced parameters (c = 11 kPa and Φ = 27°). These reduced parameters were introduced as a conservative sensitivity case to represent a potentially adverse condition and to evaluate the influence of additional strength degradation beyond reinforcement exclusion alone. The results show that the reduced-parameter case yields lower factors of safety than the unchanged-parameter case, with the difference becoming more evident under steady-state seepage and wave loading, where the dam is closer to instability. This indicates that reinforcement exclusion alone represents only one component of a potentially adverse vegetation-related condition, while the combined assumption provides a more conservative stability check under critical hydraulic scenarios.

In conclusion, the most critical stability envelope is associated with the combined presence of steady-state seepage and wave loading, particularly at higher reservoir levels and for wider reinforcement spacing or the unreinforced reference case. Conversely, the impermeable condition represented by "Water surface (No Permeability)" provides a stable baseline response in the reported outputs, enabling the incremental effects of seepage, waves, reinforcement spacing, and vegetation modelling assumptions to be isolated and compared consistently.

Chapter 5

Conclusions, Implications, and Future Work

5.1 Conclusions

This thesis investigated the stability of reinforced-soil embankment dams under combined hydraulic and mechanical actions, with particular attention to the influence of reservoir water level, seepage conditions, wave-induced loading, and vegetation-related assumptions. The study combined a focused literature review with a parametric numerical investigation carried out using Slide2 within a limit-equilibrium framework. A single reference embankment geometry was adopted, and key variables were modified systematically to isolate their influence on the computed factor of safety.

A central conclusion is that the hydraulic condition of the dam, and particularly the development of seepage and pore-water pressures, governs the stability response more strongly than any other single factor considered. When seepage is present, increases in reservoir level led to higher pore-water pressures and reduced effective stresses, producing a consistent reduction in stability. In contrast, under impermeable (non-seepage) conditions, the dam response is generally less sensitive to reservoir level changes because destabilising pore-pressure build-up does not develop within the embankment body.

Wave loading was found to play a secondary but meaningful role, especially when combined with high reservoir levels and seepage. In the context of this thesis, waves were considered as surface disturbances potentially associated with landslide impacts into mountain basins. When the embankment is already hydraulically stressed by seepage, additional hydrodynamic forcing at the upstream face can further reduce stability margins. The most conservative stability condition therefore corresponds to the combined envelope of high reservoir level, seepage, and wave loading.

Reinforcement significantly improved global stability, but its effectiveness depended on the reinforcement configuration. In particular, wider vertical spacing between reinforcement layers resulted in lower stability than denser reinforcement layouts, confirming that reinforcement density is a controlling design variable in reinforced embankment systems. As a consequence, stability checks should focus not only on the presence of reinforcement, but also on its layout, particularly in scenarios dominated by adverse hydraulic actions.

Vegetation was treated as a dual-factor issue. While the literature highlights stabilising mechanisms such as root reinforcement and hydrological regulation, the numerical analyses provided in this thesis also explored the potential adverse case where root intrusion or vegetation development interferes with the continuity of the engineered reinforcement system. This was represented through conservative scenarios in which reinforcement was omitted within a root-affected surface zone. The results showed that such a local loss of reinforcement continuity can measurably reduce the factor of safety, implying that vegetation cannot be considered automatically beneficial in reinforced embankment dams and must be managed in coordination with reinforcement and drainage functions.

Overall, the thesis demonstrates that embankment-dam stability is controlled by the interaction between hydraulic loading (water level, seepage, waves) and engineered measures

(reinforcement layout), and that vegetation must be treated as a design-and-management variable whose effects depend on how it interacts with the structural system.

5.2 Engineering Implications and Recommendations

The findings of this thesis lead to practical implications for the design and management of reinforced embankment dams.

First, seepage control should be treated as a priority in both design and operation. The results indicate that seepage is the condition that makes stability most sensitive to reservoir level and wave loading. For this reason, drainage continuity, filter performance, and seepage-path management should be addressed explicitly in stability checks and in operational rules, particularly for high-water conditions.

Second, reinforcement layout should be considered a governing parameter rather than a secondary detail. Even when the reinforcement material properties are constant, changes in reinforcement spacing can significantly alter the stability response. Conservative evaluations should therefore include the least favourable reinforcement configuration within the design range, and special attention should be given to scenarios combining high water and seepage.

Third, vegetation should be integrated through a controlled zoning and species-selection strategy. Where vegetation is used for erosion protection or ecological integration, its placement should be coordinated with the internal reinforcement system and drainage elements. The results support the need to prevent root systems from interacting with critical engineered layers, while still allowing surface coverage sufficient to limit erosion. In this sense, vegetation management should be treated as part of the dam's safety strategy rather than as an aesthetic or purely environmental measure.

Finally, the most conservative scenario envelope for stability assessment should include combined loading conditions. In the scenario set analysed in this thesis, the combination of high reservoir level, seepage, and wave loading represents the critical condition that should guide risk-averse evaluation, particularly for cases with wider reinforcement spacing or locally reduced reinforcement continuity.

5.3 Future Work

Future work should refine the coupled nature of the problem by (i) moving from steady-state to transient seepage and drawdown analyses to capture time-dependent pore-pressure evolution, (ii) extending the stability assessment to three-dimensional conditions where valley geometry and spatial heterogeneity may influence the critical mechanism, and (iii) deriving wave actions from physically based models of landslide-generated disturbances, including upstream run-up effects. In parallel, vegetation modelling could be enhanced by incorporating both root mechanical reinforcement and hydro-mechanical processes (e.g., suction changes), while systematically testing zoning strategies and species-dependent root architectures to limit adverse interactions with reinforcement and drainage systems.

References

Arnone, E. et al. (2016) 'Modeling the hydrological and mechanical effect of roots on shallow landslides,' *Water Resources Research*, *52*, pp. 8590–8612. https://doi.org/10.1002/2015WR018227.

Benson, C. H., Kucukkirca, I. E. and Scalia, J (2010) 'Properties of geosynthetics exhumed from a final cover at a solid waste landfill,' *Geotextiles and Geomembranes*, *28*, pp. 536–546. https://doi.org/10.1016/j.geotexmem.2010.03.001.

Berg, R. R., Christopher, B. R. and Samtani, N. C (2009) *Design and construction of mechanically stabilized earth walls and reinforced soil slopes (Vol*. II) (Publication No. FHWA-NHI-10-025). Federal Highway Administration, U.S. Department of Transportation.

Bishop, D. M. and Stevens, M. E (1964) *Landslides on logged areas in Southeast Alaska (U.S*. Forest Service Research Paper NOR-1). Northern Forest Experiment Station, Forest Service, U.S. Department of Agriculture.

Bordoloi, S. and Ng, C. W. W (2020) 'The effects of vegetation traits and their stability functions in bio-engineered slopes: A perspective review,' *Engineering Geology*, *275*, p. 105742. https://doi.org/10.1016/j.enggeo.2020.105742.

Cazzuffi, D., Cardile, G. and Gioffrè, D (2014) 'Geosynthetic engineering and vegetation growth in soil reinforcement applications,' *Transportation Infrastructure Geotechnology*, *1*, pp. 262–300. https://doi.org/10.1007/s40515-014-0016-1.

Cislaghi, A., Chiaradia, E. A. and Bischetti, G. B (2017) 'Including root reinforcement variability in a probabilistic 3D stability model,' *Earth Surface Processes and Landforms*, *42*, pp. 1789–1806. https://doi.org/10.1002/esp.4127.

Comité Français des Géosynthétiques (2017) *General recommendations for the use of geomembranes in barrier systems (2017 ed.)*.

Deng, Y. et al. (2020) 'Vegetation greening intensified soil drying in some semi-arid and arid areas of the world,' *Agricultural and Forest Meteorology*, *292–293*, p. 108103. https://doi.org/10.1016/j.agrformet.2020.108103.

Federal Emergency Management Agency (2014) *Overtopping protection for dams: Best practices for design, construction, problem identification and evaluation, inspection, maintenance, renovation, and repair (FEMA P-1014)*.

Giadrossich, F. et al. (2017) 'Methods to measure the mechanical behaviour of tree roots: A review,' *Ecological Engineering*, *109*, pp. 256–271. https://doi.org/10.1016/j.ecoleng.2017.08.032.

Ito, T (2010) *Tree root encroachment on levee drainage system (Master's thesis)*. University of New Mexico.

Leung, A. K. et al. (2018) 'Plant age effects on soil infiltration rate during early plant establishment,' *Géotechnique*, *68(7)*, pp. 646–652.

Leung, A. K. et al. (2015) 'Effects of the roots of Cynodon dactylon and Schefflera heptaphylla on water infiltration rate and soil hydraulic conductivity,' *Hydrological Processes*, *29*, pp. 3342–3354. https://doi.org/10.1002/hyp.10452.

Li, P. et al. (2022) 'Study on the shear strength of root-soil composite and root reinforcement mechanism,' *Forests*, *13(6)*, p. 898. https://doi.org/10.3390/f13060898.

Löbmann, M. T. et al. (2020) 'The influence of herbaceous vegetation on slope stability A review,' *Earth-Science Reviews*, *209*, p. 103328. https://doi.org/10.1016/j.earscirev.2020.103328.

Masi, E. B., Segoni, S. and Tofani, V (2021) 'Root reinforcement in slope stability models: A review,' *Geosciences*, *11(5)*, p. 212. https://doi.org/10.3390/geosciences11050212.

Ni, J. J. et al. (2018) 'Modelling hydro-mechanical reinforcements of plants to slope stability,' *Computers and Geotechnics*, *95*, pp. 99–109. https://doi.org/10.1016/j.compgeo.2017.09.001.

Olinic, T., Olinic, E.-D. and Butcaru, A.-C (2024) 'Integrating geosynthetics and vegetation for sustainable erosion control applications,' *Sustainability*, *16*, p. 10621. https://doi.org/10.3390/su162310621.

Operstein, V. and Frydman, S (2000) 'The influence of vegetation on soil strength,' *Proceedings of the Institution of Civil Engineers – Ground Improvement*, *4(2)*, pp. 81–89. https://doi.org/10.1680/grim.2000.4.2.81.

Powrie, W. and Smethurst, J (2018) *Climate and vegetation impacts on infrastructure cuttings and embankments*. University of Southampton.

Tanaka, K. et al. (2008) 'Development of test method for evaluating root resistance of waterproofing membrane,' *In Proceedings of the 11th International Conference on Durability of Building Materials and Components (11DBMC)*, *Istanbul*, pp. Turkey (May 11–14, 2008).

U.S. Army Corps of Engineers (2014) *Safety of dams Policy and procedures (Engineer Regulation No*. ER 1110-2-1156). Department of the Army.

U.S. Department of Agriculture, Natural Resources Conservation Service (1992) *Engineering field handbook, Part 650, Chapter 18: Soil bioengineering for upland slope protection and erosion reduction (210-EFH, October 1992)*.

U.S. Department of Agriculture (2007) *National engineering handbook: Technical supplement 14M Vegetated rock walls*.

Wang, H. et al. (2023) 'Temperature effects on the hydraulic properties of unsaturated rooted soils,' *Canadian Geotechnical Journal*, *60*, pp. 936–945. https://doi.org/10.1139/cgj-2022-0475.

Wu, T. H (1976) *Investigation of landslides on Prince of Wales Island, Alaska (Geotechnical Engineering Report No*. 5). Department of Civil Engineering, The Ohio State University.

Ziemer, R. R (1981) *The role of vegetation in the stability of forested slopes*. In Proceedings of the XVII IUFRO World Congress, Japan (pp. 297–308).

UNISDR (2009) *UNISDR Terminology on Disaster Risk Reduction.* Geneva: United Nations International Strategy for Disaster Reduction

Heller, V., Hager, W.H. and Minor, H.-E. (2009) *Landslide generated impulse waves in reservoirs: Basics and computation*. VAW-Mitteilungen 211. Zürich: Versuchsanstalt für Wasserbau, Hydrologie und Glaziologie (VAW), ETH Zürich.

Rocscience Inc. (2022) *Slide2 Documentation (User Guide and Help System).* Toronto, ON: Rocscience Inc. Available at: https://www.rocscience.com/help/slide2/documentation

Civil Practical Knowledge (n.d.) *Types of dams*. Available at: https://civilpracticalknowledge.com/types-of-dams/